Dissertations

Theses and Dissertations

1983

Synaptic Transmission in the Inferior Mesenteric Ganglion of the Rabbit: An Electrophysiological and Immunohistochemical Study

Mark Alan Simmons
Loyola University Chicago

SYNAPTIC TRANSMISSION IN THE INFERIOR MESENTERIC GANGLION OF THE RABBIT:

AN ELECTROPHYSIOLOGICAL AND IMMUNOHISTOCHEMICAL STUDY

by

Mark Alan Simmons

A Dissertation Submitted to the Faculty of the Graduate

School of Loyola University of Chicago in Partial

Fulfillment of the Requirements for the Degree of

Doctor of Philosophy

October

1983

ACKNOWLEDGEMENTS

DEDICATION

To Robin and Christopher for their understanding and support throughout this project and especially for their constant love.

VITA

The author, Mark Alan Simmons, is the son of LeRoy J. Simmons and Jane E. (Kraus) Simmons. He was born January 16, 1956 in Columbia, Pennsylvania and was raised in Marietta, Pennsylvania.

His elementary and secondary education were obtained in the public schools of the Donegal School District, Lancaster County, Pennsylvania, from which he graduated in 1973.

In September, 1973, he entered the University of South Carolina, and in December, 1976, received the degree of Bachelor of Science with a major in Psychology and a minor in Mathematics and Computer Science. In January, 1977, he was employed as a Research Assistant in the Behavioral Pharmacology Laboratory, Department of Psychology, University of South Carolina, by Dr. James B. Appel. He became a member of the Society for Neuroscience in 1979.

He was awarded a Basic Science Fellowship for graduate study in the Department Pharmacology at Loyola University of Chicago in July, 1979. In July, 1982, he was awarded a Fellowship by the Arthur J. Schmitt Foundation.

TABLE OF CONTENTS

LIST OF TABLES

LIST OF FIGURES

Page

LIST OF ABBREVIATIONS

ABC	Avidin:biotin complex
ACh	Acetylcholine
APP	Avian pancreatic polypeptide
BOM	Bombesin
CCK	Cholecystokinin
DAB	Diaminobenzidine
DHβE	Dihydro-β-erythoidine
DHE	Dihydroergotamine
DRG	Dorsal root ganglion
d-TC	d-Tubocurarine
E_m	Membrane potential
E_r	Resting membrane potential
EAD	Early afterdischarges
ENK	Enkephalin
F-EPSP	Fast excitatory postsynaptic potential
FITC	Fluorescein Isothiocyanate
G	Conductance
HRP	Horseradish peroxidase
5-HT	5-hydroxytryptamine, serotonin
IMG	Inferior mesenteric ganglion
LAD	Late afterdischarges
LHRH	Luteinizing hormone releasing

hormone

LN	Late negative wave
LLN	Late late negative wave
LS-EPSP	Late slow excitatory postsynaptic potential
NE	Norepinephrine
PBS	Phosphate buffered saline
R_{in}	Input resistance
SCG	Superior cervical ganglion
S-EPSP	Slow excitatory postsynaptic potential
SIF	Small intensely fluorescent
S-IPSP	Slow inhibitory postsynaptic potential
SOM	Somatostatin
SP	Substance P
τ_m	Membrane time constant
TBS	Tris-buffered saline
TTX	Tetrodotoxin
VIP	Vasoactive intestinal polypeptide

I. INTRODUCTION

The sympathetic ganglia were originally thought to act as simple relay stations from the central nervous system to the peripheral visceral organs. The ganglia received impulses exclusively from preganglionic cholinergic neurons and relayed these impulses in a diffuse fashion to the viscera via noradrenergic nerves; no integrative functions were thought to occur in the ganglia. More recently, the sympathetic ganglia, in particular the prevertebral ganglia, have been found to have a much more complex organization and, accordingly, a more integrative function has been attributed to these structures.

The prevertebral ganglia receive a number of inputs from multiple nerve trunks. Not all of these inputs originate in the preganglionic nuclei of the spinal cord; fibers also arise from cells bodies in the viscera. Additionally, afferent fibers with cell bodies in the dorsal root ganglia (DRG) traverse and apparently effect synapses in the prevertebral ganglia. Finally, a number of neuropeptides have been found in neural structures in sympathetic ganglia. Some of these peptides exert specific neurotransmitter-like effects at selected sites in the central and peripheral nervous systems and also in the prevertebral ganglia.

In the present studies, synaptic transmission in the inferior mesenteric ganglion (IMG) of the rabbit was investigated by intracellular recordings of the electrical activity of ganglionic neurons, and the

1

localization of a number of neuropeptides in this structure was studied using immunohistochemistry. The major objectives of this investigation were to delineate the basic electrical properties of these cells, to examine cholinergic transmission in this ganglion and to examine the role that certain peptides or other noncholinergic transmitters may have in synaptic transmission in this structure.

A. Structure of the Inferior Mesenteric Ganglion

1. General Organization of the Autonomic Ganglia

The autonomic ganglia are aggregates of nerve cells surrounded by glial cells and connective tissue. The ganglionic neurons receive preganglionic fibers from neurons in the central nervous system and send postganglionic fibers to the effector organs--smooth muscles, glands and the heart. The parasympathetic ganglia receive preganglionic fibers from neurons situated in the brain stem and sacral spinal cord. The sympathetic ganglia, of interest here, receive preganglionic fibers from neurons in the thoracic through lumbar spinal cord levels. The cell bodies of the sympathetic preganglionic neurons are mainly located in the nucleus intermediolateralis of the spinal cord.

Sympathetic ganglia can be classified into two types according to anatomical position--paravertebral and prevertebral. The paravertebral ganglia are the sympathetic chain ganglia. These ganglia and the commissures connecting them form the sympathetic trunks situated bilaterally along the ventro-lateral aspect of the spinal column from the first thoracic segment caudally through upper lumbar segments. Each ganglion

is connected with its corresponding spinal nerve by communicating rami. Preganglionic fibers enter the ganglia via the white rami;. postganglionic axons exit through the gray rami and join the spinal nerves to travel to the effector organs.

The prevertebral ganglia are distinct from the sympathetic trunk in the abdominal cavity (additionally the cervical ganglia may be considered prevertebral). The abdominal prevertebral ganglia lie close to the median sagittal plane of the body, ventral to the abdominal aorta. This includes the celiac, superior mesenteric and inferior mesenteric ganglia and the hypogastric and pelvic plexuses. The preganglionic fibers to these ganglia traverse the paravertebral ganglia in long nerves (Skok, 1973; Gabella, 1976).

2. Anatomy of the Inferior Mesenteric Ganglion

Detailed studies of the anatomy of the autonomic nervous system were performed by Langley and Anderson (see below); subsequent studies have confirmed the accuracy of their descriptions (Trumble, 1933). The nomenclature used by Langley and Anderson has been retained here. A schematic diagram of the rabbit IMG and surrounding structures is presented in Figure 1 of the Results section.

The IMG of the rabbit consists of a long and narrow ganglion found near the inferior mesenteric artery close to the aorta. Several fine filaments exit from the lumbar spinal cord and traverse the sympathetic trunks to enter the IMG. These are the inferior splanchnic nerves. Frequently, one or more of these fibers joins the aortic branch of the ascending mesenteric nerve to enter the ganglion (Langley & Anderson,

1896b). Five or six nerve filaments leave the upper part of the gan-
glion laterally and pass anteriorly along the inferior mesenteric vein;
these are the branches of the ascending mesenteric nerve. These
branches join strands from the superior mesenteric ganglion and give off
filaments along the vasculature to the colon. The ascending mesenteric
nerve is much larger in the rabbit than in the cat. Two other fiber
bundles leave the anterior end of the IMG, continue anteriorly near the
aorta and also join the superior mesenteric plexus. These are the
ascending aortic branches. Several nerve strands are seen emanating
from the posterior end of the IMG. The largest of these is the hypogas-
tric nerve, which in the rabbit is actually composed of two hypogastric
nerves united into a common trunk. Other fibers accompany the inferior
mesenteric artery and its branches and constitute the colonic nerves.
These are less conspicuous in the rabbit than in the cat. It is sug-
gested that more fibers for the upper part of the colon course through
the mesentery in the rabbit than in the cat; thus, the ascending mesen-
teric branches are larger and the colonic branches smaller in the rab-
bit.

3. Morphology of the Inferior Mesenteric Ganglion

The detailed structure of the rabbit IMG has been studied only to
a limited extent. Histological examinations have been performed with
respect to the IMG of the human and of the cat and the ultrastructure of
the cat IMG has been examined. In more recent studies on the neural
connections between the IMG and other structures the guinea pig prepara-
tion has been used.

a. Histology

Histological examination of the human IMG reveals ganglion cells of medium size which are stellate in form (Kuntz, 1940). The cells have long dendrites which branch relatively infrequently and radiate from the cell bodies in all directions. Some cells also have short, or accessory, dendrites with numerous short branches. Adjacent cells are intimately related through their dendrites. A single ganglion cell may become related with a relatively large number of neighboring cells. In some instances, terminal arborizations of dendrites form dendritic nests around the cell bodies of adjacent cells. Contacts are apparently formed between the cell bodies and the proximal portions of the dendrites.

Axons enter the IMG in bundles containing preganglionic fibers as well as visceral afferents traversing the ganglion. Axons leave these bundles and ramify among the dendrites. Many synaptic contacts are made with a single axon contacting more than one ganglion cell (Kuntz, 1940). Postganglionic axons arising within the IMG do not ramify among the ganglion cells but aggregate into bundles which emerge from the ganglion. The caliber of these axons is so similar to that of the preganglionic fibers that the two cannot be distinguished on the basis of size.

The morphology is essentially the same in the cat but cells with short dendrites are less common (Kuntz, 1940) and pericellular and peridendritic nests are observed less frequently (M'Fadden, Loughridge & Milroy, 1935; Kuntz, 1940). Cat ganglion cells are about 20-40 µm in size (M'Fadden et al., 1935).

Using the histochemical method of Falck and Hillarp for the fluorescent localization of monoamines (Falck, 1962), Hamberger, Norberg and Sjoqvist (1964) found noradrenergic terminals surrounding cat sympathetic ganglion cells in basket-like structures (Hamberger, Norberg & Sjoqvist, 1964). These terminals apparently correspond to the peridendritic nests of neighboring cells observed by Kuntz (1940). Of all the sympathetic ganglia examined (in both rabbit and cat) the prevertebral ganglia have the most well-developed systems of such terminals (Hamberger, Norberg & Ungerstedt, 1965). Removal of the paravertebral ganglia from L3-L7, removal of the celiac ganglia, section of the colonic nerves or section of the hypogastric nerves does not alter the peridendritic nests (Hamberger & Norberg, 1965); thus, they apparently originate within the IMG.

b. Ultrastructure

The perikarya of the IMG neurons have very few synapses (Elfvin, 1971a). Axosomatic synapses are seen only occasionally. Short and long processes are connected to the perikarya. The short processes are connected with the rest of the cytoplasm by a stalk about 100 nm in diameter. These short processes extend 1-3 µm from the surface of the cell body. The long processes are connected by a stalk which is 1-3 µm wide. Often several synaptic sites are seen on both types of processes. Sometimes, a single preganglionic terminal synapses with both a short process and the surface of the perikaryon. The presynaptic regions contain clear vesicles and are presumably acetylcholine (ACh) containing neurons. In the short cell processes small dense core vesicles are found.

These processes form dendrodendritic and dendrosomatic contacts with adjacent ganglion cells. The number of dendrodendritic contacts is about the same as the number of axodendritic contacts made by the pre-ganglionic fibers (Elfvin, 1971c). These short processes containing closely packed dense core vesicles correspond to the fluorescent basket-like networks seen with the Falck-Hillarp technique.

In addition to the classical axodendritic synapses made by the preganglionic fibers with the IMG cells, specialized axoaxonic synaptic contacts are seen between separate preganglionic cholinergic fibers (Elfvin, 1971b). Chromaffin or small intensely fluorescent (SIF) cells are practically absent in the cat IMG; however, a granule-containing cell which is apparently comparable to the SIF cell has been found in the rabbit IMG (Elfvin, 1968). These cells are about 10-25 μm in diameter and occur in groups of three to five cells.

c. Neural Connections

1) Fiber Types

In the cat, the inferior splanchnic nerves are composed mainly of small, myelinated fibers, 1-3 μm in diameter, but some unmyelinated fibers are also present (M'Fadden et al., 1935; Harris, 1943). A smaller number of fibers are found in the range of 4-6 μm and 1% are on the order of 10-12 μm (M'Fadden et al., 1935). The postganglionic fibers are mainly unmyelinated (M'Fadden et al., 1935; Harris, 1943). Some small myelinated fibers, about 2 μm in diameter, are seen scattered in the peripherally coursing nerve bundles.

2) Possible Origins of Fibers

Degeneration studies have indicated several possible sources of the fibers coursing to and through the IMG.

a) The majority of myelinated fibers in the hypogastric nerve are most likely preganglionic fibers from the lumbar spinal cord passing through the IMG to innervate cells located in the hypogastric-pelvic plexus (Kuntz, 1940; Harris, 1943).

b) Alternatively, Harris (1943) has suggested that these are preganglionic components of the sacral spinal nerves ascending in the hypogastric nerve from the pelvic plexus through the IMG to the colon; however, this does not appear to be the case since others have concluded that no fibers from the sacral spinal cord pass through the IMG to innervate the colon (Langley & Anderson 1896a; M'Fadden et al., 1935; Garry & Gillespie, 1955).

c) Visceral afferent fibers with cell bodies in the DRG (Kuntz, 1940; Harris, 1943).

d) Fibers which originate in the enteric plexuses to teminate in the IMG (Kuntz, 1940).

The latter two possibilities are the most likely in the cat colonic nerve, as very few preganglionic fibers pass through the IMG to continue in this nerve (Harris, 1943).

3) Number of Fibers

Visceral afferents. Central to the IMG, 2,500 visceral afferents were seen in the splanchnic nerves (Harris, 1943). Peripherally, a total of 5,000 afferent fibers were seen, 3,000 in the colonic nerve and

2,000 in the hypogastric nerve. The difference is explainable by assum-
ing that upon reaching the IMG each fiber from the spinal ·ganglion gives
off one collateral. An alternative explanation is that some of these
visceral afferent fibers do not have their cell bodies in the DRG, but
are fibers of enteric origin which synapse in the IMG and do not con-
tinue more centrally. This group contains both myelinated and unmyeli-
nated fibers. Most of the myelinated fibers are of small (1-3 μm), some
of medium (4-6 μm) and some of large (7-10 μm) diameter. The visceral
afferent fibers reaching the colon are exclusively unmyelinated while
some of those in the hypogastric nerve are myelinated.

    Preganglionic/Postganglionic Sympathetics. In the IMG of the cat,
approximately 3,000 postganglionic sympathetic fibers enter the IMG from
the lumbar region of the spinal cord. The ascending nerves had been
severed to allow examination exclusively of the lumbar inputs. A total
of 9,500 fibers exit the IMG in the colonic and hypogastric nerves.
Thus, 2 of 3 postganglionic sympathetic fibers in the colonic and hypo-
gastric nerves have their origin in the IMG, if one assumes that none of
the postganglionic fibers give off collaterals. Of the 4,000 pregan-
glionic fibers entering the IMG from the lumbar nerves, 1,000 pass
through and descend in the hypogastric nerve. If those fibers passing
through the ganglion effect synapses the ratio of preganglionics to
postganglionics is 1/1.5, if not the ratio is 1/3 (Harris, 1943).

    Widely varying values have been reported for the preganglionic/
postganglionic ratio in other ganglia. Several factors contribute to
this variation. First, it appears that the value obtained depends on

the animal examined. For example, in the superior cervical ganglia (SCG) of the cat reported values range from 1/11 to 1/32 (Billingsley & Ranson, 1918; Wolf, 1941), in the dog a ratio of 1/8 was calculated (Sanbe, 1961) and in the human values as high as 1/196 have been reported (Ebbesson, 1968). There is even considerable variation among primates as in the SCG of the squirrel monkey a value of 1/28 was found (Ebbesson, 1968). A second factor is the ganglion examined, as in the human lumbar sympathetic chain ganglia ratios around 1/70 have been reported (Webber, 1955). These differences partly reflect variation in the number of neurons in the ganglion rather than in the number of pre-ganglionic fibers. The number of neurons in the human SCG is about 10 times greater than the number in the same ganglion in the cat and 20 times as much as the value obtained in the rabbit, while the number of preganglionics in these species is of the same magnitude (Ebbesson, 1963). Brooks-Fournier and Coggeshall (1981) have reported a much higher ratio in the rat SCG (1/4). These authors point out that the preganglionic nerve trunks also contain sensory and postganglionic fibers. In previous work the presence of these non-preganglionic axons in the preganglionic nerve trunks was not considered. Furthermore, accurate counts of the number of the unmyelinated postganglionic axons is only possible under the electron microscope.

Low preganglionic/postganglionic ratios have been taken as support for a diffuse control of the viscera by the sympathetic system, as com-pared to a more precise control of the parasympathetic system. In view of the fact that many of the reported values of preganglionic/postgan-

glionic may overestimate the number of preganglionic fibers and underestimate the number of postganglionic fibers, this interpretation may not be justified.

B. Function of the Inferior Mesenteric Ganglion

1. Viseral Innervation

Classical studies on the effector organ responses to electrical stimulation of the IMG and associated nerve trunks were conducted by Langley and Anderson in the 1890's. Visual observation was made of the various organs, including the bladder, genital organs and gastrointestinal tract, following electrical stimulation at various sites.

a. Bladder

The IMG was shown to be involved in the innervation of the bladder. Stimulation of the lumbar nerves resulted in a contraction of the base of the bladder (Langley & Anderson, 1895b). The fibers involved in this response travel in the hypogastric nerve.

b. Genitalia

Effects were also observed on the internal genital organs--the vasa deferentia and seminal vesicles in the male and the uterus and vagina in the female (Langley & Anderson, 1895c). The response in all cases was a slight contraction of the musculature. These effects are also mediated by fibers travelling in the hypogastric nerve.

c. Gastrointestinal Tract

1) Stimulation of the Sympathetic Chain

As early as 1890, Langley had reported that the nerves to the rabbit descending colon and rectum leave the spinal cord in two regions, termed the upper and lower sets or the lumbar and sacral nerves. The nerves from the lumbar region (the sympathetic nerves) were found to travel to the IMG and then, via the ascending mesenteric, colonic and hypogastric nerves, to the colon and rectum. Stimulation of these lumbar sympathetic nerves resulted in an inhibition and pallor (vasoconstriction) of the descending colon and rectum, while stimulation of the sacral fibers (the parasympathetic nerves) produced a strong contraction (Langley, 1891).

Systematic studies on stimulation of the sympathetic chain ganglia showed that the second lumbar sympathetic nerve is the rostral-most which contains an appreciable number of fibers to the descending colon and rectum (Langley & Anderson, 1895a). Maximal effects were obtained by stimulating the fourth or fifth ganglion. By the seventh ganglion little or no response was seen; hence, the second to fifth lumbar sympathetic nerves carry fibers which affect the colon and rectum. These results have been confirmed, almost 100 years later, by Krier, Schmalz & Szurszewski (1982) who showed by stimulating the preganglionic fibers in the lumbar white rami to the cat IMG that the principal source of sympathetic innervation arises at L3 and L4.

Stimulation of the lumbar sympathetic nerves in both rabbit and cat caused pallor of the descending colon and rectum, including the

mucus membrane of the internal anal sphincter. In the rabbit inhibitory effects were seen on both muscle coats of the large intestine while a rather weak dilation of the internal anal sphincter was seen. In the cat inhibition of the descending colon and rectum was weak but there was a strong contraction of the internal anal sphincter (Langley & Anderson, 1895a).

2) Stimulation of the Nerves of the IMG

The inferior splanchnic nerves innervate the IMG and contain those branches from the sympathetic trunk which, when stimulated, cause inhibition and vasoconstriction in the colon. Inhibition and pallor in the upper part of the descending colon are observed following stimulation of the ascending mesenteric nerve. Stimulation of the colonic fibers, which travel along the inferior mesenteric artery towards the colon, results in effects on the whole of the descending colon and rectum which are greatest an inch or two on either side of the artery. Stimulation of the hypogastric nerve, which leaves the IMG caudally, reveals an inhibition and pallor in the rectum and in the adjoining part of the descending colon (Langley & Anderson, 1895a).

Following injection of nicotine or curare it was found that stimulation of the spinal branches (lumbar sympathetic nerves and inferior splanchnic nerves) to the IMG was ineffective in eliciting a response (Langley & Anderson, 1895d). As the electrodes were moved down the nerves, towards the IMG, responses were seen only upon reaching the IMG. From these studies it was concluded that the fibers from the lumbar sympathetic chain run directly to the IMG.

Nearly all the preganglionic sympathetic fibers which affect the large intestine synapse in the IMG. A considerable portion of the fibers to the bladder and internal anal sphincter, as well as a smaller and variable proportion of the fibers for the internal genital organs and sometimes a few fibers to the external genital organs, also end in the IMG (Langley & Anderson, 1895d).

2. Modulation of Intestinal Motility

Just prior to the beginning of the twentieth century, two laboratories had investigated the innervation of the large intestine and had come to the same conclusion--that stimulation of the lumbar splanchnics or of the colonic nerves results in an inhibition of the large intestine, while stimulation of the sacral nerves results in contraction (Langley & Anderson, 1895a; Bayliss & Starling, 1900). There was apparently very little interest in this part of the autonomic nervous system until the late 1920's, when interest in the role of the IMG again increased as investigations on intestinal motility advanced. In general, the visual observations of these early investigators have been subsequently confirmed with more quantitative methods.

a. In situ Studies

Following stimulation of the lumbar sympathetics, the colonic nerves or the hypogastric nerves a marked contraction of the internal anal sphincter occurs in anesthetized dogs (Learmonth & Markowitz, 1929). The effect is greatest following hypogastric nerve stimulation. The colonic nerves also exert inhibitory effects on the colon (Learmonth

& Markowitz, 1930). Section of the colonic nerves is followed immediately by an increase in intracolonic pressure and in some cases by an increased amplitude of the contractions of the colon. This reveals a tonic inhibitory influence on the musculature of the distal colon. On this basis, section of the inferior mesenteric plexus was suggested as a treatment of Hirschsprung's disease (Rankin & Learmonth, 1930, 1932) and was used successfully in a few cases (Ross, 1935). It is now known that Hirschsprung's disease is due to a congenital absence of the enteric plexuses. Current therapy involves resection of the affected region of the colon (Kleinhaus, Boley, Sheran & Sieber, 1979).

Others found that section of the preganglionics or postganglionics of the IMG or removal of the IMG had little effect on the movements of the colon in cats (M'Fadden et al., 1935). This study differed from the above in that examinations were not performed acutely, but observations were made at least one week following surgery. Colonic motility was measured by X-ray observation of the movements of radio-opaque meals or enemas. Although no hypermotility was observed, there was a decrease in transit time through the colon, apparently due to diminished resistance at the internal anal sphincter, a structure shown above to be contracted by stimulation of the fibers of the IMG.

Garry (1933b) examined the responses in the large bowel of the cat to stimulation of the lumbar sympathetic outflow. Movements of the large bowel and the anal canal were recorded by two balloons inserted through the anus. Intestinal motility was stimulated by movement, but not distention, of either of the balloons. Stimulation of the lumbar

sympathetics exerted an inhibitory influence on the response of both the large bowel and the internal anal sphincter to movement of either balloon.

In another study, the behavior of the large bowel of the cat was also measured by a balloon inserted through the anus (Garry, 1933a); when the lumbar sympathetic outflow was intact the bowel was inactive. Section of the entire lumbar outflow resulted in increased tone and rhythmical activity in the colon. Section of only the spinal rami to the IMG caused a slight increase in tone and rhythmic contractions appeared. Subsequent section of the colonic and hypogastric nerves led to a marked increase in both tone and rhythmicity. Division of the hypogastrics alone had little effect, but section of the colonics led to a marked increase in gut activity, even when the hypogastrics were intact. These studies indicated that, in the absence of lumbar spinal inputs, inhibition of the colon was maintained from the IMG via the lumbar colonic nerves.

The role of the IMG in the control of intestinal motility has also been examined in dogs (Lawson, 1934). The colonic or hypogastric nerves were sectioned for stimulation. After stimulation of the colonic nerves an inhibition of the colon was observed accompanied by a contraction of the internal anal sphincter. Stimulation of the hypogastric nerves produced consistent effects only in the distal segment of the colon and at the internal anal sphincter. When the spinal rami to the IMG were cut, the inhibitory phase was prolonged. Subsequent section of the colonic nerves when stimulating the hypogastric nerves or section of the hypo-

gastric nerves while stimulating the colonic nerves further prolonged the inhibition. Lawson (1934) concludes that the cells of the IMG act independently of preganglionic influences and that the relationships of the response of one intestinal segment to other segments depends on either automatic or reflex activity in the cells of the IMG.

b. In vitro Studies

The rabbit isolated colon has been used to examine the effects of the colonic and pelvic nerves in vitro (Garry & Gillespie, 1955). Pelvic nerve stimulation results in contraction of the colon with the maximal response occurring at 10 Hz. A contraction could be obtained with frequencies as low as 1 Hz. As reported in situ, stimulation of the colonic nerves caused an inhibition of the colon. These fibers required a higher frequency of activation as the maximal response was seen at 100 Hz and no response could be elicited below 5 Hz. The inhibition showed no fatigue and was followed by a sudden sharp contraction following cessation of stimulation. The effects of pelvic stimulation, but not the response to colonic nerve stimulation, were antagonized by hexamethonium and atropine. The inhibitory response involved an amine transmitter since it disappeared in colons taken from reserpinized animals (Gillespie & Mackenna, 1961).

3. The Inferior Mesenteric Ganglion as a Reflex Center

Prior to 1937, the evidence for independent activity in mammalian sympathetic ganglia was unconvincing, particularly in view of the prevalent concept that the ganglia served merely as relay stations from the

central nervous system to the peripheral visceral organs (Gaskell, 1916; Langley, 1921). Garry (1933a) and Lawson (1934), however, had offered evidence for continued inhibition of the intestine by the IMG following acute decentralization, but it was possible that this result was an artifact of trauma and exposure. To clarify these findings, Lawson and Holt (1937) recorded colonic motility as an index of the activity of the IMG in unanesthetized dogs. Two to four weeks following ramisection of the IMG, tone levels were decreased in the anal canal and proximal colon and raised in the middle colon. Contraction height was not uniformly affected except in the distal colon, where there was an increase. Removal of the IMG following ramisection gave essentially similar results. Basal tone levels were not uniformly affected; in some cases tone was lower. Contractility was increased throughout the colon, most in the distal colon and anal canal, least in the proximal segment. The increase in contractility following ganglionectomy was established within twelve hours and no progressive changes were noted. These results were interpreted as further evidence that control of the colon by the decentralized IMG is a result of nervous activity in the ganglion itself. Following extirpation of the lumbar segments of the sympathetic trunk and ascending mesenteric nerves, a large percentage, but not all, of the axons in the ganglia degenerate (Kuntz, 1940; Harris, 1943). Following removal of the IMG (M'Fadden et al., 1935) or section of the colonic nerves (Kuntz, 1940), intact fibers can still be seen in the distal part of the colonic nerves. Kuntz (1940) suggests that these are fibers of enteric origin which travel centripetally in the colonic nerves; thus, the IMG may be a reflex center.

Degeneration experiments revealing the persistence of axons in the distal ends of nerve fibers following nerve section more centrally further suggested that the IMG was a reflex center. To test this hypothesis, Kuntz (1940) extirpated the lumbar segments of the sympathetic trunks and severed the ascending mesenteric nerves connecting the celiac-superior mesenteric ganglion plexus with the IMG of anesthetized cats. The colon was transected in order to interrupt the enteric plexuses and balloons were placed in the proximal and distal segments of the colon. When the proximal segment was quiescent, inflation of the distal colon had no effect; but when the proximal segment was undergoing rhythmic contractions, inflation of the balloon in the distal segment commonly resulted in inhibition. In these experiments, all neural pathways from the distal segment of the large intestine to the proximal segment were interrupted, except pathways through the IMG. Thus, the response of the proximal segment following distention of the distal colon can be explained as a reflex response through the IMG. Others, however, were unable to show the persistence of intestino-intestinal reflexes through decentralized prevertebral ganglia (Youmans, Karstens & Aumann, 1942). In this study jejunal activity in dogs was measured. Inhibitory reflexes were only observed when the connections of the celiac ganglion with the spinal cord were intact.

In view of these discrepancies, Kuntz and Saccomanno (1944) combined anatomical and physiological techniques to demonstrate that the IMG can modulate reflexes in the absence of central connections. Axon terminations persist in the IMG following decentralization and intact

fibers can be found in the distal segments of nerves from the IMG following section of these nerves. On the assumption that some of these distal fibers make synapses in the IMG, they were regarded as the afferent limb of a reflex arc. The physiological experiments showed that following removal of the spinal cord from the first thoracic segment caudalward an inhibition of the proximal colon was still observed following distention of the distal segment. This response was not mediated by the enteric plexuses as the colon had been transected between the distending and recording balloons. In the acute experiments it was quite possible that the response was a pseudo-reflex, mediated through branches of the visceral afferent fibers; however, a similar response was also seen seven days after decentralization of the IMG by bilateral extirpation of the lumbar sympathetic trunk and section of the ascending and hypogastric nerves. By this time the dorsal root afferents had undergone degeneration. It is concluded that impulses arising in the colon are conducted to the IMG through axons of enteric ganglion cells. These axons synapse onto IMG neurons which transmit impulses back to the colon forming a true reflex arc. More direct evidence for the involvement of the IMG in peripheral reflex activity has been provided by the electrophysiological studies described below.

C. Electrophysiology of the Inferior Mesenteric Ganglion

The first investigations of the electrophysiology of synaptic transmission through the IMG appeared shortly after studies which recorded the electrical activity of crayfish ganglia (Adrian, 1931), sympathetic nerves (Adrian, Bronk & Phillips, 1932) and the superior cervical ganglion (Eccles, 1935).

1. Extracellular Recordings

Through the use of extracellular recordings from the nerves associated with the IMG, information has been obtained on the conduction velocity in the associated nerve fibers, on the synaptic delay occurring in the ganglion and on the conduction/reflex pathways through the ganglion.

a. Conduction Velocity and Synaptic Delay

In the cat, several types of fibers have been found in the nerve trunks associated with the IMG according to conduction velocity. Two groups of fibers were seen in the splanchnic nerves: one with a maximum conduction velocity of 10 m/sec and the second at 0.9 m/sec (Lloyd, 1937). Others calculated the conduction velocity of the fast fibers to be 2-7 m/sec and of the slower group to be 0.5-2 m/sec (Krier et al., 1982). There are only a few fibers of the latter type in the inferior splanchnics. In the hypogastric nerve the largest group is slow conducting (0.9-1.6 m/sec) while faster conducting fibers (9.7-12.8 m/sec) are fewer in number (Lloyd, 1937). Adrian et al. (1932) described slow fibers conducting at 0.8 m/sec in the hypogastric nerve of the cat.

In the rabbit IMG _in vitro_, the inferior splanchnic fibers conduct at a rate not less than 5 m/sec (Brown & Pascoe, 1952). These results were obtained at temperatures from 20-22°C. Three groups of fibers are seen in the ascending mesenteric nerve. The largest group consists of fibers conducting at 0.45 m/sec; these are postganglionic fibers. A smaller number of lower threshold fibers conduct at 2 m/sec and do not synapse in the ganglion. A small group of high threshold fibers conduct

at 0.25 m/sec. These are presumably preganglionic fibers of small size. The synaptic delay following ascending or inferior splanchnic nerve stimulation is similar (see below).

Estimates of the synaptic delay for these responses have varied from around 5 to 33 msec. Synaptic delay in the IMG of the cat in situ was determined to be between 4.5 and 6 msec (Lloyd, 1937). A similar value was reported in a later study where the minimum synaptic delay was calculated to be 5 msec (Job & Lundberg, 1952). In the celiac-superior mesenteric ganglion of the guinea pig in vitro at 37°C a synaptic delay of 9.3 msec has been reported (Kreulen & Szurszewski, 1979b). In the rabbit IMG in vitro a much longer delay of 33 msec was found at 20-22°C (Brown & Pascoe, 1952).

b. Pathways Through the Ganglion

Studies on cat, rabbit and guinea pig IMG have delineated a complex network of conduction pathways through this ganglion. For example, in the cat IMG in situ stimulation of the inferior splanchnic nerves resulted in synaptic responses in the colonic and hypogastric nerves (Lloyd, 1937). Following stimulation of the hypogastric nerve synaptic responses were recorded in both the same nerve and in the colonic nerve while an antidromic response was seen in the inferior splanchnic nerves (Lloyd, 1937; Job & Lundberg, 1952). In the rabbit IMG in vitro synaptic responses were recorded in the ascending mesenteric nerve following stimulation of the same nerve or following stimulation of the inferior splanchnic nerves (Brown & Pascoe, 1952).

In vivo experiments on the connections of the guinea pig IMG have also illustrated the complexity of synaptic connections in. this ganglion (Davison & Hersteinsson, 1975). Following stimulation of any one of the nerve trunks of the IMG synaptic responses can be recorded from the same nerve or from any of the other nerves. The only exception to this is that stimulation of inferior splanchnic fibers does not evoke activity in any of the other splanchnic fibers. Thus, all of the nerves associated with the guinea pig IMG contain fibers which make synaptic contacts in the ganglion and also contain postganglionic fibers except for the inferior splanchnic fibers, which may not contain postganglionics.

c. Peripheral Reflex Pathways

Job & Lundberg (1952) examined the responses in the colonic and hypogastric nerves of the cat following hypogastric nerve stimulation. Degeneration after excision of the sympathetic ganglia from the ninth thoracic to the fifth lumbar level, section of the dorsal and ventral roots or section of the preganglionic nerves did not alter the responses; thus, the presynaptic fibers which carry the reflex do not originate central to the IMG. If the hypogastric nerve is sectioned and allowed to degenerate, stimulation and recording on the peripheral part of this nerve reveals an action potential. Consequently, the origin of these fibers must be located peripherally to the IMG.

Similar findings have been obtained in other studies. McLennan & Pascoe (1954) examined the origin of the high threshold, slow conducting fibers observed in the ascending mesenteric nerve by Brown & Pascoe (1952). Degeneration following section of the inferior splanchnic

fibers, vagal fibers or the sympathetic trunks did not affect these fibers. Variable effects were seen following removal of the celiac-superior mesenteric ganglion complex. As noted above, some of the fibers in the ascending branches do intermingle with the celiac-superior mesenteric plexus while others course towards the colon; hence, removal of the celiac-superior mesenteric complex would remove some of these fibers. Section of the ascending branches themselves was the only manipulation which resulted in a disappearance of the response; however, section of the ascending mesenteric nerve did not exclusively involve the slow preganglionic fibers but also involved postganglionic fibers. To solve this problem, the ascending branches were severed close to the ganglion and, after degenerationof the postganglionic fibers, the segment of the nerve rostral to the section was examined. The slow fibers remained; therefore, the cells of origin must lie in the rostral distribution of the ascending mesenteric nerves. These fibers definitely do not enter the abdomen in the vagi or thoracic splanchnics and are probably not collaterals of dorsal root afferents. As has been suggested for the cat IMG, the most likely explanation in the rabbit is that these are fibers of enteric origin.

Recording from the colonic nerves in vivo in anesthetized cats most commonly revealed irregularly grouped discharges (De Groat & Krier, 1979). Injection of ganglionic blocking agents blocked the activity while section of the inferior splanchnic nerves reduced the activity in the colonic nerves. The activity in the colonic nerves was found to depend on activity from the upper lumbar levels of the cord. This was

illustrated by the finding that transection of the cervical (C2-C3) or thoracic (T10-T13) spinal cord did not alter colonic nerve activity; but, procaine injected at L3-L4 or bilateral section of the lumbar ventral roots markedly depressed colonic nerve activity. Furthermore, colonic nerve activity was correlated with intestinal motility. Procaine injection or ablation of the spinal cord at L1-L5 decreased colonic nerve activity, and thereby increased intraluminal pressure and unmasked or enhanced slow rhythmic waves in the colon. Subsequent section of the colonic nerves resulted in a further increase in basal pressure and of the intestinal contractions. This indicates that the isolated lumbar spinal cord as well as the decentralized IMG can generate tonic inhibitory input to the large intestine (De Groat & Krier, 1979).

Following stimulation of the colonic nerves an outcoming asynchronous reflex activity could be recorded in the same nerves. The reflexes were depressed by hexamethonium. Section of the lumbar spinal dorsal roots or ablation of the cord from L1-L5 markedly reduced, but did not abolish, the response to colonic nerve stimulation (De Groat & Krier, 1979). This indicates at least two possible reflexes involved in colonic nerve activity. First, a spinal reflex which depends on the integrity of the dorsal root afferents and second, a peripheral reflex initiated in the IMG itself.

2. Intracellular Recordings

Several studies have examined the electrical properties of single cells in the guinea pig IMG (see below). These studies also serve to illustrate the complexity of synaptic transmission in the IMG with

respect to multiple input pathways. Additionally, the use of an isolated IMG-colon preparation has allowed direct comparison of intracellular responses to the activity of the colon. Most recently, intracellular recordings have revealed that peptides exert specific effects on these cells and may play a role in synaptic transmission in this ganglion.

a. Basic Properties of Ganglion Cells

The first intracellular studies on this ganglion used the guinea pig IMG in vitro (Crowcroft & Szurszewski, 1971). Three types of cells were found in the IMG. Most were of the first type, which responded to direct intracellular or presynaptic stimulation with an action potential. The maximum resting membrane potential (E_r) in these cells was -65 mV. The second type of cell had a more negative E_r, ranging from -75 to -85 mV, and required larger depolarizations to initiate action potentials. The third type of cell also had a high E_r, but was inexcitable; these are presumably glial cells.

There is evidence that the Type II cells may have actually been damaged Type I cells. Neild (1978) observed that during the first minute of penetration, some Type I cells spontaneously hyperpolarized to become Type II cells. These cells would then gradually depolarize over a period of 5 to 10 min and again become Type I, although the impalement was usually lost before complete recovery. A similar phenomenon was seen in the present studies on neurons in the rabbit IMG. Most subsequent studies have described only one type of excitable cell with E_r around -50 mV (Szurszewski & Weems, 1976; Krier et al., 1982).

In the guinea pig IMG, a depolarization of 10-20 mV elicits an action potential which is often > 100 mV in amplitude (Crowcroft & Szurszewski, 1971). With sustained depolarizations the cells fire at frequencies up to 150-170 spikes per sec. With hyperpolarizing currents, some cells exhibit linear current-voltage relationships, while other cells rectify beyond 15-20 mV more negative than E_r. Input resistance (R_{in}) ranges from 40-150 MΩ. A 5-18 mV depolarization is needed to reach threshold for an action potential in the cat IMG. Reported values of R_{in} for the neurons in the cat IMG have a range of 15-56 MΩ with a mean of 46 MΩ (Krier et al., 1982).

b. Synaptic Inputs to Ganglion Cells

Most cells in the guinea pig IMG receive synaptic input from all of the nerve trunks entering the ganglion (Crowcroft & Szurszewski, 1971). Examination of the increase in the nicotinc fast excitatory postsynaptic potentials (F-EPSP) with increasing stimulus intensity revealed that each neuron in the guinea pig IMG receives at least ten presynaptic inputs from each of the colonic and ascending mesenteric nerves, three to five inputs via each hypogastric nerve and one to three fibers from each splanchnic nerve; therefore, the total number of inputs to a single cell in this ganglion would approximate 40. In the cat IMG it was found that some cells receive synaptic input from two or three different lumbar sympathetic rami, most often from adjacent segments. The number of inputs from a single ramus to one cell ranged from 1-13 with a mean of 5 per cell (Krier et al., 1982).

Following the fast nicotinic responses, an afterhyperpolarization of up to 15 mV lasting 0.2 to 0.5 sec and an afterdepolarization of up to 5 mV and lasting as long as 10 sec were observed. The amplitude of the afterhyperpolarization was positively related to the number of action potentials. This afterhyperpolarization was not seen during nicotinic blockade which prevented repetitive spiking. The afterdepolarization was observed in the presence of cholinergic antagonists. A much more prolonged response was seen in three of six cells examined following presynaptic stimulation at 15-30 Hz for 1 sec. This response consisted of an increase of R_{in} with no detectable change in E_r. During the increased R_{in}, direct depolarizing pulses were more effective in eliciting action potentials. This effect lasted about 2 min. No slow hyperpolarizing responses were observed (Crowcroft & Szurszewski, 1971).

c. IMG-Colon Preparations

The hypothesis that the IMG receives input from neurons in the colon has been confirmed using an in vitro IMG-colon preparation (Crowcroft, Holman & Szurszewski, 1971). This preparation consists of the IMG attached to the colon by the colonic nerves. The preparation is placed in a two compartment organ bath, the IMG in one compartment and the colon in the other. In this manner the input to IMG neurons can be examined by intracellular recording and drugs can be applied selectively to the IMG or to the colon. With this preparation, continuous electrical activity consisting of action potentials or F-EPSPs was recorded from neurons in all regions of the IMG. This spontaneous activity was indistinguishable from that elicited by submaximal stimulation of the

nerve trunks connected to the IMG. When the colonic nerves were cut an immediate and irreversible abolition of the spontaneous activity occurred. In addition, when the colonic nerves were left intact, spontaneous activity was reversibly abolished by application of tetrodotoxin (TTX) to the colon. At this time, stimulation of the other nerve trunks to the IMG was still effective in eliciting a synaptic response; thus, the spontaneous activity must be initiated in the colon. Application of the cholinergic nicotinic antagonist dihydro-β-erythoidine (DHβE) to the IMG blocked both spontaneous and evoked activity indicating that spontaneous activity in the IMG is mediated by the activation of nicotinic receptors. DHβE applied to the colon depressed, but did not completely abolish, the spontaneous activity recorded from the IMG cells while not affecting nerve-evoked responses. Part of the spontaneous activity from the colon, therefore, must result from cholinergic activation in the colon.

The activity in the IMG cells is related to intestinal intraluminal pressure. The input to the IMG from the colon in vitro can be activated by raising the intraluminal pressure of the colon above 5 cm H_2O; the input to the IMG increased as pressure increased above this level (Weems & Szurszewski, 1977). At least part of this input, therefore, seems to be dependent on mechanoreceptors in the gut. Mechanoreceptors have been classified as slowly adpating or rapidly adapting and both types are found in the gastrointestinal tract. Since a continuous increase in intraluminal pressure did not result in an adaptation of the afferent input it is presumed to be from the slowly adapting type of mechanoreceptor.

Agents which have a relaxant effect on the intestine also resulted in a decrease in the spontaneous activity recorded from IMG cells. Papaverine, isoproterenol, adenosine triphosphate and atropine all exhibited this effect. Carbachol, ACh and serotonin (5-HT), which excite the colon, increased the synaptic activity. The effects of carbachol and ACh were blocked by atropine applied to the colon (Crowcroft et al., 1971; Szurszewski & Weems, 1976).

Furthermore, repetitive stimulation of the nerve trunks to the IMG has been shown to result in a transient inhibition of the spontaneous activity from the colon. Following stimulation at 20 Hz for 1 sec the inhibition lasted 1.5 sec. An increase in duration or frequency of stimulation resulted in a longer period of inhibition. The inhibition was not due to the afterhyperpolarization following action potentials. The inhibition was mimicked by application of norepinephrine (NE) to the colon, but only a slight inhibitory effect was seen when NE was added to the IMG. Both the synaptic and the NE inhibition of the spontaneous activity were antagonized by addition of the α-adrenergic antagonists phentolamine and phenoxybenzamine to the colon (Crowcroft et al., 1971). In reserpinized animals repetitive stimulation of the nerve trunks failed to inhibit the spontaneous synaptic activity (Szurszewski & Weems, 1976). A period of enhanced excitability followed the synaptically induced inhibition. This probably correlates with the increased R_{in} seen above.

These results provide direct evidence for a peripheral reflex arc involving the IMG and the distal colon. The noradrenergic cells of the IMG act to depress the activity of excitatory neurons in the colon. In

turn, these neurons send fibers to the IMG in a feedback loop similar to recurrent inhibition. Since blockade of the nicotinic receptors in the IMG suppresses the spontaneous activity, the fibers from the colon must release ACh. Simlarly, DHβE was able to suppress, but not completely, the spontaneous activity when applied to the colon; thus, some, but not all, of the enteric cholinergic neurons must themselves be driven by cholinergic inputs.

Similar reflex activity involving the colon was also seen in other prevertebral ganglia, the celiac and superior mesenteric ganglia. The preparation consisted of the celiac-superior mesenteric ganglion attached to an orad segment of the colon via the celiac nerves and the IMG attached to an aborad segment of the colon via the colonic nerves and the superior mesenteric ganglion and IMG connected by the ascending mesenteric nerve (Kreulen & Szurszewski, 1979a). As in the IMG, spontaneous synaptic activity was observed in the neurons of the celiac ganglion. This activity disappeared when the celiac nerves were cut. With this preparation the two segments of the colon could be distended separately. When one segment was distended, inhibition was usually observed in the other segment. This reflex must be mediated by the prevertbral ganglia as the only connections of the two segments were through these ganglia. When the ascending mesenteric nerves connecting the ganglia were severed this reflex disappeared.

D. Noncholinergic Transmission in Sympathetic Ganglia

Excitatory transmission in sympathetic ganglia not blocked by cholinergic antagonists was first identified in bullfrog paravertebral

ganglia. Henceforth, slow noncholinergic depolarizations have been identified in the IMG and myenteric plexus of the guinea pig and in the SCG of the rabbit.

1. Bullfrog Sympathetic Ganglia

a. Description of Slow Potentials

With extracellular electrodes on the postganglionic fibers of the ninth or tenth ganglion of the bullfrog sympathetic chain, Nishi & Koketsu (1968) observed early afterdischarges (EAD) and late afterdischarges (LAD) following repetitive stimulation of the preganglionic fibers. The EAD appeared during stimulation, reached a maximum immediately following cessation of stimulation and diminished in about 30 sec (at 25°C). This response was blocked by atropine. In contrast, the LAD occurred immediately or shortly after the cessation of stimulation, reached a maximum in about 30 sec and lasted for more than 2 min; furthermore, this response was insensitive to cholinergic antagonists. Using sucrose gap recordings, potential changes of the whole ganglion were measured which correspond in time to the EAD and LAD; these are the late negative (LN) and late late negative (LLN) potentials, repsectively. Direct evidence that the LN and LLN waves are postsynaptic potentials was obtained by intracellular recordings which revealed a long lasting depolarization of the ganglion cells, the amplitude of which was dependent on the frequency and duration of preganglionic stimulation. Atropine depressed the initial phase of this slow depolarization while enhancing the late phase. Hence, the early component of the slow depolarization is the slow excitatory postsynaptic potential

(S-EPSP) (Libet & Tosaka, 1966); it relates to the EAD and LN wave. The latter component of the depolarization, which corresponds to the LAD and LLN wave, is not blocked by cholinergic antagonists and is referred to as the late slow excitatory postsynaptic potential (LS-EPSP).

A S-EPSP and a slow inhibitory postsynaptic potential (S-IPSP) can also be recorded from sympathetic ganglion cells (Kuba & Koketsu, 1978). The S-EPSP is due to an action of ACh on muscarinic receptors of the ganglion cells (Libet, 1970). The S-IPSP is also sensitive to muscarinic blockade; however, the exact nature of this potential is in dispute (Horn & Dodd, 1983). These potentials have not been examined in detail in this thesis.

A LS-EPSP is observed in 90% of the B cells and 75% of the C cells in the bullfrog ninth and tenth lumbar ganglia (Jan & Jan, 1982). The optimal frequency for the LS-EPSP is 5-10 Hz; with 20-50 stimuli, the LS-EPSP amplitude is 5-10 mV. In 80% of the cells, the LS-EPSP is accompanied by an increase in R_{in}.

b. The Transmitter of the LS-EPSP in the Bullfrog

The transmitter mediating the LS-EPSP in the bullfrog has been recently identified to be a luteinizing hormone releasing hormone (LHRH)-like peptide (Jan, Jan & Kuffler, 1979, 1980; Jan & Jan, 1982). Several findings have led to this conclusion:

1) An LHRH-like substance is found in the bullfrog sympathetic chain by radioimmunoassay. This substance is not identical to mammalian LHRH.

2) After section of the preganglionic nerves, 95% of this LHRH-like peptide disappears from the ganglion while the content triples in the spinal nerves proximal to the cut; thus, the LHRH-like peptide is contained in the preganglionic fibers.

3) LHRH-immunoreactive fibers have been identified surrounding the cell bodies of the ganglionic neurons.

4) An LHRH-like peptide can be released in a Ca^{++}-dependent manner by raising K^+ concentration or by stimulation of the preganglionic nerves.

5) When applied to the ganglion cells by pressure ejection, LHRH causes a slow depolarization.

   a) This depolarization is accompanied by an increased R_{in}, as is the LS-EPSP.

   b) When Ca^{++} in the Ringer solution is replaced by Mg^{++}, in order to prevent transmitter release, the response following presynaptic stimulation is blocked. The response to applied LHRH is unchanged under these conditions, indicating a direct action of LHRH on the postsynaptic membrane.

6) The effects of various analogs of LHRH in the bullfrog ganglia is the same as the effects of these analogs on the release of luteinizing hormone in rats. Analog antagonists block the LS-EPSP and the response to applied LHRH while analog agonists mimic the LS-EPSP. None of these compounds affected cholinergic transmission.

Another peptide, substance P (SP), also depolarizes and increases R_{in} of neurons in the bullfrog ganglia by a direct postsynaptic action

(Jan & Jan, 1982). SP does not appear to be involved in the generation of the LS-EPSP since no cross-desensitization is observed between SP and the LS-EPSP in the bullfrog and LHRH analogs have no effect on the SP responses. Also, LHRH is still effective after desensitization of the cells to SP; therefore, LHRH and SP must act at different sites. Although SP-immunoreactivity is contained in bundles of axons passing through the ganglion, no SP-postive synaptic boutons are seen and the distribution of SP-fibers is distinct from that of the LHRH fibers which surround C cells.

2. Guinea Pig Celiac Ganglion

A slow noncholinergic depolarization has recently been recorded from cells in the guinea pig celiac ganglion (Dun & Ma, 1983). This response was observed in 70% of the cells in this ganglion. The response was very long lasting with a mean duration of 160 sec and its amplitude averaged about 5 mV. The response was accompanied by an increase or no change in R_{in}.

Pharmacological analysis of this response indicated that, in some of the celiac ganglion cells, the slow depolarization may be mediated by 5-HT (Dun, Kiraly & Ma, 1983). Several lines of evidence led to the conclusion that this response is mediated by 5-HT. First, 5-HT depolarized 63% of the cells in this ganglion. The membrane resistance change during the 5-HT induced depolarization and the nerve evoked response were always the same in a given cell. Also, the effects of membrane polarization on the 5-HT and nerve responses were always changed in parallel. Secondly, pharmacolgical manipulations indicated an involvement

of 5-HT. The 5-HT receptor antagonist cyproheptadine suppressed the noncholinergic depolarization and the 5-HT induced response. Superfusing the ganglion with fluoxetine, a 5-HT uptake inhibitor, increased the amplitude of both the LS-EPSP and the 5-HT response. The 5-HT precursor, L-tryptophan, also resulted in an enhancement of the LS-EPSP, but not of the 5-HT response. The final evidence was obtained from immunohistochemical studies which showed the presence of 5-HT immunoreactive fibers in this ganglion.

3. Guinea Pig Inferior Mesenteric Ganglion

a. Characteristics of the LS-EPSP

A mammalian counterpart of the LS-EPSP observed in amphibian ganglia was first reported in the guinea pig IMG (Neild, 1978). Stimulation of the hypogastric nerves at 20-30 Hz for 1-5 sec results in a depolarization of 2-20 mV (Neild, 1978; Dun & Jiang, 1982), the average value being about 4 mV (Dun & Jiang, 1982). The depolarization usually appears 0.5-5 sec after the stimulus burst, reaching a peak in 10-25 sec (Neild, 1978; Tsunoo, Konishi & Otsuka, 1982). The half decay time of the response has been reported to be 51 sec (Tsunoo et al., 1982), although the mean total duration has been found to be only 54 sec (Dun & Jiang, 1982) or 90 sec (Neild, 1978). The time course ranges from 20 sec to 4 min following hypogastric nerve stimulation at 10-30 Hz for 1-5 sec. A slow depolarization was observed in 70-80% of the cells in the guinea pig IMG (Neild, 1978; Tsunoo et al., 1982). This response is very similar to the LS-EPSP observed in bullfrog sympathetic ganglia and will be referred to also as the LS-EPSP.

There is a great diversity in the types of membrane resistance changes which have been reported to accompany the LS-EPSP in the guinea pig IMG. In the first study on this slow depolarization (Neild, 1978), a decrease of R_{in} was observed in 96% of the cells. A decrease of 15% was observed for responses < 7 mV in amplitude and of 26% when the response was > 7 mV. This seems to be consistent with a rectification of the membrane with depolarization. The author claims, however, that while a depolarization of the cell by passing current through the electrode did result in a decreased R_{in}, the decrease was never as great as that seen during the synaptically evoked depolarization. In the remaining cells (4%) an increase in R_{in} was observed. The cells were not clamped in a study which found that for a small depolarization an increase in R_{in} was usually observed (Konishi, Tsunoo & Otsuka, 1979b), but if the depolarization exceeded 15 mV R_{in} usually decreased. It is concluded that the observed decrease is probably due to delayed rectification of the membrane.

Unfortunately, when the cell is held at E_r during the response, so resistance changes can be examined in the absence of membrane potential (E_m) changes, a variety of results are still obtained and the nature of the resistance change differs according to different investigators. Dun and Jiang (1982) found three types of resistance change: 1) an increase of 21% beginning 20-30 sec following stimulation was seen in 45% of the cells, 2) a small (16%) decrease followed by a sustained increase of about 25%, was seen in 32% of the cells and 3) a monophasic increase averaging 22% occurred in the remainder. Tsunoo et al. (1982) reported only two types of changes when the cells were held at E_r: an increase of 30% in two thirds of the cells and no change in the remainder.

The relationship between E_m and the LS-EPSP also varies. In some cells, membrane hyperpolarization resulted in an increased LS-EPSP amplitude (Dun & Jiang, 1982). In other cells the amplitude decreased at moderately hyperpolarized levels while further hyperpolarization resulted in a return of the LS-EPSP. In conclusion, it appears that the ionic mechanism of the LS-EPSP is complex, involving changes in membrane conductance to more than one ion species.

The amplitude of the slow depolarization is positively correlated with the frequency and duration of presynaptic stimulation. Neild (1978) found that with a 2 sec duration the lowest effective frequency was 10 Hz, but if a 1 Hz stimulus is continued for several seconds a small, but detectable, depolarization can be evoked (Dun & Jiang, 1982). In most cells, the maximum depolarization is elicited at 20-30 Hz for 2-5 sec while at higher frequencies the depolarization becomes progressively smaller (Dun & Jiang, 1982). The slow depolarization was not affected by d-tubocurarine (d-TC), atropine or guanethidine, indicating that it is not mediated by cholinergic or adrenergic receptors, but was reversibly abolished by the replacement of external Ca^{++} with Mg^{++} (Neild, 1978), indicating that it is probably a result of the action of a synaptically released transmitter. Also, the occurrence of a LS-EPSP in the guinea pig IMG does not follow stimulation of specific nerve trunks associated with the ganglion, but a LS-EPSP can be seen in some cells following stimulation of any of the nerve trunks entering the ganglion (Dun & Jiang, 1982; Tsunoo et al., 1982). Different outcomes do, however, result from dorsal and ventral root stimulation: ventral root stimulation (L2,L3) produces only F-EPSPs, while dorsal root stimulation elicits only a LS-EPSP (Tsunoo et al., 1982).

There is also evidence for a LS-EPSP in the rabbit SCG where the LLN wave has been recorded (Ashe & Libet, 1981). The amplitude of the response was found to depend on both the frequency and duration of pre-synaptic stimulation. These authors conclude that the number of impulses is the most important factor in determining the amplitude of the LLN response. The pharmacology of the LLN wave recorded from the rabbit SCG has not been investigated.

b. The Transmitter of the LS-EPSP in the Guinea Pig

When SP was applied to the guinea pig IMG a depolarization ensued which was electrophysiologically and pharmacologically similar to the LS-EPSP elicited by repetitive stimulation of the hypogastric nerves (Dun & Karczmar, 1979). Following desensitization by continuous application of SP, presynaptic stimulation failed to elicit the LS-EPSP. Thus, it was suggested that SP may be involved in LS-EPSP in the guinea pig IMG. These findings have been confirmed and extended.

1) Actions of Substance P

When applied to the guinea pig IMG by superfusion, SP (0.5 µM) caused a depolarization in about 85% of the ganglionic neurons, a biphasic response in 5% and no effect in the remaining 10% (Dun & Minota, 1981). The biphasic response consisted of an initial small hyperpolarization followed by a depolarization. The average amplitude of the response in those cells exhibiting a monophasic depolarization was 9 mV. With a 10-20 sec application of SP the response lasted a little over 3 min. SP acts directly on the post-synaptic membrane since the SP response was not altered in a low Ca^{++}/high Mg^{++} Krebs or by TTX (Dun &

Minota, 1981; Tsunoo et al., 1982). D-TC (50 µM), atropine (1 µM), DHβE, and hexamethonium had no effect, ruling out an action of ACh (Dun & Minota, 1981; Tsunoo et al., 1982). In neurons clamped at E_r of around -50 to -60 mV, SP elicited two types of changes in R_{in}. In half of the cells R_{in} increased briefly by 20%, followed by a more prolonged decrease of 23%. In the other half of the cells, an increase of about 25% was observed. In cells with E_r higher than -70 mV, the depolarization caused by SP was much larger and accompanied by a large increase in R_{in}. Much of this increase was probably due to anomalous rectification of the membrane since the current-voltage relations of these cells exhibited anomalous rectification and these cells exhibited a much smaller increase in R_{in} when the membrane potential was clamped at E_r.

The effects of E_m on the SP response were of two types. In some cells, conditioning hyperpolarization of the membrane enhanced the SP depolarization. The extrapolated equilibrium potential for these cells averaged -32 mV. In the second type of cell, the SP depolarization was attenuated as E_m approached the potassium equilibrium potential. When external Na^+ is replaced by sucrose or Tris, the SP depolarization is reduced to about 20% of the control response. In addition, high K^+ reduces the response by about one half (Dun & Minota, 1981).

The action of SP on the neurons of the guinea pig IMG thus seems to involve changes in conductance to more than one ion including a combination of increased sodium conductane (G_{Na}) and decreased potassium conductance (G_K). Substance P has been shown to depolarize neurons at various sites in the central and peripheral nervous systems (Krnjevic, 1977; Otsuka & Konishi, 1977; Katayama & North, 1978; Nicoll, 1978);

however, the mechanism of action depends on the neurons being examined. An increased R_{in} was observed in the myenteric plexus of the guinea pig (Katayama & North, 1978) and in cat motoneurons (Krnjevic, 1977), while both a decrease and increase was seen in the guinea pig IMG (Dun & Minota, 1981). A decreased R_{in} was observed in spinal motoneurons (Nicoll, 1978).

One suggestion for the different conductance changes observed in the IMG in response to SP is that G_{Na} activation and G_K inactivation occur at different locations on the cell (Dun & Minota, 1981). Whenever G_K was found to constitute the primary effect of SP, the peptide was applied iontophoretically to the soma of the neuron, while in those studies using bath application where the entire neuronal surface is exposed to SP, various resistance changes have been observed. It is possible then that G_K inactivation occurs primarily at the soma membrane while G_{Na} activation is the predominant effect away from the soma membrane, for instance on the dendritic membrane.

2) Substance P Mimics the LS-EPSP

Several lines of evidence support the hypothesis that SP is the transmitter of the LS-EPSP in the guinea pig IMG. First, changes in R_{in} during an SP depolarization are similar to those which occur during a synaptically induced depolarization. For a particular cell both the LS-EPSP and SP depolarization are associated with a membrane resistance change of the same type (Dun & Jiang, 1982; Tsunoo et al., 1982).

Second, the LS-EPSP has been shown to disappear following desensitzation with SP. With prolonged application of SP the LS-EPSP could

not be elicited. Following washout of SP the LS-EPSP returned (Dun & Jiang, 1982; Tsunoo et al., 1982). Also, an SP analog which differentially antagonizes the effects of SP on smooth muscle has a depressant effect on the LS-EPSP in the guinea pig IMG in a concentration-dependent manner (Jiang, Dun & Karczmar, 1982a). This effect seems specific for the LS-EPSP since the nicotinic F-EPSP is unaffected as is the muscarinic slow excitatory postsynaptic potential in the rabbit SCG.

Other substances which have been suggested as possible transmitters have also been tested on the guinea pig IMG, but do not affect the LS-EPSP (Tsunoo et al., 1982). Angiotensin II depolarized cells in the IMG; an angiotensin II antagonist blocked the depolarizing action of angiotensin II but did not affect the LS-EPSP or SP depolarization. LHRH failed to depolarize IMG cells. 5-HT, however, did depolarize the cells; this action was antagonized by methysergide, but methysergide did not affect LS-EPSP or SP depolarization. Norepinephrine and γ-amino butyric acid also depolarized IMG cells and were antagonized by phentolamine and picrotoxin, respectively. Neither of these antagonists affected the LS-EPSP or SP depolarization. The following substances were without effect on IMG cells: L-glutamate, glycine, thyrotropin-releasing hormone and somatostatin (SOM).

3) Release of Substance P

Using radioimmunoassay techniques it has been shown that an SP-immunoreactive material can be released from the IMG following incubation of the ganglion in a high K^+ solution (Konishi et al., 1979b) and that this release is Ca^{++}-dependent. Following section of the inferior

splanchnic nerves to the IMG, an accumulation of SP was found in the central stump of these nerves. Proximal to the section the SP content was 4 times greater than that in the ganglionic segments indicating that the cell bodies of origin of the SP fibers are not located within the IMG. Similar effects were observed following hypogastric nerve section (Tsunoo et al., 1982).

4) Release and Depletion of SP by Capsaicin

Further evidence for the involvement of SP in the LS-EPSP is provided by studies on capsaicin. This compound has been shown to cause the release and subsequent depletion of SP (Jessell, Iversen & Cuello, 1978; Gamse, Leeman, Holzer & Lembeck, 1981a; Gamse, Wax, Zigmond, & Leeman, 1981b). Application of capsaicin (0.5-100 μM) to the guinea pig IMG caused a depolarization occured which was similar to the LS-EPSP (Tsunoo et al., 1982; Dun & Kiraly, 1983). The peak amplitude of the LS-EPSP which could be elicited was positively correlated to the amplitude of the depolarization following capsaicin application in a given cell, but the duration of the capsaicin depolarization was significantly longer than the LS-EPSP. Capsaicin only caused a depolarization in those cells exhibiting a LS-EPSP and did not affect E_m, R_{in} or the F-EPSP in those cells that did not show a LS-EPSP. Capsaicin apparently resulted in a depletion of the transmitter of the LS-EPSP since following the application of capsaicin, nerve stimulation failed to elicit a LS-EPSP. In a few cells, however, a partial restoration of the LS-EPSP was seen about an hour after washout of capsaicin. Also, a second application of capsaicin was usually ineffective in eliciting a depolar-

ization. After capsaicin, however, SP was still effective in eliciting a slow depolarization, indicating no change in postsynaptic sensitivity. In any given cell, the three depolarizations, synaptic, SP or capsaicin, always caused similar resistance changes.

Further evidence for a presynaptic site of action of capsaicin was obtained by experiments in Ca^{++}-free perfusing solution. In this case, capsaicin was ineffective. In ganglia pretreated with TTX, however, a capsaicin depolarization could still be induced. This supports the hypothesis that capsaicin causes a presynaptic release of transmitter that does not depend on the generation of action potentials. Capsaicin was ineffective in a few cells (8%). In these cells, the LS-EPSP was not affected by prolonged superfusion with SP. In bullfrog ganglia, where the mediator of the LS-EPSP is presumed to be an LHRH-like peptide, capsaicin had no effect (Dun & Kiraly, 1983).

Capsaicin (0.9-1.5 μM) also stimulated the release of SP into a perfusate of the IMG in vitro (Tsunoo et al., 1982). The amount of SP released following incubation in capsaicin-containing solution was about 5 times greater than spontaneous release. The release of another neuropeptide, vasoactvie intestinal polypeptide (VIP), which has also been localized to the IMG by immunohistochemistry, was not affected by capsaicin. The effects of capsaicin on the release of SP is not observed in a low Ca^{++}/high Mg^{++} medium.

In conclusion, the electrophysiological evidence above supports the hypothesis that peptides mediate the LS-EPSP, SP in the guinea pig IMG and LHRH in the bullfrog paravertebral ganglia. These data are further supported by the immunohistochemical studies and retrograde tracing experiments presented in following sections.

4. Effects of Enkephalins in the Guinea Pig IMG

The opiate peptides have also been shown to exert specific effects on neural transmission in the guinea pig IMG. Met-enkephalin, Leu-enkephalin and $(D-Ala^2)$-Met-enkephalinamide, a metabolically stable Met-enkephalin analog, all exert similar effects, the only quantitative difference being that $(D-Ala^2)$-Met-enkephalinamide is more potent (Konishi, Tsunoo & Otsuka, 1979a); thus, these substances will be referred to collectively as enkephalins (ENK).

When the IMG is perfused with a solution containing ENK the amplitude of the F-EPSP evoked by presynaptic stimulation was depressed by about 50% (Konishi et al., 1979a). ENK had little or no effect on either E_m or R_{in}. The ENK effect was mediated by opiate receptors since it was blocked by the specific opiate antagonist naloxone. Naloxone itself did not produce a significant change of the amplitude of the F-EPSP. ENK did not affect the response to iontophoretically applied ACh or SP, indicating no change in the sensitivity of the postsynaptic membrane. Quantal analysis revealed that the effect of ENK was to increase the number of failures of F-EPSPs and to reduce quantal content. These results suggested a presynaptic site of action of ENK in this preparation.

A presynaptic site of action has also been suggested for ENK effects on the LS-EPSP in this ganglion (Jiang, Simmons & Dun, 1982b). ENK depressed the amplitude of the LS-EPSP in about 70% of the cells tested by an average of 30%. In 90% of these cells ENK was without effect on either E_m or R_{in}. Pretreatment of the ganglion with naloxone or naltrexone effectively prevented the effects of ENK in all cells

tested. The direct effects of SP on the postsynaptic membrane were not affected by ENK or the antagonists. Additionally, it was found that the administration of naloxone or naltrexone alone to the IMG resulted in an increased amplitude of the LS-EPSP in about one half of the cells. These findings suggest that endogenous ENK may play a role in the modulation of the LS-EPSP in this ganglion and that the site of action of ENK would be presynaptic.

E. The Localization of Peptides in the IMG

Immunoreactivity to a number of peptides has been examined in the sympathetic ganglia of the guinea pig, cat and rat. Avian pancreatic polypeptide (APP), bombesin (BOM), cholecystokinin (CCK), ENK, SOM and VIP immunoreactivity have been demonstrated in the IMG of several species; however, there are no reports concerning rabbit sympathetic ganglia.

1. Avian Pancreatic Polypeptide

In the rat, APP-like immunoreactivity was observed in the cell bodies of the superior cervical, stellate and celiac ganglia. APP immunoreactivity was also observed in the sympathetic ganglia of the cat. The highest proportion of labeled cells was found in the celiac ganglion. Many cells were seen in the superior cervical and seventh lumbar ganglia. Somewhat lower numbers were found in the superior and inferior mesenteric ganglia. No APP immunoreactivity was seen to occur in varicose nerve terminals in these ganglia (Lundberg, Hokfelt, Anggard, Kimmel, Goldstein & Markey, 1980; Lundberg, Hokfelt, Anggard, Terenius, Elde, Markey, Goldstein & Kimmel, 1982). A large number of the cells in

the superior cervical ganglion of the guinea pig were also found to be APP-positive. APP-like immunoreactive cell bodies were also found in the prevertebral ganglia of the guinea pig. In the celiac-superior mesenteric complex the number of APP labeled cells varied in different regions of the ganglion, while in the inferior mesenteric ganglion the cells were distributed more evenly (Lundberg et al., 1982).

2. Bombesin

Dense networks of bombesin-immunoreactive nerve fibers have been observed in the celiac-superior mesenteric ganglion complex of the rat and guinea pig and in the guinea pig IMG (Schultzberg, 1983). No mention is made of BOM-immunoreactivity in the rat IMG. In the rat celiac-superior mesenteric ganglion and in the guinea pig IMG the fibers were evenly distributed. In the guinea pig celiac-superior mesenteric ganglion fibers were not seen in all regions of the ganglion. Radioimmunoassay also revealed differences between the rat and guinea pig celiac ganglia with regard to BOM content--the rat ganglion contained four times more BOM per gram of tissue than the guinea pig ganglion.

3. Cholecystokinin

CCK has also been observed in the guinea pig IMG and celiac ganglion (Dalsgaard, Hokfelt, Schultzberg, Lundberg, Terenius, Dockray & Goldstein, 1983). CCK fibers form a dense network surrounding the ganglion cells in the guinea pig IMG.

4. Enkephalins

In the IMG of the guinea pig dense networks of ENK-immunoreactive nerve terminals exhibiting strongly fluorescent varicosities and thin intervaricose fibers were observed following incubation with either met-or leu-ENK antisera (Schultzberg, Hokfelt, Lundberg, Terenius, Elfvin & Elde, 1978; Schultzberg, Hokfelt, Terenius, Elfvin, Lundberg, Brandt, Elde & Goldstein, 1979). The majority of principal ganglionic neurons were surrounded by strands of fluorescent fibers but sometimes small groups of cells were seen which lacked fluorescence. No ENK-immunoreactivity was present in the principal ganglionic neurons but a few SIF cells apparently contained ENK. A smaller number of strongly fluorescent fibers were seen in the celiac-superior mesenteric ganglion surrounding a smaller percentage of the ganglion cells. A few ENK-immunoreactive fibers were also present in the superior cervical ganglion.

The rat IMG and celiac-superior mesenteric complex contain medium to strongly fluorescent varicose nerve terminals using met-ENK antisera while a weaker fluorescence was seen after incubation with leu-ENK antisera (Schultzberg et al., 1979). The density of the ENK fluorescence varied throughout the ganglion with many fluorescent strands in some areas and few in other parts. The rat superior cervical ganglion, in addition to a patchy network of ENK fibers similar to the prevertebral ganglia, also exhibited a medium intensity fluorescence in a minority of the ganglionic neurons.

5. Somatostatin

Unlike the above peptides which were found in nerve ·fibers in the IMG, SOM has been found to be present in the cell bodies of most sympathetic ganglia studied, including the superior cervical, celiac-superior mesenteric and inferior mesenteric ganglia of the guinea pig and the middle cervical, celiac-superior mesenteric and inferior mesenteric ganglia of the rat (Hokfelt, Elfvin, Elde, Schultzberg, Goldstein & Luft, 1977a). The immunofluorescence was localized in the cytoplasm, often forming a continuous ring around the nucleus and extending short distances into the cell processes.

As with the other neuropeptides, the most intense labeling was seen in the abdominal prevertebral ganglia, particularly in the guinea pig (Hokfelt et al., 1977a). About two thirds of the principal ganglion cells in this ganglion were labeled. Sixty percent of the cells in the inferior part of celiac-superior mesenteric ganglion were labeled while only 25% were labeled in the superior part of this complex. Very few cells were labeled in the superior cervical ganglion.

In the rat the appearance and distribution of SOM-immunoreactivity was similar to that seen in the guinea pig. Although the numbers were not quantified, the number of cells labeled was less numerous (Hokfelt et al., 1977a).

6. Substance P

All sympathetic ganglia studied to date including: the superior cervical, stellate, celiac-superior mesenteric and inferior mesenteric ganglia of the guinea pig; the superior cervical, celiac-superior and

inferior mesenteric ganglia of the cat; and the superior cervical, middle cervical, stellate, celiac-superior mesenteric and inferior mesenteric ganglia of the rat, have been found to contain SP immunoreactive fibers in varying amounts (Hokfelt, Elfvin, Schultzberg, Goldstein & Nilsson, 1977c). No SP immunoreactivity was observed in the cell bodies of the sympathetic ganglionic neurons in this study (Hokfelt et al., 1977c); however, SP immunofluorescence has been observed in most of the cell bodies in cultures of the superior cervical ganglia of neonatal rats (Kessler, Adler, Bohn & Black, 1981).

In the guinea pig, the highest density of SP immunoreactive fibers was found in the celiac-superior mesenteric and inferior mesenteric ganglia (Hokfelt et al., 1977c). In the IMG strongly fluorescent beaded fibers were seen with the number of fibers varying in different parts of the ganglion. Fluorescent nerve bundles frequently apposed and surrounded ganglion cell somata. In the celiac-superior mesenteric ganglion, the appearance was somewhat different with the axons running singly, rather than in bundles, and forming a more delicate network. Comparatively few SP immunoreactive fibers were seen in the stellate and superior cervical ganglia.

In the cat IMG and celiac-superior mesenteric ganglia, SP immunoreactivity was found to be of a more moderate intensity than in the same ganglia in the guinea pig (Hokfelt et al., 1977c). Thin, non-varicose axons of low fluorescence intensity and nerve terminals with strongly fluorescent varicosites frequently were seen surrounding the ganglion cells. In the superior cervical ganglion only a few fluorescent fibers were present.

In the rat IMG and celiac-superior mesenteric ganglia, a moderate SP fluorescence formed a plexus surrounding almost all of the ganglion cells. In the stellate, superior cervical and middle cervical ganglia only singly occurring fibers were present (Hokfelt et al., 1977c).

7. Vasoactive Intestinal Polypeptide

The vast majority of cells in the guinea pig IMG were surrounded by a very dense network of strongly VIP-immunoreactive varicose nerve fibers (Hokfelt, Elfvin, Schultzberg, Fuxe, Said, Mutt & Goldstein, 1977b). Occasionally, small groups of principal ganglionic neurons were seen devoid of fluorescent fibers. The inferior part of the celiac-superior mesenteric ganglion complex had a similar distribution of VIP-immunoreactive fibers. Additionally, single cell bodies were labeled, usually occurring in areas where relatively few fluorescent fibers were seen. The superior part of the celiac-superior mesenteric complex contains similar dense networks interspersed with more frequently occurring areas containing a few or no fibers. In the superior cervical ganglion a sparse network of thin fibers was present, but no cell bodies were immunoreactive.

VIP-immunofluorescence was generally much less intense in the rat ganglia and cell bodies were never labeled (Hokfelt et al., 1977b). In the IMG and the celiac-superior mesenteric ganglion plexus, a regular network of weakly fluorescent fibers was seen surrounding most of the ganglionic neurons. In the superior cervical ganglion, single varicose fibers were observed while the middle cervical ganglion showed no VIP-immunoreactivity.

8. Coexistence of Peptides and Noradrenaline

As seen above, APP-, SOM- and VIP-immunorecactive principal ganglion cell somata have been found in the prevertebral ganglia. Recently, the pattern of coexistence of the various peptides has been studied and the cells have been classified according to the presence or absence of specific peptide immunoreactivity (Lundberg et al., 1982).

In the guinea pig IMG, the principal ganglion cells have been categorized into four types according to peptide immunoreactivity (Lundberg et al., 1982). The first type of cell contains both somatostatin and noradrenaline. The second type of cell contains both APP and noradrenaline. These two types were found to be mutually exclusive in that APP- and SOM-immunoreactivity were never observed in the same neurons. The third type of cell contains only noradrenaline, showing no immunoreactivity to APP, SOM or VIP. The fourth type of cell is the singly occurring VIP-immunoreactive cell. This type was not labeled by antibodies to tyrosine hydroxylase or dopamine-β-hydroxylase and therefore is thought to contain VIP but not noradrenaline.

F. Tracing Pathways of the IMG

The physiological studies mentioned above provide evidence for a complicated system of pathways to and from the IMG. Additionally, the immunohistochemical findings suggest that neuropeptides are involved in neurotransmission in this ganglion. Anatomical studies on the connectivity of the IMG have recently been combined with peptide immunohistochemistry to further examine these pathways. These studies provide direct evidence for inputs to the IMG from a variety of sites and for

the presence of peptides in specific pathways of the ganglion. These findings also support the electrophysiological findings which suggest a neurotramsmitter function of peptides in this ganglion. All of the following studies have used the guinea pig IMG.

1. Application of HRP to the IMG

Following injection of horseradish peroxidase (HRP) into the IMG widely distributed labeled cell bodies were seen (Dalsgaard & Elfvin, 1982). In the celiac-superior mesenteric plexus labeled cells appeared singly or in small groups and were apparently distributed at random. HRP-labeled cell bodies were also observed in ganglia of the pelvic plexus at the most caudal end of the hypogastric nerves and usually occurred singly. A small number of HRP-positive cell bodies were also observed in the nodose ganglia. After injection of the fluorescent tracer True blue into the IMG, labeled cell bodies were also seen in the enteric nervous system and in the DRG. Some of the cell bodies of the ganglia in the myenteric plexus of the distal colon were clearly labeled. Also, in the submucus plexus an occasional fluorescent cell was seen.

2. Application of HRP to the Nerve Trunks

Following application of HRP to the severed ends of the hypogastric nerve, labeled cell bodies could be seen in the IMG, in the celiac-superior mesenteric plexus, in the spinal cord and also in the DRG (Dalsgaard & Elfvin, 1982). A number of randomly distributed postganglionic neurons were labeled in the IMG, while only a few labeled cells appeared in the celiac-superior mesenteric ganglia. Confirming the

physiological findings that a significant number of preganglionic fibers descend in the hypogastric nerve, sympathetic preganglionic cell bodies labeled with HRP were found in the nucleus intermediolateralis and nucleus intercalatus of the spinal cord.

When HRP was applied to the cut colonic nerves heavily labeled cells were seen in the IMG (Dalsgaard & Elfvin, 1982). Cells were also labeled in the caudal part of the superior mesenteric ganglion. Labeled axons could be detected in the ascending mesenteric nerve connecting the IMG with the superior mesenteric ganglion. Labeled cells could also be found in the DRG, but no cells filled with HRP were seen in the spinal cord.

HRP tracing studies have also shown that the connections of the IMG, the celiac and the superior mesenteric ganglia with the colon are different (Kreulen & Szurszewski, 1979b). When HRP was applied to the cut ends of the celiac nerves, which travel to the colon from the celiac ganglion, labeled cells were observed in the celiac ganglion, a few cells in the superior mesenteric ganglion, but no cells in the IMG were labeled. When applied to the colonic nerves, dense filling was observed throughout the IMG, in some cells in the superior mesenteric ganglion and very few in the celiac ganglion. This anatomical finding correlates with electrophysiological studies. A higher percentage of neurons in the rostral part of the celiac ganglion receive input from celiac nerves than from the ascending mesenteric nerves (Kreulen & Szurszewski, 1979a). In the IMG, however, the inputs are not patterned; cells in all parts of the IMG receive synaptic inputs from all of the associated nerve trunks (Crowcroft & Szurszewski, 1971).

3. Preganglionic Fibers to the IMG

The HRP technique has been used to study in detail the origin of the preganglionic fibers to the IMG (Dalsgaard & Elfvin, 1979). The sympathetic nuclei in the spinal cord include the nucleus intermediolateralis, the nucleus intercalatus and the nucleus intermediomedialis. After application of HRP to the guinea pig IMG, labeled preganglionic neurons were found in the intermediolateralis and intercalatus nuclei. The cells were located bilaterally in the spinal cord, in contrast to the superior cervical ganglia which receive fibers only from the ipsilateral cord. Labeled cells could be found from the level of T13 to L4. Only a few cells were seen at these limiting levels. In agreement with the physiological studies, the highest proportion of labeled cells were seen at L2 and L3.

4. Enkephalin-containing Preganglionic Neurons

As mentioned previously, a dense network of enkephalin-containing nerve terminals was found to surround the ganglion cells in the guinea pig IMG (Schultzberg et al., 1978, 1979). The origin of these fibers has been studied using a combination of retrograde tracing and immunohistochemistry.

Following incubation of slices from the L2 and L3 levels of the spinal cord with antibodies to enkephalin many fluorescent cell bodies were seen in the nuclei which contain the sympathetic preganglionic neurons (Dalsgaard, Hokfelt, Elfvin & Terenius, 1982b). Most of the enkephalin immunoreactive cells were in the nucleus intermediolateralis with a few in the nucleus intercalatus. These cells have been compared with

the labeling obtained following application of a retrogradely trans-ported dye to the IMG. About 40% of the cells which contained enkepah-lin were also found to be preganglionic to the IMG. Of the remaining cells some were labeled with enkephalin only and some with the tracer only. At the electron microscopic level numerous axo-axonic contacts were observed in the guinea pig IMG, as reported previously for the cat IMG (Elfvin, 1971b).

These results give strong evidence for the existence of enkepha-lin-containing preganglionic neurons originating in the L2 and L3 levels of the spinal sympathetic nuclei projecting to the IMG. Again, The ana-tomical findings correspond well to the physiological findings as enke-phalins have been shown to exert a presynaptic inhibitory effect on synaptic transmission in the IMG (Konishi et al., 1979a; Jiang et al., 1982b).

5. Substance P-containing Sensory Neurons

When HRP was applied to the IMG labeled cell bodies were also found in the DRG at the T13 to L5 levels (Elfvin & Dalsgaard, 1977). Labeled cells occurred in the L2 and L3 DRG in rather large numbers. A similar distribution of labeled cells in the DRG was seen following application of HRP to the cut ends of the hypogastric or colonic nerves. This indicates that the fibers of the DRG traverse the IMG, probably on a course to the viscera.

When the inferior splanchnic nerves were severed, there was a marked accumulation of SP-immunoreactive material in the central stumps of these nerves indicating that SP is being transported from cell bodies

central to the IMG (Matthews & Cuello, 1982). When combined with section of the ascending mesenteric nerve there was a complete loss of SP-immunoreactive fibers from the IMG. When the hypogastric or colonic nerves were sectioned the appearance of the SP network in the IMG did not change, but there was an accumulation of immunoreactivity in the ganglionic stumps of these nerves. Additionally, capsaicin treatment completely abolished the SP-immunoreactivity from the IMG. At the ultrastructural level using peroxidase-antiperoxidase immunohistochemistry SP-immunoreactivity was seen in vesicle-containing nerve varicosities in the IMG. Some of these fibers made synapses with dendrites in the ganglion and showed features typical of axo-dendritic synapses

In a further study, retrograde tracing was again combined with immunohistochemistry for the localization of substance P in the DRG (Dalsgaard, Hokfelt, Elfvin, Skirboll & Emson, 1982a). As seen following HRP transport, the fluorescent dye retrogradely transported from the IMG was seen in the cell bodies of the DRG, usually in singly occurring small cells, but occasionally in small groups. Incubation of the sections of the DRG with antisera to SP revealed the occurrence of small evenly distributed SP-labeled cells. Comparison of the retrogradely-labeled cells with the SP-immunoreactive cells revealed that some of the cells were labeled with both techniques. There were also DRG cells labeled by only one of the techniques.

Electrophysiological studies have demonstrated that SP is the probable mediator of the LS-EPSP in this ganglion and have suggested that the SP fibers are collaterals of primary sensory neurons (Dun & Jiang, 1982; Tsunoo et al., 1982). The anatomical studies combining

SP-immunohistochemistry and retrograde tracing strongly support this hypothesis.

6. Peptidergic Neurons from the Colon

In contrast to ENK and SP fibers which originate centrally to the IMG in the spinal cord and DRG, respectively, the other peptides which have been found in the IMG appear to have a peripheral origin, at least in the guinea pig IMG. These include BOM, CCK and VIP.

a. Bombesin

In the normal guinea pig a dense network of BOM-immunoreactive fibers was observed in the guinea pig IMG (Dalsgaard et al., 1983; Schultzberg, 1983). These fibers remained following section of the splanchnic, ascending mesenteric and hypogastric nerves, leaving the colonic nerves. When the colonic nerves were ligated BOM-immunoreactivity accumulated distal to the ligation. BOM fibers were not observed in the other nerves. These results indicated that the BOM fibers reach the IMG exclusively via the colonic nerves (Dalsgaard et al., 1983). These fibers may be involved in an afferent projection from the colon to the IMG since BOM-immunoreactivity has been observed in the gastrointestinal tract (Dockray, Vaillant & Walsh, 1979).

b. Cholecystokinin

The normally dense network of CCK-immunoreactive fibers in the guinea pig IMG disappears following complete denervation of this ganglion (Dalsgaard et al., 1983). Similar to the case with BOM, cutting all the nerves except the colonic nerves revealed a pattern of CCK

fibers similar to that seen in the normal animals. Ligation of the colonic nerves resulted in an accumulation of CCK-immunoreactivity distally. Although a few CCK fibers were found in the other nerves, CCK fibers to the IMG travel mainly in the colonic nerves. CCK-immunoreactive cell bodies have been found in the gastrointestinal tract (Schultzberg, Hokfelt, Nilsson, Terenius, Rehfeld, Brown, Elde, Goldstein & Said, 1980) and may project from the colon to the IMG.

c. Vasoactive Intestinal Polypeptide

The VIP fibers appear to take several routes to the IMG. The major supply of VIP fibers was found to travel in the hypogastric and colonic nerves. Some VIP fibers also enter via the ascending mesenteric nerve and a few via the inferior splanchnic nerves. When the colonic or hypogastric nerves were ligated a heavy accumulation of immunoreactivity was seen distal to the ligature, with a small amount seen proximally. In the ascending mesenteric nerve there was accumulation on both sides of the ligature and in the inferior splanchnic nerves the accumulation was proximal to the IMG (Dalsgaard et al., 1983). Thus, the VIP fibers reach the ganglion through several different pathways. Most fibers originate in the distal colon, suggesting yet another peptidegic afferent pathway from the colon to the IMG. Some neurons must also enter through the hypogastric nerve; these probably originate from VIP cells in the pelvic plexus. The fibers entering in the ascending mesenteric nerve may originate in the celiac-superior mesenteric ganglion since VIP-containing cells have been described there (Hokfelt et al., 1977b).

The above data have led to an evolution in our concept of the function of the IMG. These studies have shown that, at least in the guinea pig, the IMG consists of a sophisticated neural network involved in the integration of both central and peripheral neural inputs. Some postsynaptic potentials in the IMG are mediated (in the case of SP) or modulated (in the case of ENK) by peptides in addition to the "classical" transmitter, ACh.

II. SPECIFIC AIMS

The subject of this dissertation is the examination of synaptic transmission in the inferior mesenteric ganglion of the rabbit. The hypotheses tested are:

1. Are the basic electrical properties of the neurons in the rabbit IMG similar to those of cells contained in other sympathetic ganglia? This will be examined with intracellular recordings from the IMG in vitro. The passive electrical properties to be measured include: resting membrane potential, membrane time constant and membrane voltage-current relations. Active properties of the cells which will be examined include: action potential threshold, amplitude and duration, and afterhyperpolarization amplitude, half-decay time and duration. Somatic action potentials will be elicited by direct intracellular current injection (direct spike) or by electrical stimulation of the cell axon (antidromic spike).

2. Do rabbit IMG neurons resemble cells in the guinea pig IMG with regard to nicotinic cholinergic inputs? To answer this question the properties of the F-EPSP will be examined. The action potential elicited by suprathreshold presynaptic stimulation (orthodromic spike) will be characterized according to the criteria used for the direct and antidromic action potentials described

61

above. Additionally, the synaptic potentials following stimulation of the various nerve trunks associated with the ganglion will be examined to determine the number of inputs received by a single cell in the rabbit IMG.

3. Does a late slow excitatory postsynaptic potential occur in the neurons of the rabbit IMG? To test this, the responses of the cells to repetitive presynaptic stimulation will be examined in the presence of cholinergic antagonists. The slow response will be characterized as to its amplitude, time course and accompanying input resistance changes. Also, the dependence of the response on the frequency and duration of stimulation will be determined.

4. Is the LS-EPSP in the rabbit IMG mediated by substance P, as is apparently the case in the guinea pig IMG? Immunohistochemical and pharmacological techniques will be combined to test this hypothesis. To examine the involvement of certain putative transmitters in this response, SP and several other substances will be applied during intracellular recordings to determine if they mimic or antagonize the LS-EPSP. Lastly, the presence of SP and other neuropeptides in neural structures within the rabbit IMG will be examined by immunohistochemistry.

III. METHODS

White rabbits (male, 1.5-2.0 kg) were used for both electrophy-
siological (Purves, 1981) and immunohistochemical (Sternberger, 1979)
experiments.

A. Electrophysiological Studies

1. Dissection of the IMG and Associated Nerve Trunks

The rabbits were sacrificed by cervical dislocation, the abdomen
immediately opened and the intestines moved to the animal's left side,
thus exposing the posterior wall of the abdomen. Thereafter, the dis-
section was conducted under a dissecting microscope. The inferior mes-
enteric artery is easily located as it exits the aorta. The IMG is seen
about a centimeter along this artery.

The peritoneum overlying the ganglion and associated nerve trunks
was first cut. Next, the nerve trunks were carefully isolated. The
aortic branch of the ascending mesenteric nerve extends rostrally from
the IMG and was isolated most easily. The main portion of the ascending
mesenteric nerve exits laterally from the IMG and travels along the
ascending mesenteric vein; therefore, this nerve trunk had to be care-
fully stripped from the associated vascular tissue. Isolation of the
hypogastric nerve required clamping of the inferior mesenteric artery
which passes through the caudal part of the ganglionic tissue. Follow-

ing isolation of the various nerve trunks, the ganglion was freed of connective tissue and removed from the animal. During the dissection oxygenated Krebs solution was applied to the ganglion and surrounding structures.

After excision, the IMG was placed in a beaker containing Krebs solution and transferred to the recording chamber. This chamber (0.5 ml capacity) consisted of a plexiglass bath lined with Sylgard. The ganglion was secured in the bath by pins inserted through the edge of the ganglion or through the connective tissue surrounding the ganglion, with care being taken not to damage the entering nerves. Connective tissue was removed as thoroughly as possible from the ganglion and the nerve trunks. The distal ends of the nerve trunks were ligated and pulled into glass capillary tubes. Silver wire electrodes were inserted into these tubes for electrical stimulation of the nerve trunks. The ganglion was constantly perfused with a modified Krebs-bicarbonate buffer (117 mM NaCl; 4.7 mM KCl; 1.2 mM MgCl; 1.2 mM Na H_2PO4; 2.5 mM $CaCl_2$; 25 mM $NaHCO_3$; 11.5 mM glucose; gassed with 95% O_2/5% CO_2) at 36-37°C. The flow rate was approximately 2.5 ml/min. All drugs were dissolved in this solution and applied by superfusion. The drugs used and the sources of each are listed in Table 1.

2. Intracellular Recordings

The electrodes used for intracellular recording consisted of glass capillary tubing of 1.0 or 1.2 mm outer diameter, with extruded fiber, pulled to give a resistance of 30-60 MΩ when filled with 3M KCl. Electrodes of this type typically have outer tip diameters of < 0.5 μm

TABLE 1

DRUGS USED IN THE PRESENT STUDIES
AND THEIR SOURCES

Drug	Source
Atropine sulfate	Sigma
Capsaicin	Sigma
Dihydroergotamine tartrate	Sigma
5-Hydroxytryptamine creatinine sulfate	Sigma
Luteinizing hormone releasing hormone	Bachem, Peninsula
$(D-p-Glu^1, D-Phe^2, D-Trp^3, ^6)$ − Luteinizing hormone releasing hormone	Peninsula
Norepinephrine hydrochloride	Sigma
Substance P	Bachem, Peninsula, Sigma
$(D-Arg^1, D-Pro^2, D-Trp^7, ^9, Leu^{11})$ − Substance P	Dr. S. Rosell
$(D-Pro^2, D-Phe^7, D-Trp^9)$ − Substance P	Peninsula
d-Tubocurarine chloride	Sigma
Vasoactive intestinal polypeptide (porcine)	Bachem, Peninsula

(Purves, 1981). The electrodes were back-filled with 3M KCl. Potentials were recorded using a WPI Model M-701 electrometer which contains active bridge circuitry for injecting current through the microelectrode. The outputs of the M-701 were connected to a dual beam oscilloscope (Tektronix Type 502A) for the simultaneous display of recorded potentials and monitor of applied current. A camera attached to the oscilloscope provided permanent records of "fast" electrical events. Output was also displayed on a Gould Brush pen recorder (Model 2200). In figures reproduced from the pen recorder tracings the action potential amplitude is attenuated due to the frequency response of the recorder. A Grass stimulator (Model S-8) was used for the injection of intracellular current and another for stimulation of the nerve trunks.

a. Impalement of a Principal Ganglionic Neuron

To obtain a successful impalement of a ganglion cell, the electrode was moved slowly through the ganglion under manual control with the micromanipulator. Ganglion cells were impaled by staccato tapping on the micromanipulator or by overcompensation of the negative capacity adjustment to oscillation (Baylor, Fuortes & O'Bryan, 1971). Upon impalement a sudden potential change of -40 mV to -60 mV was observed. A successful impalement was confirmed by observing the electrotonic potential following the passage of anodal current pulses and the action potential following cathodal pulses. A cell was considered suitable for study if it had a rapidly rising action potential > 50 mV in amplitude. Data collection was begun after allowing sufficient time for the cell to stabilize.

b. Statistical Analyses

All values are expressed as the mean ± standard error of the mean.
Data comparisons of ratio level data were made using the t-test when
comparing two groups of data and analysis of variance followed by Dun-
can's multiple range test for comparisons involving more than two
groups. For nominal level data a X^2 test was used. A level of signifi-
cance of 0.05 was chosen. All statistical analyses were performed using
the Statistical Analysis System (SAS) computer program.

B. Immunohistochemical Studies

The immunohistochemical procedure involves five basic steps: 1)
fixation of the tissue, 2) sectioning of the tissue, 3) incubation with
primary antiserum, 4) incubation with labeled antibodies and 5) micro-
scopic examination of the stained tissue. The buffers used in these
experiments are listed in Table 2.

Two different immunostaining procedures were used. The first
technique involved the use of a fluorescein isothiocyanate labeled sec-
ondary antibody; this is the FITC technique. In the second procedure a
biotinylated secondary antibody was used followed by an avi-
din:biotinylated horseradish peroxidase complex; this is the ABC techni-
que.

TABLE 2

BUFFERS USED IN THE IMMUNOHISTOCHEMICAL EXPERIMENTS

Solution	Composition
Ca^{++}-free Tyrode's	116 mM NaCl; 5.4 mM KCl; 1.6 mM $MgCl_2$; 0.4 mM $MgSO_4$; 1.2 mM NaH_2PO_4; 5.6 mM Glucose; 26.2 mM $NaHCO_3$
Fixative	0.05 M NaH_2PO ; 0.05 M Na_2HPO_4; + 4% paraformaldehyde or 0.4% ρ-benzoquinone
Sorenson's	0.03 M KH_2PO_4; 0.07 M Na_2HPO_4
Phosphate Buffered Saline	0.05 M Na_2HPO_4; 0.14 M NaCl
Tris Buffered Saline	0.05 M Trizma-7.6; 0.15 M NaCl

1. Fixation of Tissue

a. Transcardial Perfusion

Rabbits were anesthetized with pentobarbital (35 mg/kg i.p.), the chest opened and a perfusion cannula inserted through the left ventricle into the aorta. The animal was first perfused with 500 ml ice cold Ca^{++}-free Tyrode's solution followed by 1-2 L of ice cold fixative (4% paraformaldehyde in sodium phosphate buffer). The IMG was then removed, placed in a refrigerator in fixative for 90 min and then transferred to Sorenson's buffer containing 5% or 10% sucrose for at least 12 hr before sectioning.

b. Post-fixation

Following dissection of the IMG or following an electrophysiological experiment the IMG was placed directly into the fixative (either 4% paraformaldehyde or 0.4% p-benzoquinone in sodium phosphate buffer) and left overnight in the refrigerator. The following day the IMG was transferred to Sorenson's buffer containing 5% or 10% sucrose and left for at least 12 hr prior to sectioning.

2. Sectioning of Tissue

The IMG was sliced into thin sections (15 um) on a cryostat-microtome at -20°C. The sections were thaw-mounted onto gelatinized microscope slides. The mounted sections were then warmed to room temperature for 20 min and rehydrated in phosphate buffered saline (PBS) or Tris buffered saline (TBS).

3. Incubation with the Primary Antibody

After rehydration, the sections were incubated with the primary antibody. The primary antibody uses as its antigen the substance to be localized. These antibodies were diluted in 0.3% Triton X-100 in PBS and applied to the microscope slides. For the FITC-labeling the sections were incubated overnight at 4°C. For the ABC technique the sections were incubated 60 min at room temperature. All primary antibodies were raised in rabbits and obtained from ImmunoNuclear Corporation.

4. Incubation with the Labeled Antibodies

After blotting off the primary antibody and rinsing the sections for 20 min in buffer, the secondary antibody was applied for 30 min at room temperature. For immunofluorescence this consisted of FITC-labeled goat anti-rabbit IgG applied for 30 min at room temperature. These sections were then mounted in PBS:glycerin (1:3) and examined under a fluorescence microscope.

For the ABC technique the secondary antibody was biotinylated goat anti-rabbit IgG. Following another rinse, an avidin:biotinylated horseradish peroxidase complex was applied. Avidin has an extremely high affinity for biotin and the binding of avidin to biotin is practically irreversible; thus, avidin serves to link the biotinylated secondary antibody and the biotinylated horseradish peroxidase complex. This complex was applied for one hour. Following another rinse, the sections were reacted with diaminobenzidine (DAB) solution. DAB is oxidized by horseradish peroxidase to form a brown precipitate thus revealing the localization of the antigen of interest. The sections were then dehydrated, coverslipped and examined under a light microscope.

5. Controls for Labeling Specificity

Immunohistochemical results must be interpreted with caution since antisera may react not only with the antigen against which they were raised but also with structurally related compounds, e. g. precursors of the antigen. For this reason, immunohistochemical results are discussed in terms of "immunoreactivity" or "like-immunoreactivity" (Hokfelt, Lundberg, Schultzberg, Johansson, Skirboll, Anggard, Fredholm, Hamberger, Pernow, Rehfeld & Goldstein, 1980). This also emphasizes the need for proper controls with immunohistochemical studies.

There are two types of immunohistochemical controls termed first level controls and second level controls (Larsson, 1981). First level controls examine the specificity of the interaction between the primary antibody and the tissue antigen. Second level controls are used to evaluate the quality of the tissue and to evaluate the detection system. For the first level controls, or preabsorption controls, the primary antibodies at working dilutions were incubated overnight at $4^{\circ}C$ with 1 µg/ml of the antigen. The primary antibody should combine with the antigen during this incubation, making its binding sites unavailable for combination with the antigen in the tissue.

The second level controls, which involve the omission of antibodies at various stages, were particularly important in these studies since all of the primary antibodies used were raised in rabbits. It was necessary, therefore, to use an anti-rabbit IgG secondary antibody, for example, goat anti-rabbit IgG. Thus, an anti-rabbit antibody was being applied to a rabbit peripheral tissue. Consequently, it was expected

that problems might occur with unwanted binding of the secondary anti-
body. The original studies using an FITC-labeled goat anti-rabbit IgG
secondary antibody revealed a high degree of background fluorescence in
the rabbit IMG, but not in rabbit brain sections, in the absence of a
primary antibody. These results indicated that, in addition to binding
to the primary antibody, the FITC-labeled secondary antibody was binding
to rabbit IgGs present in this peripheral tissue, but not in the central
nervous system which is less accessible to IgGs. The procedure chosen
to decrease this background staining was to pre-treat the IMG sections
with a solution of 1 volume $KMnO_4$ (2.5%) and 1 volume H_2SO_4 (5%) in
50-100 volumes H_2O before applying the primary antibody. This treatment
has been used to elute antibodies from immunohistochemically stained
sections in double-labeling experiments (Tramu, Pillez & Leonardelli,
1978). It was found that this treatment resulted in a marked decrease
in background fluorescence. The other second level control with the
FITC technique was omission of the secondary antibody, which gave blank
specimens. With the ABC technique, a similar problem was encountered;
however, the biotinylated goat anti-rabbit IgG secondary antibody can be
applied at a much lower concentration with this technique. Here, the
background staining was much less intense, leaving the stained nerve
fibers more clearly visible. Other second level controls for the ABC
technique were omission of the secondary antibody, omission of the ABC
complex, omission of the DAB step and omission of all antibodies.

IV. RESULTS

A. Anatomy

The rabbit IMG is an elliptoid ganglion located just rostral to or surrounding the inferior mesenteric artery, peripheral to the exit of this artery from the abdominal aorta (Figure 1). The ganglion may be up to 1 cm in length and 2 mm thick at its widest point. Frequently, two clusters of ganglion cells are seen, with the major part of the IMG superior to the inferior mesenteric artery connected by nerve strands with a smaller accessory ganglion inferior to the artery. At other times, the accessory part of the IMG is indistinguishable and the IMG appears as a continuous ring of tissue surrounding the inferior mesenteric artery.

The large number of nerves in the vicinity of the IMG form a frequently intermingling plexus of fibers. Some of these fibers enter or exit the IMG. The major nerve trunks of the ganglion are the ascending mesenteric nerve, the aortic branch of the ascending mesenteric nerve, the hypogastric nerve and the inferior splanchnic nerves.

As it exits the IMG, the ascending mesenteric nerve is not a single nerve, but consists of several groups of fibers which leave the IMG laterally and join to course rostrally along the inferior mesenteric vein. Some of these fibers can be followed to the superior mesenteric-

FIGURE 1.   Anatomical arrangement of the inferior mesenteric ganglion

and surrounding structures.

AB - Aortic branch of the ascending mesenteric nerve; AMN -

Ascending mesenteric nerve; AP - Accessory part of the inferior

mesenteric ganglion; HGN - Hypogastric nerve; IMA - Inferior

mesenteric artery; IMG - Inferior mesenteric ganglion; IMV -

Inferior mesenteric vein; ISN - Inferior splanchnic nerves.

FIGURE 1
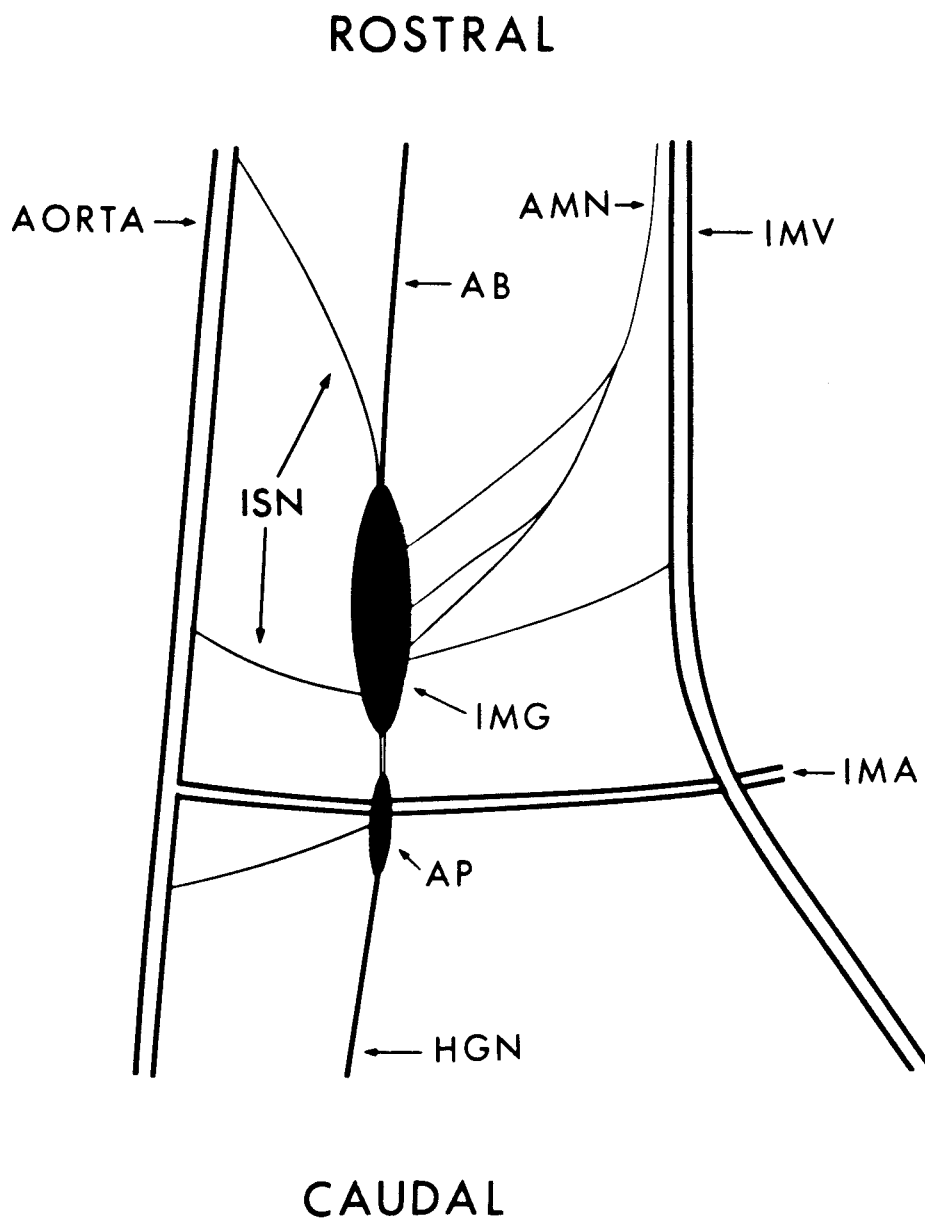
celiac ganglion plexus while others travel along the vasculature toward the colon. The aortic branch of the ascending mesenteric nerve exits the rostral pole of the IMG and also travels toward the superior mesenteric-celiac plexus. The hypogastric nerve exits the caudal pole of the IMG or the accessory part of the IMG, if present, and travels toward the hypogastric-pelvic plexus. The inferior splanchnic nerves include one to three very fine and delicate branches which enter the medial side of the IMG. These nerves contain the classical preganglionic sympathetic fibers. Frequently, one of the inferior splanchnic nerves joins the aortic branch of the ascending mesenteric nerve to enter the rostral pole of the ganglion. Other fibers from the IMG travel peripherally along the inferior mesenteric artery to innervate the colon. These are apparently comparable to the colonic nerves in the guinea pig and are much less prominent in the rabbit than in other species.

B. Passive Membrane Properties

Several measurements were made to characterize the basic electrical properties of IMG neurons. The passive membrane properties examined include E_r, R_{in} and membrane time constant (τ_m). These electrical properties are listed and compared to the properties of other sympathetic ganglion cells in Table 3.

Membrane potential was measured as the potential change occurring upon removal of the recording electrode from the cell. The average E_r of the rabbit IMG cells was found to be -49 ± 1 mV (n=71) ranging from -35 to -70 mV. These values do not appear to differ from the E_r

TABLE 3

BASIC MEMBRANE ELECTRICAL PROPERTIES OF RABBIT IMG CELLS

COMPARED WITH THE PROPERTIES OF OTHER SYMPATHETIC GANGLION CELLS

	Rabbit IMG			Rabbit SCG	Guinea Pig IMG	Guinea Pig SCG	Cat IMG	Frog Paravertebral
	$\bar{x}$ ± S.E.M.	Range	n					
Resting Membrane Potential (mV)	-49 ± 1	-35 to -70	71	-55[7]	-52[6]	-45 to -90[4]	-52[8]	-65 [1]
Input Resistance (MΩ)	37 ± 2	8 to 160	129	40[7]	40 to 150[5]	41[4]	46[8]	20 [1]
Membrane Time Constant (ms)	8 ± 1	2 to 21	29	10.5[7]		4.4[4]		10.6[1]
Threshold Depolarization (mV)	12 ± 1	7 to 25	21	20[3]	10 to 20[5]	17[4]	5 to 18[8]	25 [1]
Rheobase (nA)	0.2 ± 0.03	0.05 to 0.35	12	0.22[3]		0.11[4]		0.31[2]
Chronaxie (ms)	13 ± 3	0.6 to 35	12			8.4[4]		
Maximum Frequency of Firing (Hz)	66 ± 8	50 to 100	6		150 to 170[5]			80[2]

1. Nishi & Koketsu, 1960
2. Hunt & Riker, 1966
3. Erulkar & Woodward, 1968
4. Perri, Sacchi & Casella, 1970
5. Crowcroft & Szurszewski, 1971
6. Szurszewski & Weems, 1978
7. Wallis & North, 1978
8. Krier, Schmalz & Szurszewski, 1982

reported in other studies on mammalian sympathetic neurons, but the mean is somewhat less than the value reported in the bullfrog (Table 3). The frequency distribution of the observed E_r is plotted in Figure 2. On the basis of this distribution the cells in the rabbit IMG are of a single type.

The measurement of R_{in} was calculated using Ohm's law: $R_{in} = V / I$, where I = the current applied through the electrode in nA, V = the resultant potential change in mV and R_{in} = the calculated input resistance in MΩ. The pulses were of sufficient duration for the potential change to reach a steady state. While monitoring R_{in} on the pen recorder 200 msec pulses were commonly used; this is well within the frequency response of the recorder. In some cells a series of current pulses of various amplitudes was applied to construct a voltage-current curve for the cell to reveal the dependence of R_{in} on E_m. The voltage-current relationship of a typical rabbit IMG neuron is shown in Figure 3. The slope resistance of this cell was 42 MΩ. This cell did not show a decrease in resistance, i. e. anomalous rectification, in the voltage range to 40 mV more negative than E_r, as was found to be typical of the rabbit IMG cells; however, in some of the cells examined beyond this level, the slope resistance did decrease. Delayed rectification was evident with depolarizing pulses. Since the voltage-current curves revealed little rectification of the membrane in the range of 0-30 mV more negative than E_r, in most experiments R_{in} was calculated from the application of a single current intensity ranging from 0.1-0.25 nA in

FIGURE 2. Frequency distribution of resting membrane potentials.

Each bar represents the number of cells with resting membrane

potentials falling within 5 mV intervals. The midpoints of the

intervals are labeled from -40 to -65 mV.

FIGURE 2
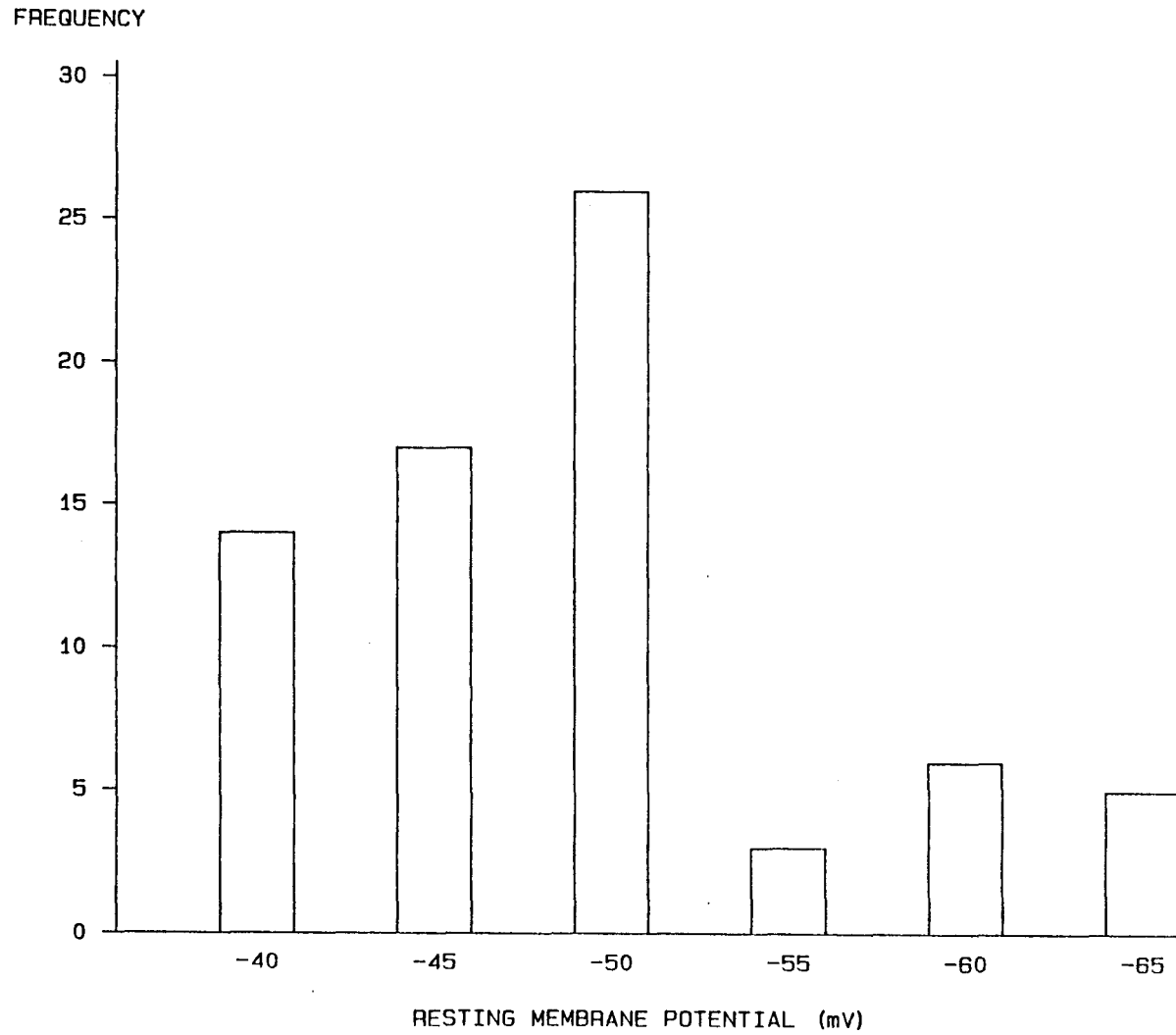
FIGURE 3. Voltage-current relationship of an IMG neuron.

A: Oscilloscope record. Top - Current pulses injected into the cell. Bottom - Resultant electrotonic potentials of the cell. Horizontal Calibration - 20 msec, Vertical Calibration - 1 nA (top), 10 mV (bottom). B: Voltage-current plot of the data obtained from the record in A. The line is the least squares regression line through the filled circles (r^2=.99). The open circles represent the steady-state voltage change for the depolarizing pulses.
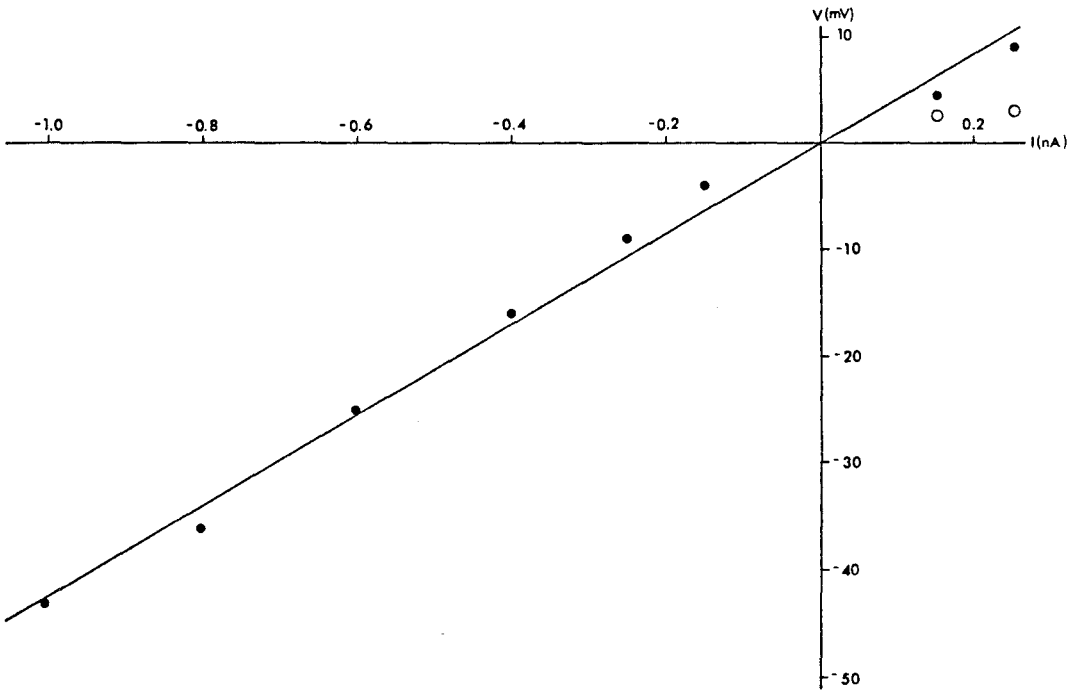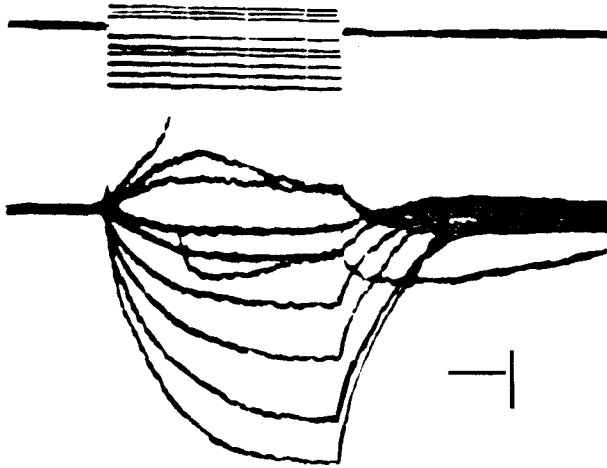
FIGURE 3

various cells. Once again, a unimodal distribution is obtained when the frequency distribution of the observed R_{in} is plotted (Figure 4). The mean R_{in} of 129 cells was 37 ± 2 MΩ, which is similar to the reported R_{in} of other sympathetic ganglion cells (Table 3).

Using the oscilloscope records, τ_m was calculated as the time in msec required for the anelectrotonic potential to reach $1-1/e$ (63%) of its maximum value. Figure 5 shows the frequency distribution of the recorded τ_m which ranged from 2 to 21 msec with a mean of 8 msec.

C. Active Membrane Electrical Properties

Active membrane properties measured include threshold for the initiation of action potentials, rheobase, chronaxie, action potential amplitude and duration, and amplitude, duration and half decay time of the action potential afterhyperpolarization.

An average depolarization of 12 mV from E_r was needed in the rabbit IMG neurons to reach the threshold for action potential initiation. This value is consistent with that reported elsewhere (Table 3). A frequency distribution of the thresholds is plotted in Figure 6. The threshold was similar following either direct intracellular stimulation or following orthodromic activation of the cells. The rheobase is the threshold stimulus intensity for a long current pulse. The rheobase for these cells was 0.2 nA. At twice this current, the chronaxie, a pulse of 13 msec duration was required to reach threshold. With long, high intensity current pulses these cells fired repetitive action potentials at a frequency up to 100 Hz. Usually, the firing rate was higher at the beginning of the pulse and then slowed to a steady rate. The cells did not show accommodation to pulses up to 200 msec duration.

FIGURE 4.   Frequency distribution of input resistances.

Each bar represents the number of cells with input resistances

falling within the 5 MΩ intervals.   The midpoints of the

intervals are labeled from 15 to 70 MΩ.
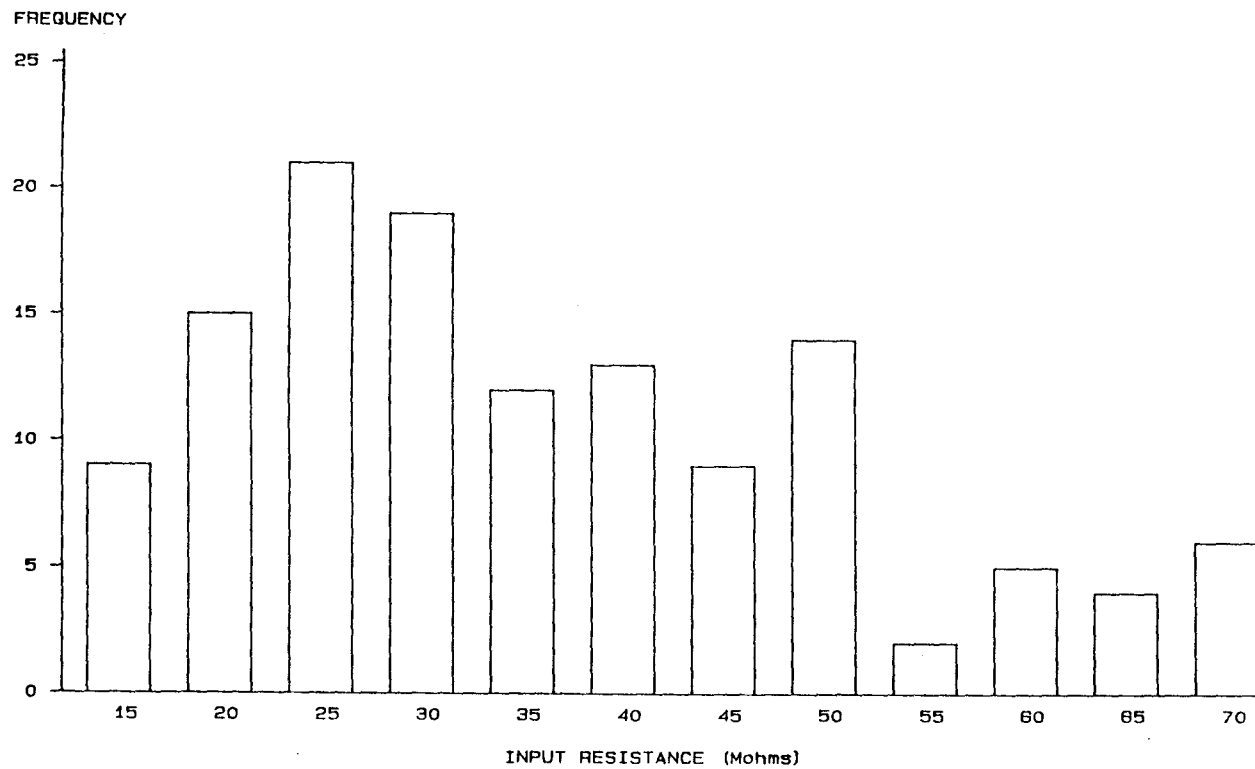
FIGURE 4

FIGURE 5. Frequency distribution of membrane time constants.

Each bar represents the number of cells with membrane time

constants falling within the 3 msec intervals. The midpoints of

the intervals are labeled from 3 to 18 msec.

FIGURE 5
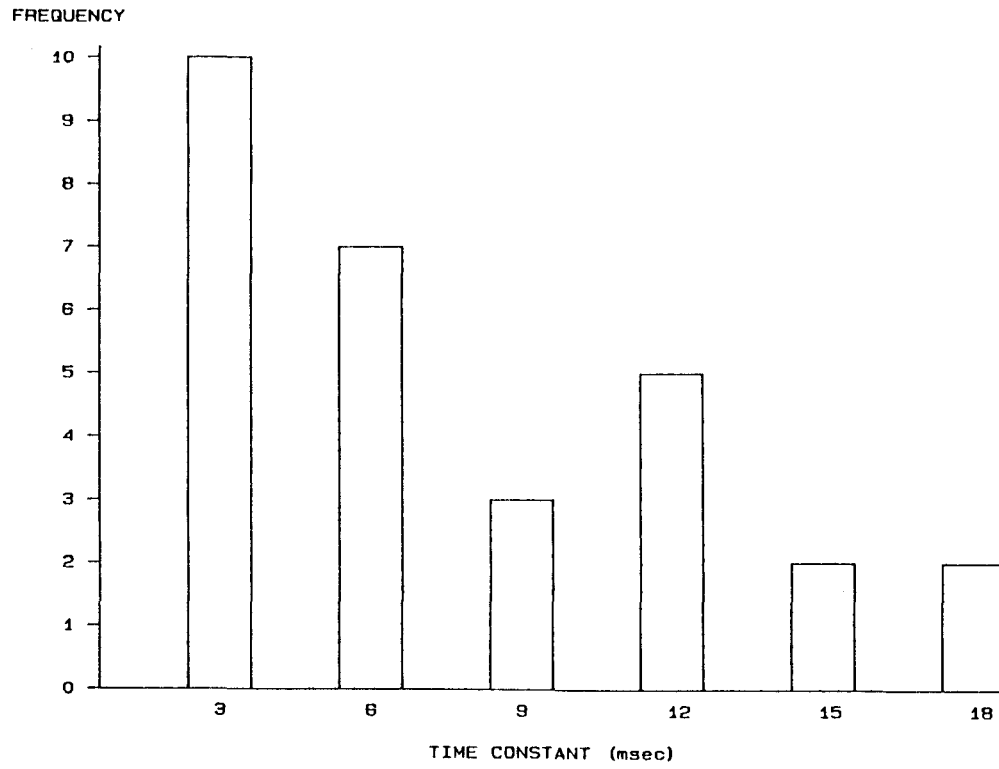
FIGURE 6. Frequency distribution of thresholds for the action

potential.

Each bar represents the number of cells with thresholds falling

within the 2 mV intervals. The midpoints of the intervals are

labeled from 8 to 16 mV.

FIGURE 6
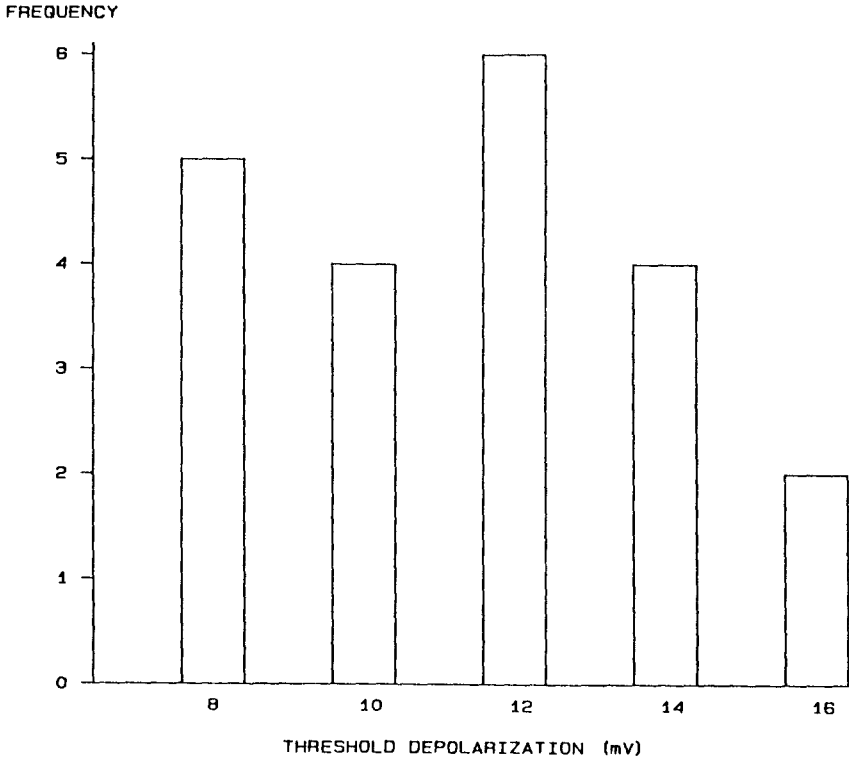
The action potential in the rabbit IMG cells was studied following

either direct intracellular stimulation with short cathodal pulses,

antidromic stimulation or orthodromic stimulation. The characteristics

of the action potential following each of these stimuli is shown in

Table 4. An antidromic spike was rarely seen in these cells. Of a

total of 204 cells, only 8 exhibited an antidromic spike. The action

potential amplitude was about 65 mV. With an E_r of -50 mV this gives an

overshoot of 15 mV. Action potential duration averaged about 4 msec.

The spike was followed by an afterhyperpolarization of 11 mV with a

duration of 250 msec. Analysis of variance followed by Duncan's

multiple range test showed that the characteristics of the direct,

antidromic and synaptic spikes were not significantly different. Since

several studies in other sympathetic ganglia have reported the

orthodromic spike to be smaller than the direct spike, a paired t-test

was performed on spike amplitude for those cells in which both

orthodromic and direct spikes were measured. This test revealed that

there was no difference between the orthodromic and direct spike

amplitude in rabbit IMG neurons.

The afterhyperpolarization following the action potential returned

to E_r in a biphasic manner, with an initial rapid decay followed by a

slower, long-lasting phase. Two K^+ conductances have been shown to

contribute to the repolarizing phase of the action potential: a voltage-

dependent G_K and a Ca^{++}-activated G_K. It was hypothesized that the

biphasic slope and long duration of the afterhyperpolarization may be

TABLE 4

CHARACTERISTICS OF THE DIRECT, ANTIDROMIC
AND ORTHODROMIC ACTION POTENTIALS IN RABBIT IMG CELLS

	Direct			Antidromic			Orthodromic		
Amplitude (mV)	65	± 3	(19)	68	± 3	(7)	63	± 3	(10)
Duration (msec)	4.2	± 0.4	(14)	3.4	± 0.3	(7)	4.3	± 0.6	(7)
After hyperpolarization – Amplitude (mV)	10	± 0.6	(22)	12	± 0.3	(7)	11	± 0.8	(10)
Duration (msec)	248	± 18	(13)	253	± 19	(5)	288	± 18	(7)
Half Decay Time (msec)	89	± 11	(20)	73	± 20	(6)	126	± 14	(10)

Values are mean ± S.E.M.

n   in parentheses

due to a Ca^{++}-activated G_K, as has been shown in a variety of other neurons including sympathetic postganglionic neurons (Meech, 1978). Figure 7B shows an antidromic reponse in normal Krebs and in low Ca^{++} Krebs. The latter part of the decay of the afterhyperpolarization becomes shortened and, as seen in the inset, the amplitude of the afterhyperpolarization is decreased in a low Ca^{++} solution.

D. Fast Excitatory Postsynaptic Potential

Synaptic responses were elicited by stimulation of the nerve trunks entering the IMG. Several observations were made on the F-EPSPs in these cells.

1. Characteristics of the F-EPSP

The amplitudes of the F-EPSPs varied from a few mV to threshold. Because these cells receive a large number of nicotinic cholinergic inputs, it was frequently difficult to elicit a single F-EPSP. These data are for those cells where it was possible with low intensity pre-ganglionic pulses to elicit what appeared to be a single F-EPSP. The F-EPSP reached its maximum amplitude in 7 ± 0.6 msec (n=11) and lasted 42 ± 3 msec (n=10). The time required for the F-EPSP to decay from peak amplitude to 37% (1/e) of this peak was calculated for comparison to τ_m. The time constant of decay of the F-EPSP was 18 ± 2 msec (n = 11). In these 11 cells τ_m averaged 9 msec. A paired t-test revealed the time constant of decay of the F-EPSP was significantly longer (p < 0.0001) than the membrane time constant.

FIGURE 7.   Effects of low Ca^{++}/high Mg^{++} solution on the orthodromic and
antidromic responses in a rabbit IMG neuron.

A: Top - Orthodromic response following stimulation of the
aortic branch of the ascending mesenteric nerve. Bottom - The
orthodromic reponse is abolished in low Ca^{++}/high Mg^{++} Krebs
solution. Horizontal Calibration - 10 msec, Vertical Calibration
- 10 mV. B: Top - Antidromic response in the same cell
following stimulation of the ascending mesenteric nerve. Note
the long time course and biphasic shape of the spike
afterhyperpolarization. Bottom - In low Ca^{++}/high Mg^{++} Krebs
solution an antidromic spike is still present, but the
afterhyperpolarization is shortened and its biphasic shape is no
longer evident. Horizontal Calibration - 50 msec, Vertical
Calibration - 10 mV. Inset - The antidromic response at higher
sweep speed in normal Krebs solution (1) and in low Ca^{++}/high
Mg^{++} solution (2). The lowering of Ca^{++} results in a decreased
amplitude of the afterhyperpolarization. Horizontal Calibration
- 5 msec, Vertical Calibration - 10 mV.

FIGURE 7
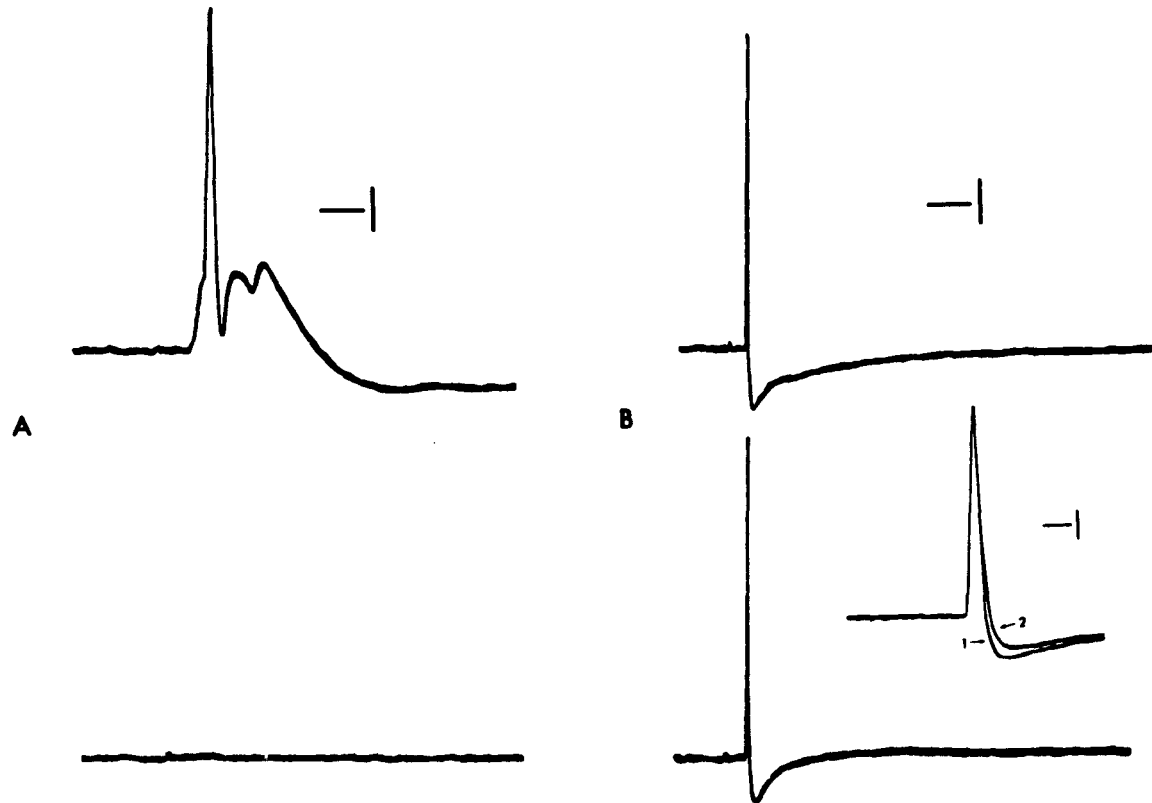
2. Blockade by d-Tubocurarine

The F-EPSP recorded from postganglionic sympathetic neurons has been shown to be generated by the action of ACh on nicotinic receptors of the postganglionic cell membrane of a number of species (Blackman, Ginsborg & Ray, 1963; Eccles, 1963; Nishi, 1974; Kuba & Koketsu, 1978). To test the hypothesis that the F-EPSP in rabbit IMG cells was similar to that in other sympathetic ganglia, d-TC was applied to 20 ganglion cells. As demonstrated by Figure 8, the F-EPSP in the rabbit IMG is blocked by this nicotinic receptor antagonist. In this experiment an antidromic spike followed by a F-EPSP on the afterhyperpolarization of the antidromic action potential were recorded using a digital waveform storage module of the pen recorder. The initial part of each panel shows the electrotonic pulses that were elicited by hyperpolarizing current pulses in order to monitor R_{in}. This is followed by the antidromic spike and F-EPSP at high sweep speed. The application of d-TC (50 μM) first decreased (Figure 8B) and then completely antagonized (Figure 8C) the F-EPSP while not affecting E_m, R_{in} or the antidromic response.

3. Blockade in low Ca^{++} solution

Low Ca^{++} also effectively and reversibly abolished the F-EPSP. Figure 7A shows a F-EPSP elicited by stimulation of the ascending mesenteric nerve. The top panel shows the response in normal Krebs solution. Following perfusion with low Ca^{++} Krebs, the F-EPSP is completely blocked, but an antidromic response can still be elicited (Figure 7B).

FIGURE 8.   Effects of d-tubocurarine on the fast excitatory postsynaptic

potential.

The initial part of each tracing shows membrane potential and

electrotonic potentials elicited by hyperpolarizing current

pulses (lower tracing). This is followed by an antidromic spike

and a F-EPSP superimposed on the spike afterhyperpolarization.

A: Control response. B: Response after 4 min in Krebs

containing d-tubocurarine (50 µM). The F-EPSP is attenuated

while E_m, R_{in} and the antidromic spike are unaffected. C: After

8 min in d-tubocurarine the F-EPSP is abolished. Horizontal

calibration - 20 sec for the initial part of each record, 5 msec

for the latter part of each record, Vertical calibration - 10 mv

(upper tracing), 0.5 nA (lower tracing).

FIGURE 8
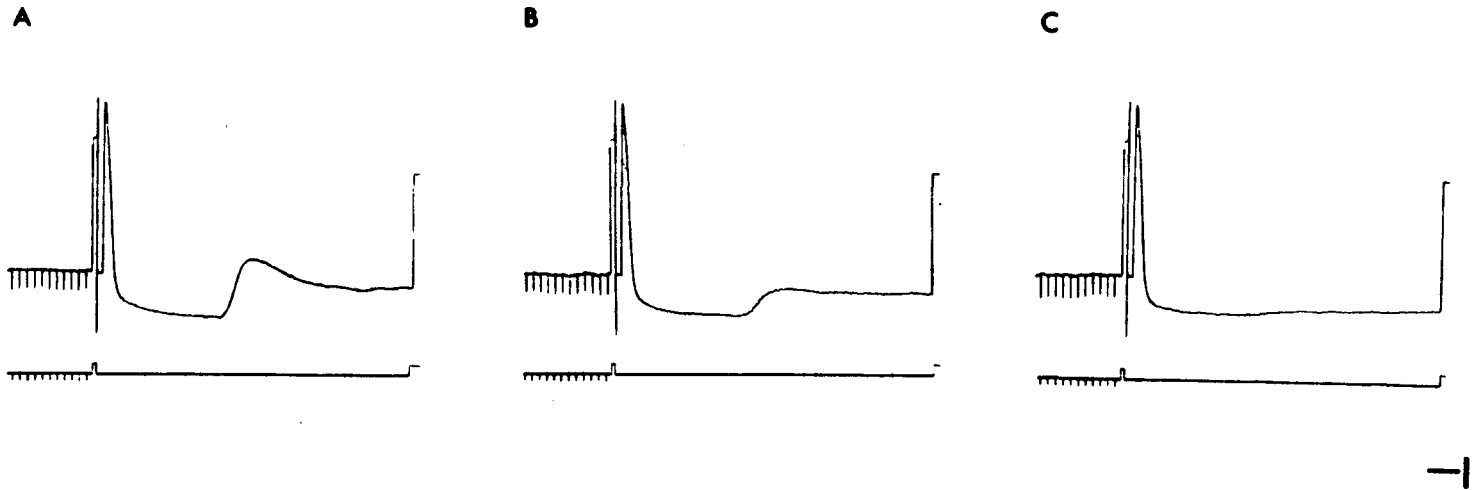
4. Number of Inputs

The fast synaptic inputs to cells in the guinea pig IMG are more complicated than the input to cells in the paravertebral sympathetic ganglia in that stimulation of any of the nerve trunks attached to this ganglion can elicit several F-EPSPs (Crowcroft & Szurszewski, 1971). The number of inputs to a single cell in the rabbit IMG was, therefore, examined by stimulating the various nerve trunks with presynaptic pulses of increasing amplitude and duration. Both of these manipulations resulted in the appearance of an increasing number of F-EPSPs. An approximation of the number of fast nicotinic inputs to the cells was made by counting the F-EPSPs occurring with different latencies follow-ing the presynaptic stimulation and by examining stepwise increases in amplitude of F-EPSPs occurring at the same latency (Nja & Purves, 1977).

It was found that in 98% (65 of 66) of the cells a F-EPSP could be elicited following aortic branch stimulation, in 97% (108 of 111) fol-lowing ascending mesenteric nerve stimulation and in 96% (49 of 51) fol-lowing hypogastric nerve stimulation. Every cell responded with a F-EPSP following stimulation of at least one of the nerves. When the response to stimulation to two nerves was tested it was found that 94% (63 of 67) of the cells exhibited F-EPSPs following stimulation of each of the nerves. These inputs rarely consisted of a single F-EPSP from any of the nerves, but usually consisted of multiple F-EPSPs as shown in Figures 9, 10 & 11. These figures show the synaptic inputs received by a single cell in the rabbit IMG from the aortic branch (Figure 9), from the ascending mesenteric nerve (Figure 10) and from the hypogastric

FIGURE 9. Synaptic inputs to a cell of the rabbit IMG following

stimulation of the aortic branch of the ascending mesenteric

nerve.

A-K show the F-EPSPs occurring following stimulation of the

aortic branch of the ascending mesenteric nerve with pulses of

increasing intensity. As the stimulus intensity is increased an

increasing number of F-EPSPs occur in the postganglionic cell.

Horizontal Calibration - 20 msec, Vertical Calibration - 10 mV.

FIGURE 9
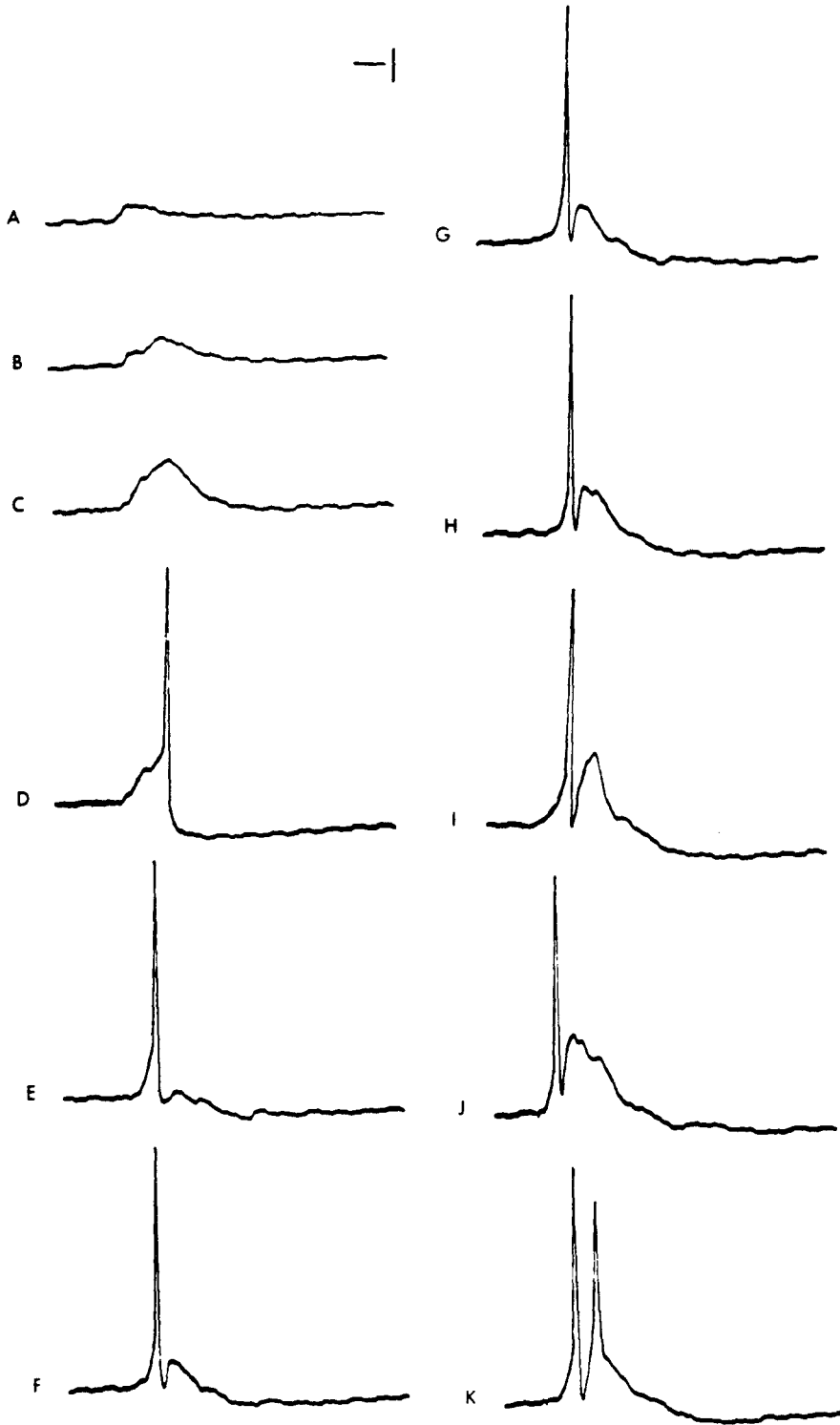
FIGURE 10.   Synaptic inputs to a cell of the rabbit IMG following

stimulation of the ascending mesenteric nerve.

A-K show the F-EPSPs occurring following stimualtion of the

ascending mesenteric nerve with pulses of increasing intensity.

As the stimulus intensity is increased an increasing number of F-

EPSPs occur in the postganglionic cell.   Horizontal Calibration -

20 msec, Vertical Calibration - 10 mV.

FIGURE 10
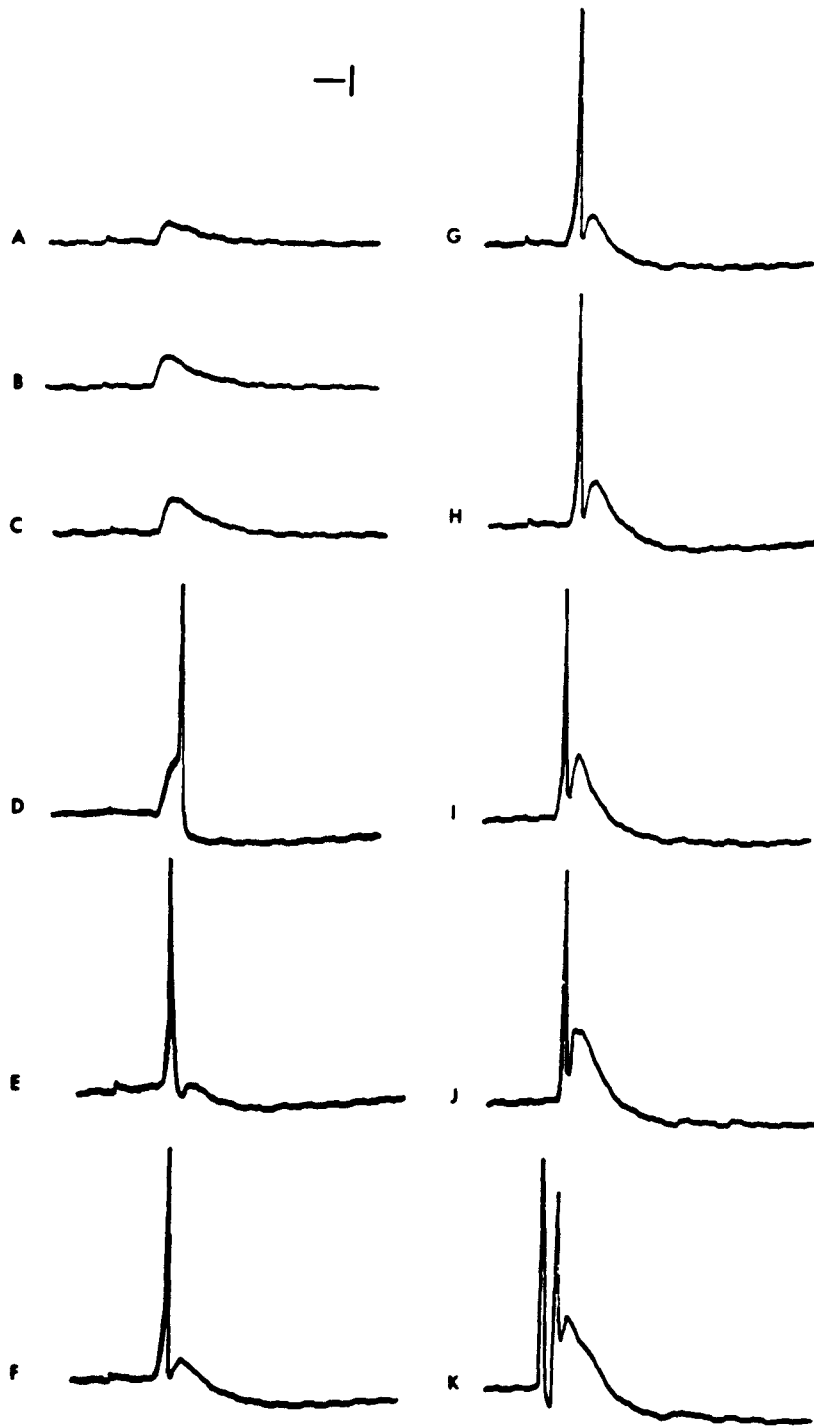
FIGURE 11. Synaptic inputs to a cell of the rabbit IMG following

stimulation of the hypogastric nerve.

A-D show the F-EPSPs occurring following stimualtion of the

hypogastric nerve with pulses of increasing intensity. As the

stimulus intensity is increased an increasing number of F-EPSPs

occur in the postganglionic cell. Horizontal Calibration - 20

msec, Vertical Calibration - 10 mV.

FIGURE 11
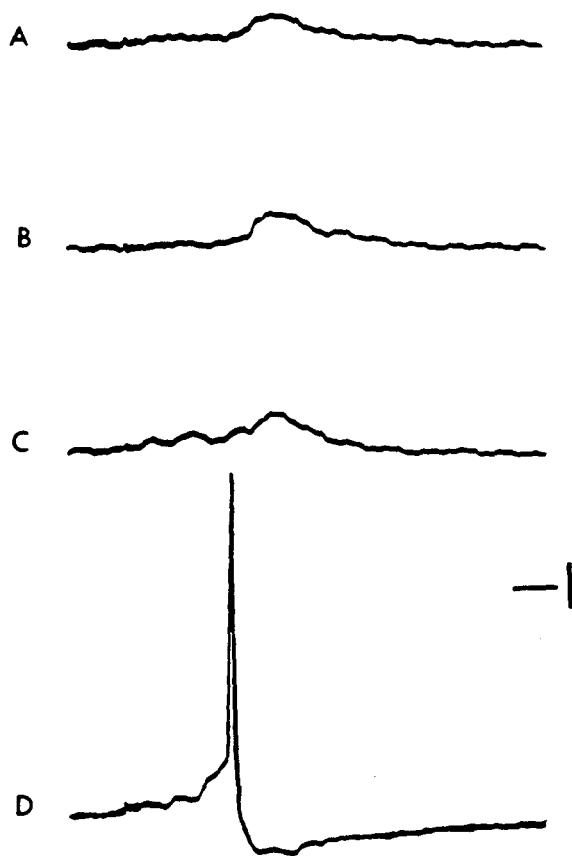
nerve (Figure 11). It was calculated that this particular cell received 17 inputs from the aortic branch, 14 from the ascending mesenteric nerve and 9 from the hypogastric nerve, giving a total of 40 inputs. The average number of inputs received by the cells was 12 from the aortic branch (n=11), 19 from the ascending mesenteric nerve (n=6) and 11 from the hypogastric nerve (n=5). Thus, the average cell in the rabbit IMG receives at least 42 nicotinic cholinergic inputs.

E. Conduction Velocity of Pre- and Postganglionic Fibers

The conduction velocity of the postganglionic fibers of the rabbit IMG was estimated in 5 of the cells which exhibited an antidromic spike. The distance from the stimulating electrode to the recording electrode was measured using an eyepiece micrometer in the microscope. Conduction velocity was calculated by dividing this distance by the latency from the stimulus artifact to the beginning of the upstroke of the antidromic spike. The values obtained ranged from 0.25-0.50 m/sec. The mean was 0.35 ± 0.05 m/sec.

The calculation of the conduction velocity of the preganglionic fibers was slightly more complicated. First, a single cell received a number of preganglionic inputs which were temporally dispersed; there-fore, the latency was measured from stimulus artifact to the upstroke of the first and subsequent F-EPSPs in a given cell. Secondly, this latency, from stimulus artifact to beginning of F-EPSP, does not only involve conduction of the impulse but also involves a synaptic delay. To account for this a factor of 9 msec was subtracted from the observed latency to obtain conduction time (Kreulen & Szurszewski, 1979b). Using

this method, two groups of preganglionic fibers were found with regard to conduction velocity. The largest group was slow conducting fibers which had conduction velocities ranging from 0.15-0.60 m/sec, with a mean of 0.24 ± 0.03 m/sec. A smaller number of fibers had conduction velocities ranging from 1.5-6.0 m/sec with a mean of 2.9 ± 0.6 m/sec.

F. Slow Excitatory Postsynaptic Potential

In addition to a nicotinic cholinergic response, some cells in the rabbit IMG also exhibited a slow muscarinic EPSP. This response was evident following repetitive presynaptic stimulation. The response of a cell to stimulation of the ascending mesenteric nerve at 16 Hz for 3 sec is shown in Figure 12. Following perfusion with Krebs containing atropine (1 μM), the slow depolarization following the initial F-EPSPs is blocked. Of the cells examined, very few (3 of 41, 7%) exhibited a S-EPSP and no LS-EPSP. In many cells, both a S-EPSP and LS-EPSP were seen (see below).

G. Late Slow Excitatory Postsynaptic Potential

In addition to the muscarinic S-EPSP, a much longer lasting depolarization was observed in some cells of the rabbit IMG following repetitive nerve stimulation.

1. Noncholinergic Nature of the LS-EPSP

This long lasting depolarization was insensitive to antagonism of nicotinic and muscarinic cholinergic receptors. Figure 13A shows a slow depolarization elicited by stimulation of the ascending mesenteric nerve at 16 Hz for 3 sec. Perfusion of the ganglion with d-TC (50 μM) effec-

FIGURE 12. Muscarinic slow depolarization in a rabbit IMG neuron.

A: Following stimulation of the ascending mesenteric nerve at 16 Hz for 3 sec a slow depolarization occurs following the F-EPSPs (initial vertical tracings). B: The depolarization is abolished after 4 min in Krebs containing atropine (1 µM) and an afterhyperpolarization following the repetitive cellular spiking is apparent. In this cell, the slow depolarization is pharmacologically similar to the muscarinic S-EPSP.

FIGURE 12

A

B

60 sec

10 mV
0.5 nA
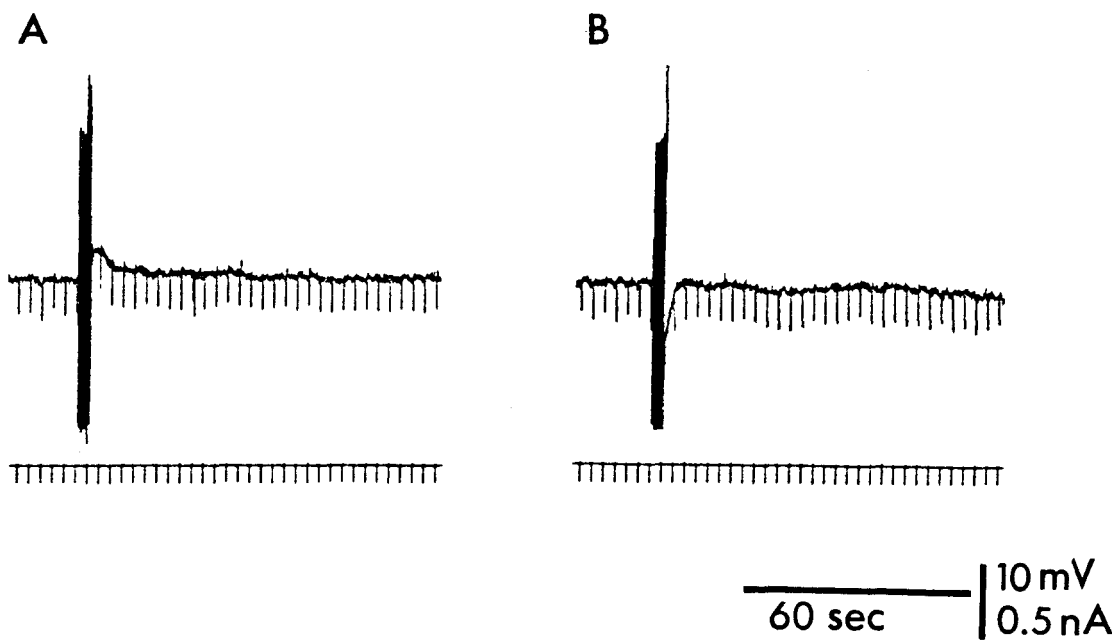
tively blocked the F-EPSPs (initial vertical tracings) but did not affect the slow depolarization (Figure 13B, n=19). Addition of atropine (1 µM) also did not affect this response, although the rise time of the depolarization was increased (Figure 13C).

As noted earlier, a muscarinic S-EPSP also occurred in some neurons in the rabbit IMG. On this basis, it was thought that the increased rise time of the LS-EPSP after the addition of atropine, as seen in Figure 13, might be due to the blockade of a muscarinic S-EPSP. To assess the contribution of the muscarinic component to the slow depolarization, the response of 14 cells was examined before and after perfusion of the IMG with atropine (1 µM). Antagonism of the muscarinic receptors had no effect on the peak amplitude, R_{in} change or duration of the depolarization, but in 10 of the cells an increase in the time to peak of the reponse was observed. In these cells the time to peak was increased from an average of 3 sec to an average of 9 sec. One of these cells is shown before and after addition of atropine in Figures 14 and 15, respectively. In normal Krebs solution the depolarization following nerve stimulation has peaked at the end of the stimulus train (Figure 14, top). Following perfusion with atropine (1 µM) the peak is not reached until several seconds following the cessation of nerve stimulation (Figure 15, top). The bottom tracings of these figures illustrate that an increased R_{in} was observed both in the presence (Figure 14) and absence (Figure 15) of atropine.

FIGURE 13.   Noncholinergic slow depolarization in a rabbit IMG neuron.

A: Following stimulation of the ascending mesenteric nerve at 16

Hz for 3 sec a long lasting depolarization is observed following

the F-EPSPs (initial vertical tracings).   B: After 5 min

perfusion with d-tubocurarine (50 μM) the initial F-EPSPs are

completely blocked, but the slow depolarization remains.   C:

Addition of atropine (1 μM) to the perfusate causes an increase

in the rise time of the slow response, but does not antagonize

the long lasting depolarization.

FIGURE 13
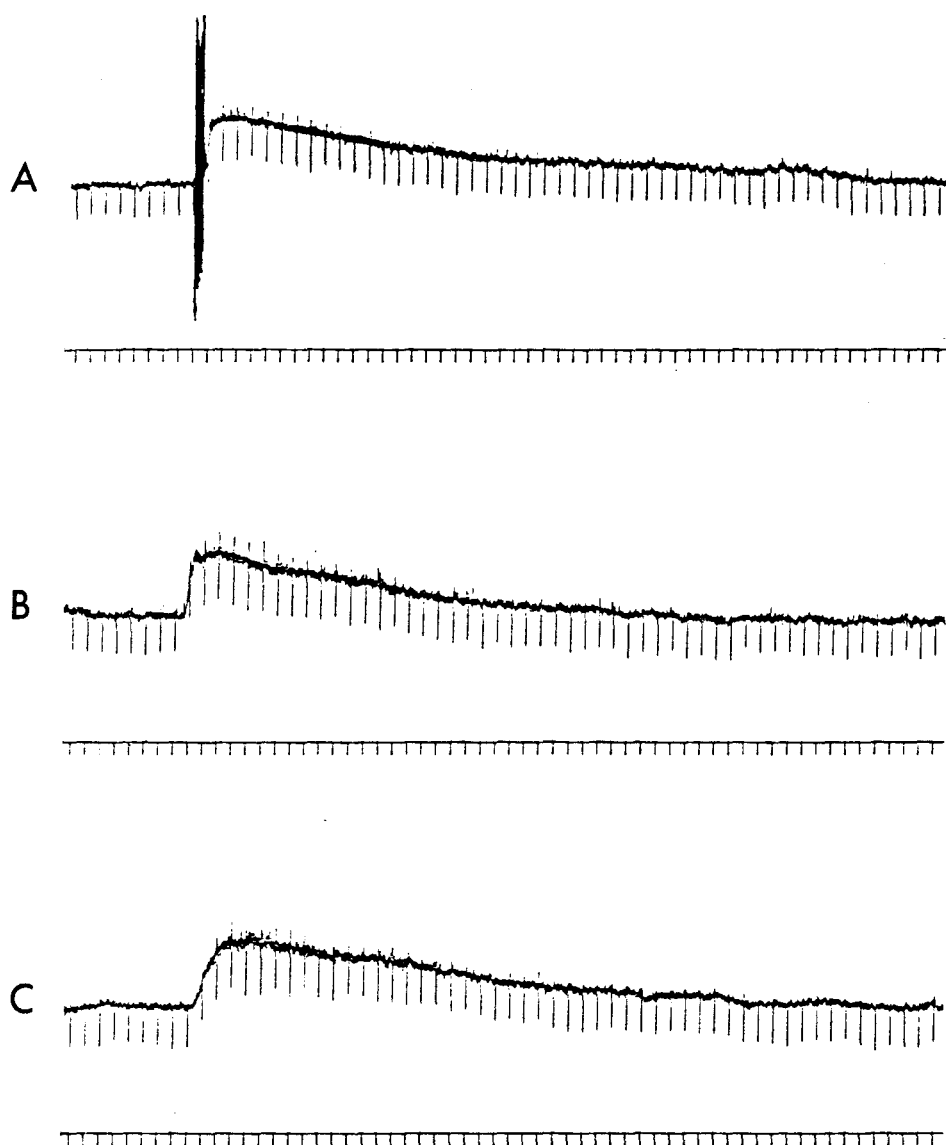
60 sec   5 mV / 0.5 nA

FIGURE 14. Late slow excitatory postsynaptic potential and accompanying

membrane resistance changes in a rabbit IMG neuron following

stimulation of either of two nerve trunks.

Top: Membrane potential change in a ganglionic cell following

stimulation of the aortic branch of the ascending mesenteric

nerve (AB) or following stimulation of the ascending mesenteric

nerve (AMN) at 30 Hz for 3 sec. Bottom: Membrane resistance

change in the same cell following stimulation of the aortic

branch of the ascending mesenteric nerve (AB) or following

stimulation of the ascending mesenteric nerve (AMN) at 30 Hz for

3 sec. The cell was held at E_r following stimulation by passage

through the recording electrode of hyperpolarizing current (lower

tracing). Note that stimulation causes an increase in R_{in} with a

time course contiguous with the LS-EPSP.

FIGURE 14
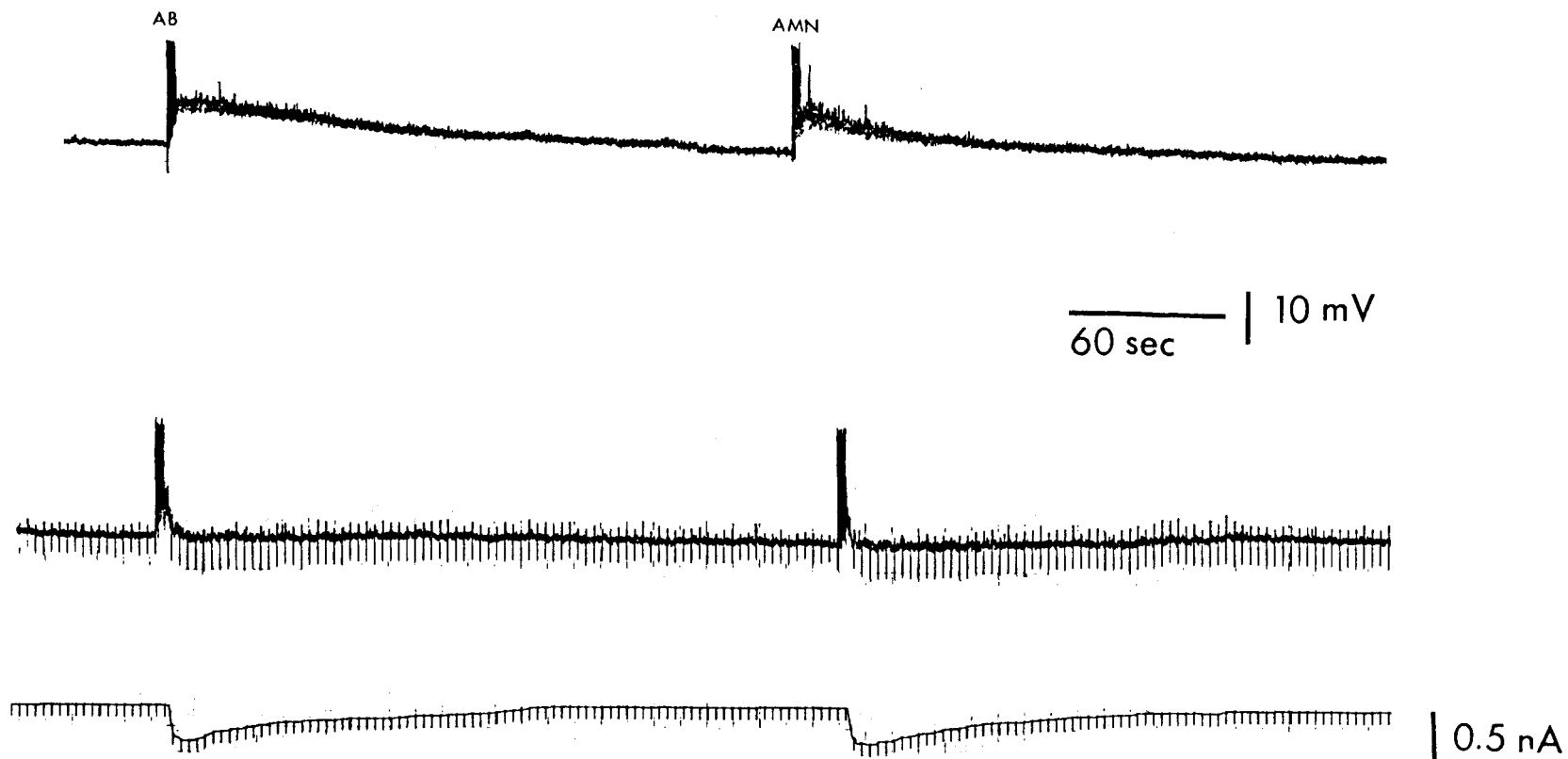
FIGURE 15. Late slow excitatory postsynaptic potential and accompanying

membrane resistance changes in a rabbit IMG neuron following

stimulation of either of two nerve trunks in the presence of

atropine (1 μM).

These responses were obtained from the same cell as the previous

figure following perfusion with atropine (1 μM). Top: Membrane

potential change in a ganglionic cell following stimulation of

the aortic branch of the ascending mesenteric nerve (AB) or

following stimulation of the ascending mesenteric nerve (AMN) at

30 Hz for 3 sec. Note the increased rise time of the response

compared to Figure 14. Bottom: Membrane resistance change in

the same cell following stimulation of the aortic branch of the

ascending mesenteric nerve (AB) or following stimulation of the

ascending mesenteric nerve (AMN) at 30 Hz for 3 sec in the

presence of atropine (1 μM). The cell was held at E_r following

stimulation by current passed through the recording electrode

(lower tracing). In the absence of a muscarinic component, the

depolarization is still accompanied by an increased R_{in}, although

slower in onset.

FIGURE 15
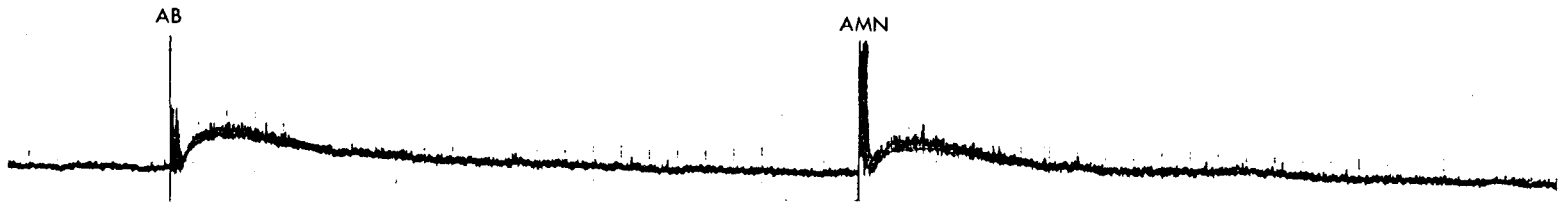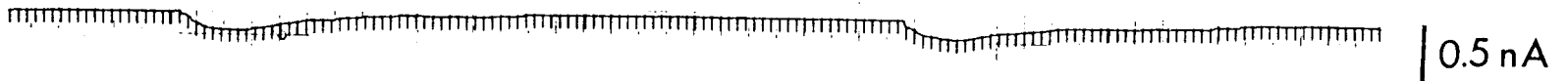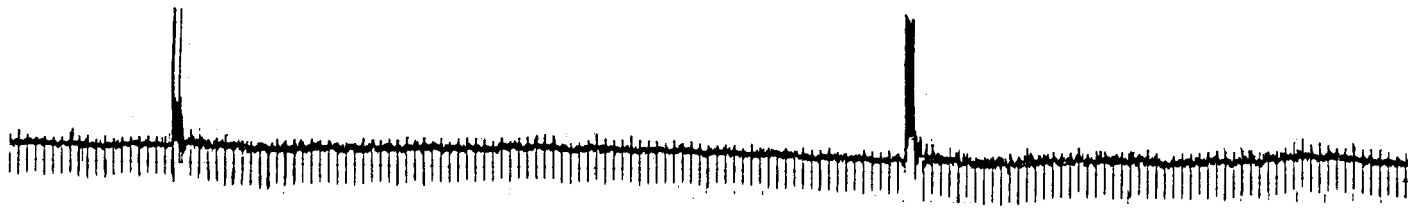
2. Characteristics of the LS-EPSP

The characteristics of the LS-EPSP are listed in Table 5. These data are for responses following presynaptic stimulation at 30 Hz for 3 sec in the presence of atropine. For examples of typical LS-EPSPs in rabbit IMG cells see Figures 13 and 15. In several cells, hyperpolarizing current was passed through the recording electrode to nullify the depolarization to examine the R_{in} change in the absence of E_m changes. One of these cells is shown in Figure 15. This figure shows the responses elicited following repetitive presynaptic stimulation of the ascending mesenteric nerve and the aortic branch of the ascending mesenteric nerve. The top panel shows the potential change. In the bottom panel, the depolarization was nullified by the passage of current through the recording electrode (manual clamp) and an increased R_{in} was observed. An average increase in R_{in} of 31% (n=20) was observed when the depolarization was prevented by manual clamp. This mean is slightly larger than the the increase observed with depolarization (Table 5) but this difference is not statistically significant (paired t-test). A decrease in R_{in} was not observed during the LS-EPSP in any of the cells studied. In about 8% of the cells, however, a detectable change in R_{in} was not evident.

3. Occurrence of the LS-EPSP

Of all the cells tested, 63% (155 of 247) exhibited a detectable LS-EPSP. The percentage of cells which showed a LS-EPSP varied, depending to some extent on the nerve being stimulated. A LS-EPSP was observed in 70% (54 of 77) of the cells following stimulation of the

TABLE 5

CHARACTERISTICS OF THE LATE SLOW EXCITATORY
POSTSYNAPTIC POTENTIAL IN RABBIT IMG CELLS
(Following preganglionic stimulation at 30 Hz
for 3 sec in the presence of atropine (1μM))

	Mean	±	S.E.M.	Range			n
Amplitude (mV)	4.3	±	0.3	1	–	13	64
Time to Peak (sec)	10.0	±	0.6	<3	–	27	63
Duration (sec)	159	±	13	23	–	390	38
Half Decay (sec)	61	±	5	17	–	218	54
% Increase in R_{in}	27	±	2	0	–	75	48

aortic branch of the ascending mesenteric nerve, in 61% (69 of 110) following stimulation of the ascending mesenteric nerve and in 52% (32 of 60) following hypogastric nerve stimulation. A X^2 test revealed that these differences in the proportion of cells showing a LS-EPSP following stimulation of the different nerves was not statistically significant.

The response following separate stimulation of two of the nerve trunks was also studied. In 36% (28 of 78) of the cells a LS-EPSP could be elicited following stimulation of both nerves tested. An example of such a cell is shown in Figure 15.

4. Topography of Cells Showing a LS-EPSP

As noted in the previous section, a F-EPSP could be elicited in practically every cell in the IMG following stimulation of any of the associated nerve trunks irrespective of the location of the cell in the ganglion. Since the LS-EPSP was not detected in every cell studied, it was of interest to determine whether or not there was a topographical organization of the noncholinergic inputs to the ganglion. This possibility was analyzed by noting the relative positions of the cells which did or did not exhibit a LS-EPSP following stimulation of the various nerve trunks on a map of the shape of the IMG. This map illustrates the position of the cell in the rostrocaudal-mediolateral plane. These results are shown in Figure 16. From this figure it can be seen that a LS-EPSP could be elicited in cells located throughout the ganglion, regardless of the nerve trunk being stimulated.

FIGURE 16.   Topographical localization of the neurons in the rat it IMG

which did or did not exhibit a LS-EPSP following stimulation of

the different nerve trunks.

Filled circles - Location of cells which did exhibit a LS-EPSP.

Open circles - Location of cells which did not exhibit a LS-EPSP.

AB: Cells examined following stimulation of the aortic branch of

the ascending mesenteric nerve.   AMN: Cells examined following

stimulation of the ascending mesenteric nerve.   HGN: Cells

examined following stimulation of the hypogastric nerve.

AB　　　　　　　　AMN　　　FIGURE 16　　　HGN
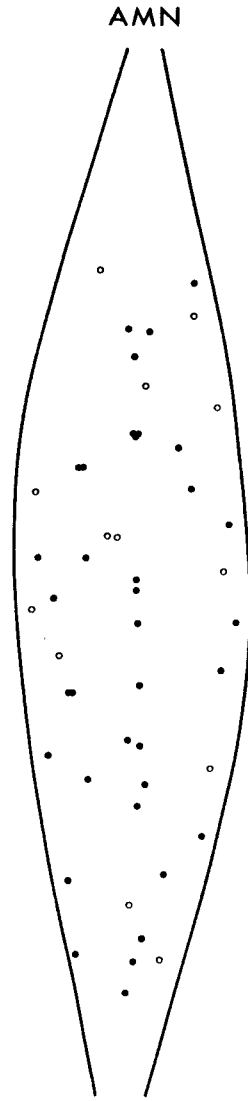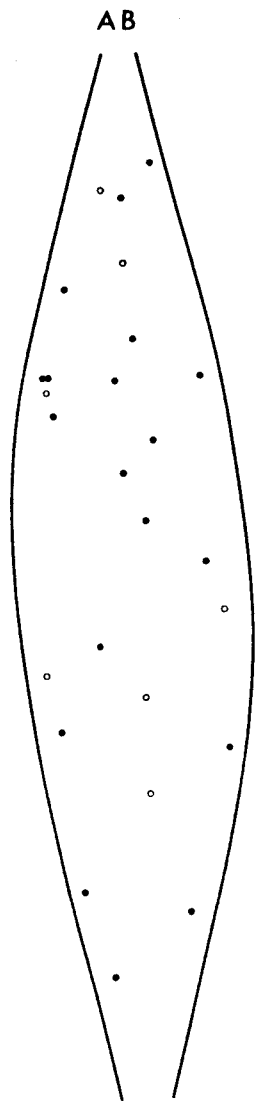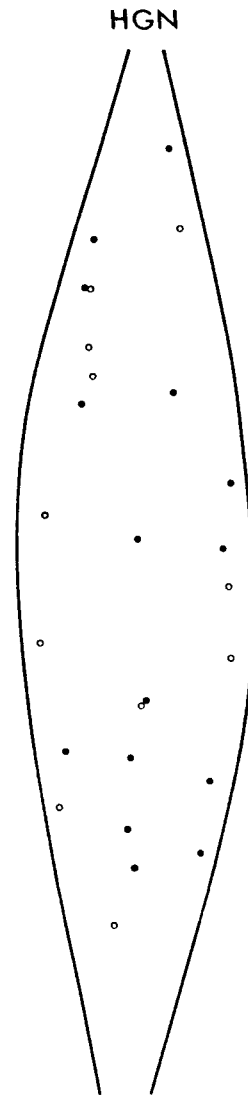
5. Synaptic Mediation of the LS-EPSP

Several experiments were conducted to ascertain that the LS-EPSP is indeed the result of the action of a synaptically released neurotransmitter. The possibility that the repetitive discharges which follow a train of preganglionic stimuli could themselves generate a slow potential change is ruled out by the following findings. First, direct intracellular stimulation at stimulus parameters which elicited repetitive firing of the cell similar to the firing seen with the preganglionic train did not evoke a slow depolarization of the cells (n=6). Second, the LS-EPSP was not affected following the blockade of the spikes by d-TC (Figure 13). Additionally, repetitive nerve stimulation failed to elicit a LS-EPSP in the presence of TTX (1 μM, n=4). TTX blocks voltage-sensitive Na^+ channels in the nerve terminal membrane (Narahashi, 1974) thus preventing the propagation of action potentials into the nerve endings. As shown by Figure 17, TTX completely blocked both the F- and LS-EPSPs. This effect of TTX was reversed with prolonged washing.

Since the release of chemical transmitters from the preganglionic terminal is dependent on the influx of Ca^{++}, the release should be impaired in a low Ca^{++} solution. Figure 18 shows the F- and LS-EPSPs before, during and after perfusion with low Ca^{++} (0.25 mM)/high Mg^{++} (12 mM) Krebs solution. As illustrated, both the F- and LS-EPSP disappear in this medium. This result was confirmed in 5 other cells.

Collectively, these results provide strong evidence that the LS-EPSP is indeed a postsynaptic potential mediated by the release of a chemical transmitter.

FIGURE 17. Effects of tetrodotoxin on the LS-EPSP in a rabbit IMG

neuron.

Con: F- and LS-EPSPs occur in a rabbit IMG cell following

ascending mesenteric nerve stimulation (8 Hz, 3 sec) in the

presence of atropine (1 µM). TTX: After application of

tetrodotoxin (1 µM) for 5 min both the F- and LS-EPSPs are

blocked (stimulus artifact still apparent). Anelectrotonic

potentials elicited by hyperpolarizing current pulses of 0.1 nA,

200 msec duration, were employed to monitor R_{in} of this cell.

FIGURE 17

Con

TTX

10 mV

60 sec
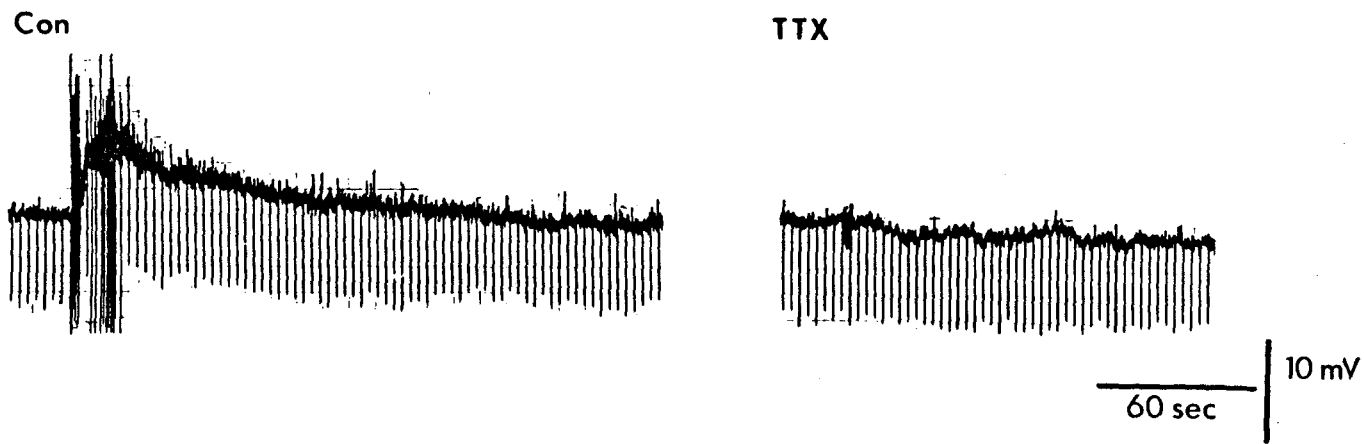
FIGURE 18. Effects of low Ca^{++}/high Mg^{++} Krebs solution on the LS-EPSP.
Con: F- and LS-EPSPs elicited in a rabbit IMG neuron following
stimulation of the ascending mesenteric nerve (16 Hz for 3 sec).
Low Ca: After 4 min perfusion with low Ca^{++}/high Mg^{++} Krebs the
cell is depolarized by 10 mV and the LS-EPSP greatly attenuated.
Hyperpolarizing current was then applied to return E_m to the
original E_r. The F- and LS-EPSP have completely disappeared at
this point and following removal of the hyperpolarizing current.
Wash: Following 8 min in normal Krebs E_m and the F- and LS-EPSPs
return to the control level.

FIGURE 18
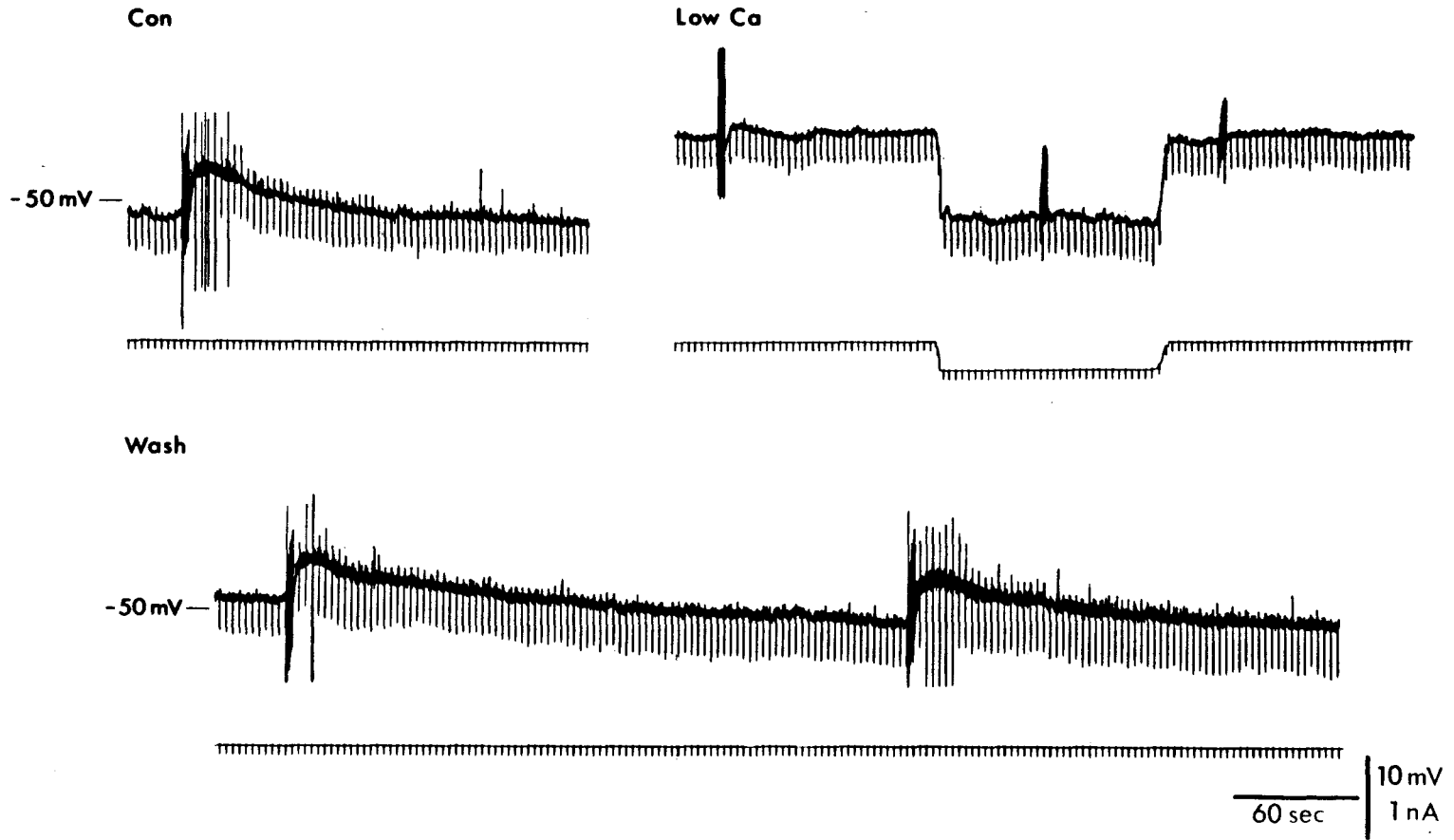
6. Relationship Between Presynaptic Stimuli and LS-EPSP

The relationship between the amplitude of the LS-EPSP and the frequency and duration of the presynaptic stimulus train was also studied. The frequency was varied from 1-100 Hz and the durations from 1-6 sec. The response of the cell to preganglionic stimulation at 30 Hz for 3 sec was chosen as a reference. The results obtained with other stimulus parameters are expressed as the percent of the response at this reference for a given cell.

The response of one cell to increasing the frequency and duration of the presynaptic stimulus train is shown in Figure 19. The left panel shows the responses to a 3 sec train of stimuli at frequencies from 2 to 100 Hz. The LS-EPSP first becomes evident at 4 Hz and is maximal at 32 Hz. With a 6 sec train a small depolarization is visible even at the 2 Hz frequency. From this figure it can be seen that the amplitude of the LS-EPSP is directly proportional, within limits, to the number of presynaptic impulses. The relationship between presynaptic stimuli and the LS-EPSP is described in more detail below.

a. Effects of Stimulus Frequency

The amplitude of the LS-EPSP was found to be correlated with the frequency of presynaptic stimulation. Figure 20 shows a plot of the percent amplitude of the responses obtained at frequencies from 2-100 Hz. The duration of stimulation was 3 sec. The two most simple equations to describe this distribution would be a hyperbolic function of the form: % amplitude = (a × Hz) / (b + Hz) or a logarithmic function of the form % amplitude = a log Hz, where a and b are constants. Regres-

FIGURE 19. Response of a cell in the rabbit IMG to presynaptic

stimulation of increasing frequency and duration.

Left: Responses following a 3 sec train of presynaptic pulses.

Right: Responses following a 6 sec train of presynaptic pulses.

The frequency of the presynaptic pulses for these train durations

is increased from 2-100 Hz as labeled on the left side. Note the

dependency of the amplitude of the LS-EPSP on the frequency and

duration of nerve stimuli. In the presence of atropine (1 μM).

Horizontal calibration - 30 sec, Vertical calibration - 10 mV.

FIGURE 19
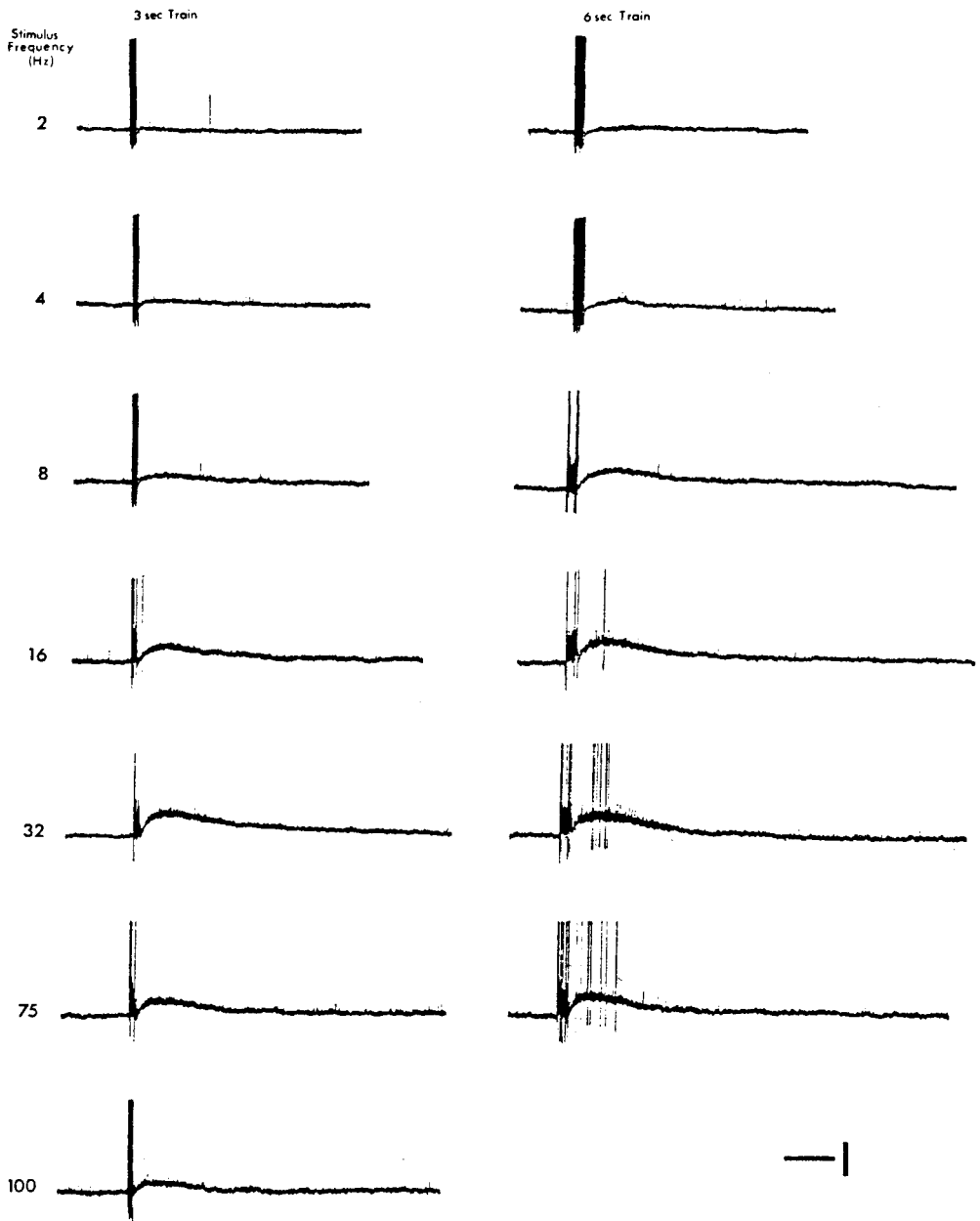
sion analysis was performed to determine which of these functions best described the relationship obtained here. The r^2 values obtained for the fits to the hyperbolic and logarithmic equations were .61 and .44, respectively, revealing a better fit of the hyperbolic distribution. The line drawn on Figure 20 was fit by the equation % amplitude = (123 × Hz) / (11 + Hz), 0 < Hz < 100. The coefficients were obtained from the regression analysis.

b. Effects of Stimulus Duration

The amplitude of the LS-EPSP was also found to increase with increasing duration of stimulation. This relationship is shown on Figure 21. The stimulation in this case was at 30 Hz and the duration was varied from 1-6 sec.

c. Number of Pulses

Since the amplitude of the LS-EPSP depends on both the frequency and duration of the presynaptic stimulation, it follows that there would be a similar relationship to the number of presynaptic pulses, which is the product of frequency and duration. As seen on Figure 22, there is a clear increase in the amplitude of the LS-EPSP as the number of presy- naptic impulses increases. The same analysis used for the frequency plot was used to determine the best fit line for this data. For number of pulses vs. % amplitude an r^2 value of .72 was obtained. The line on Figure 22 is described by the equation: % amplitude = (123 × Pulses) / (32 + Pulses), 0 Pulses < 300.

FIGURE 20. Relationship between frequency of nerve stimulation and

amplitude of the LS-EPSP.

Duration of stimulation was 3 sec. Ordinate - Percent amplitude

of the response obtained at 30 Hz. Abscissa - Frequency of

stimulation. The graph shows the mean ± 1 standard deviation for

the responses obtained at each frequency. The line is fitted by

the equation: % amplitude = (123 × Hz) / (11 + Hz), 0 < Hz <

100.

FIGURE 20

FREQUENCY OF STIMULATION/SEC
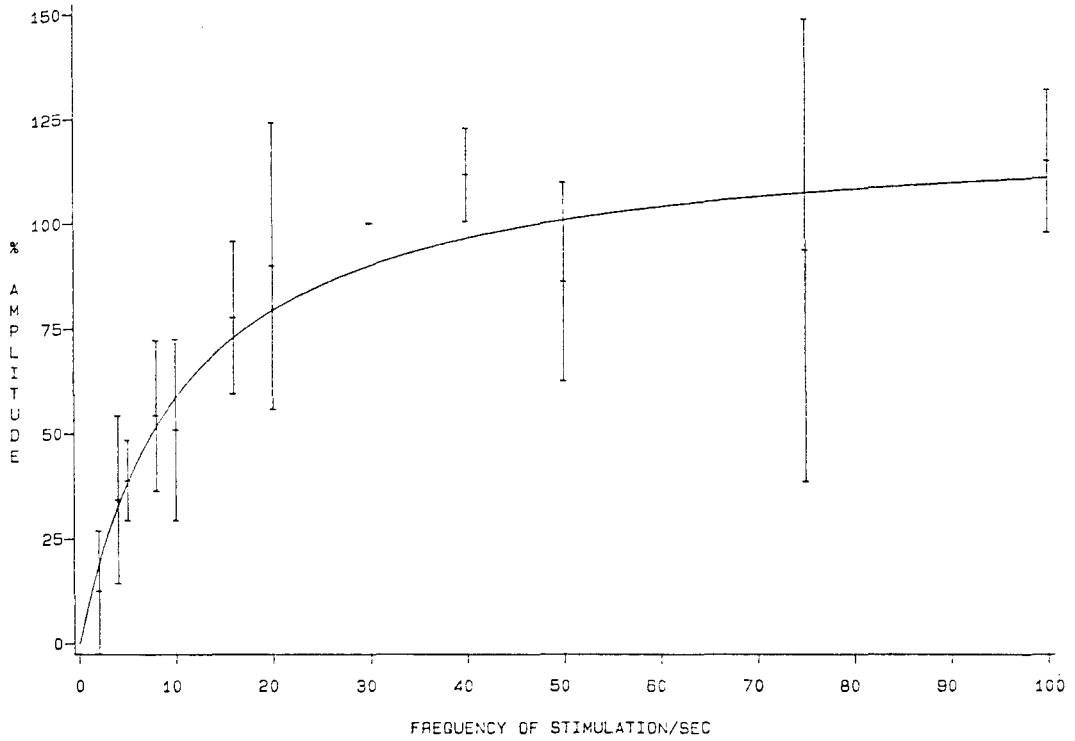
FIGURE 21.   Relationship between the duration of the presynaptic train
and amplitude of the LS-EPSP.

Frequency of stimulation was 30 Hz.   Ordinate - Percent amplitude
of the response obtained with a 3 sec train.   Abscissa - Duration
of stimulation in sec.   The graph shows the mean ± 1 standard
deviation for for the responses obtained at each duration.

FIGURE 21

DURATION OF STIMULATION (SEC)
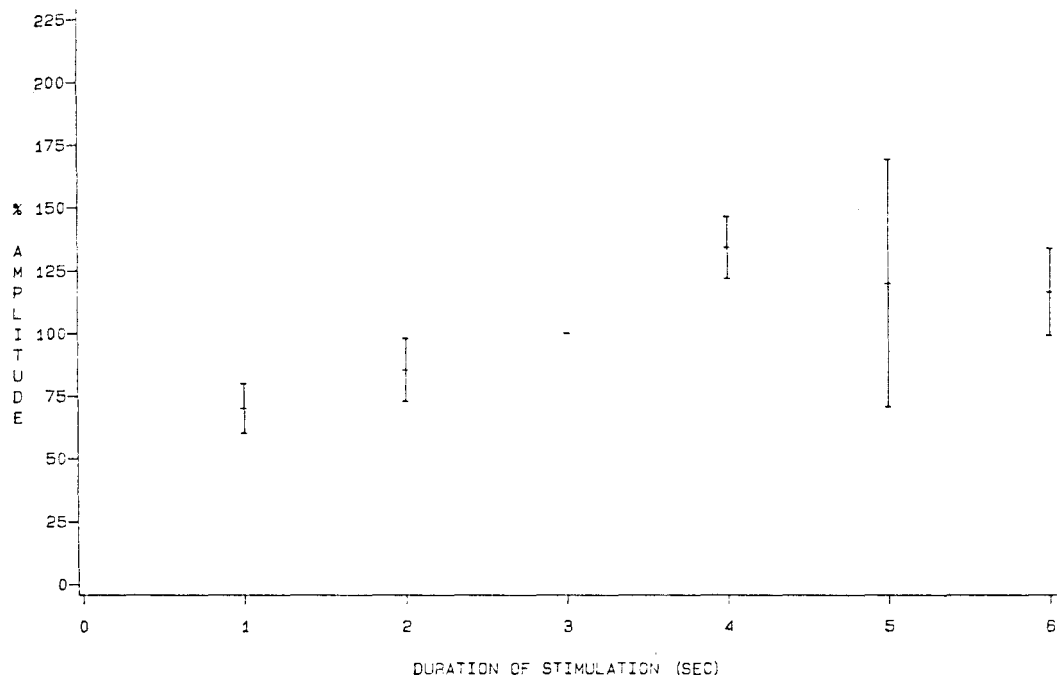
FIGURE 22. Relationship between the number of presynaptic pulses and

amplitude of the LS-EPSP.

Ordinate - Percent amplitude of the response obtained with 90

pulses. Abscissa - Number of pulses in the stimulus train. The

graph shows the mean ± 1 standard deviation for the responses

obtained at each value of pulses. The line is fitted by the

equation: % amplitude = (123 × Pulses) / (32 + Pulses), 0 <

Pulses < 300.

FIGURE 22
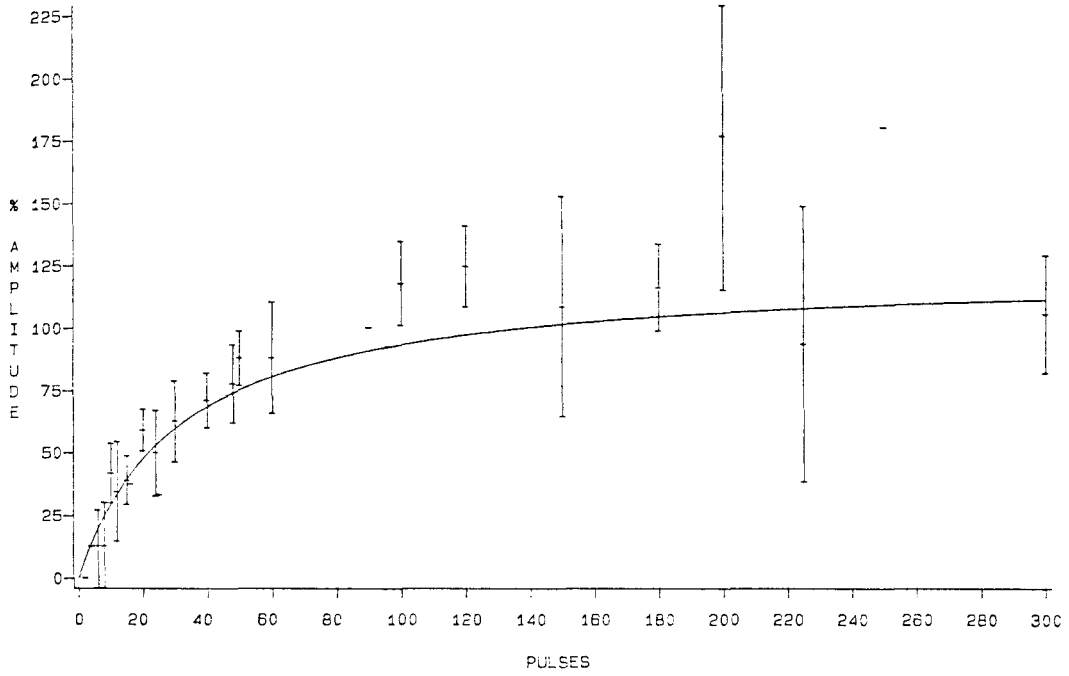
7. Effects of High Potassium on the LS-EPSP

According to the ionic theory of electrogenesis, potential changes of neurons are due to changes in membrane permeability to one or more ions. The fact that the LS-EPSP consisted of a depolarization accompanied by a decrease in membrane conductance suggested that the equilibrium potential for the ion species involved was more negative than E_r; thus, the most likely ion involved in this response would be K^+. To test this possibility, the concentration of KCl in the Krebs solution was increased and the membrane was hyperpolarized. Figure 23 shows the effects of raising $[K_o]$ to 20 mM and subsequent hyperpolarization of the cell on membrane potential, the spike afterhyperpolarization and the LS-EPSP. The spike afterhyperpolarization was monitored since it is known to involve an increase in K^+ conductance and should disappear at the K^+ equilibrium potential (E_K). Following perfusion with high K^+ Krebs the cell is depolarized by 6 mV and the afterhyperpolarization and the LS-EPSP are reduced in amplitude. Subsequently hyperpolarizing the membrane to -50 mV results in a disappearance of both the afterhyperpolarization and the LS-EPSP. Further hyperpolarization did not result in a reversal of the LS-EPSP. In 6 other cells tested similar results were obtained. According to the Nernst equation, and assuming $[K_i]$=160 mM, in normal Krebs E_K=-95 mV. In 20 mM K^+ E_K is lowered to -56 mV. In the high K^+ Krebs the LS-EPSP disappeared near the level of E_K. This indicates that a decrease in K^+ conductance is probably involved in the electrogenesis of the LS-EPSP. Changes in Cl^- conductance are probably not involved in the LS-EPSP. Since KCl-filled electrodes were used in

FIGURE 23. Effects of high K^+ and membrane hyperpolarization on the
direct spike and LS-EPSP in a rabbit IMG neuron.
Arrowheads - Direct spike, Arrows - Stimulation of the aortic
branch of the ascending mesenteric nerve (30 Hz, 3 sec). Top:
Responses in normal Krebs solution. Note afterhyperpolarization
of direct spike and amplitude of LS-EPSP. Middle: In 20 mM K^+
the cell is depolarized by 6 mV. The afterhyperpolarization of
the direct spike is smaller and the amplitude of the LS-EPSP is
decreased. Bottom: Hyperpolarization to -50 mV by current
injection results in a disappearance of the
afterhyperpolarization and of the LS-EPSP.

FIGURE 23
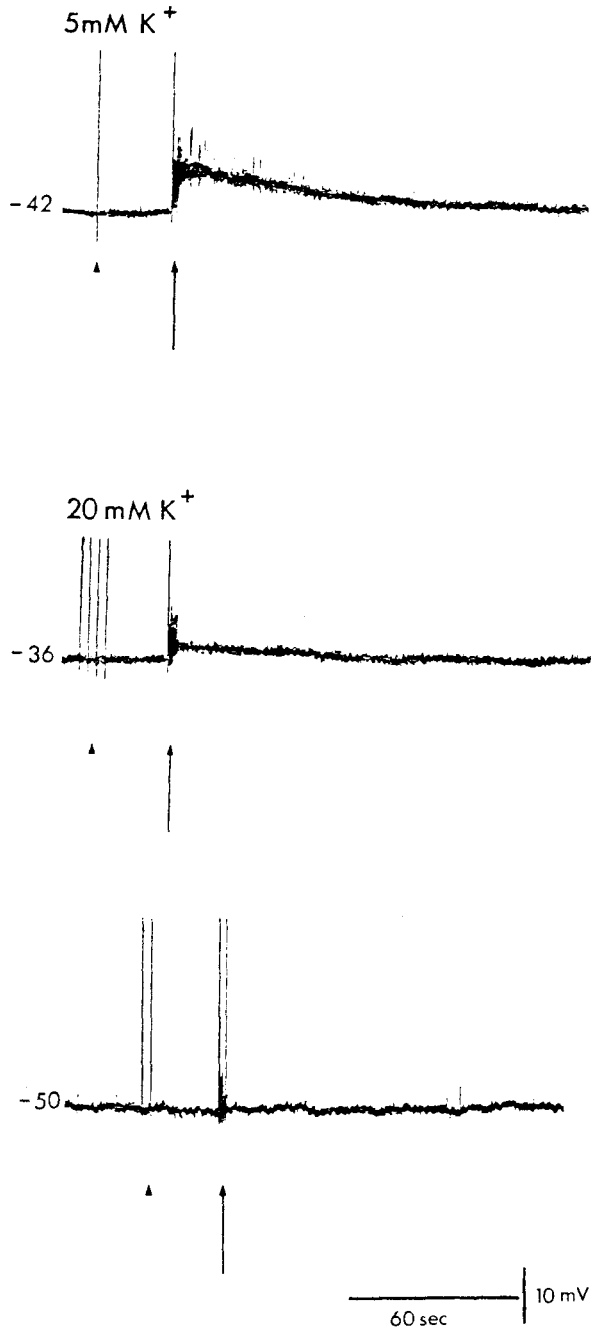
these studies, diffusion of Cl^- from the electrode into the cell would tend to make the Cl^- equilibrium potential more positive than E_r.

8. Pharmacology of the LS-EPSP

In both bullfrog paravertebral ganglia (Jan et al., 1979, 1980; Jan & Jan, 1982) and in the guinea pig IMG (Jiang et al., 1982a) peptides have been proposed as mediators of the LS-EPSP. Experiments using several classes of drugs were carried out to examine the possibility that the LS-EPSP in the rabbit IMG may be mediated by a peptidergic transmitter.

a. 5-Hydroxytryptamine

This substance has recently been shown to depolarize neurons in the guinea pig celiac ganglion and has been proposed as the mediator of a noncholinergic slow depolarization in this ganglion (Dun & Ma, 1983). 5-HT has also been suggested as a mediator of the slow noncholinergic potential in the guinea pig myenteric plexus (Wood & Mayer, 1978). When applied to the rabbit IMG, 5-HT had a depolarizing effect on 3 of 15 cells tested. In all cases this depolarization was accompanied by an increase in membrane resistance. One of the cells which was sensitive to 5-HT is shown in Figure 24. The LS-EPSP elicited in this cell had a particularly long-lasting duration (Figure 24, top). When applied to the ganglion, 5-HT (100 μM) resulted in a depolarization of 9 mv (Fig. 24, middle). During the 5-HT depolarization, the membrane potential was momentarily returned to the resting level during which time nerve stimulation elicited a LS-EPSP of much smaller amplitude accompanied by an

140

FIGURE 24. Effects of 5-hydroxytryptamine on membrane potential, input

resistance and the LS-EPSP in a rabbit IMG neuron.   .

5-HT (100 µM) application is indicated by the bar. Arrows

indicate stimulation of the ascending mesenteric nerve (16 Hz for

3 sec). Top: Nerve stimulation results in a large, 9 mV, long

lasting, over 6 min, depolarization. Middle: 5-HT (100 µM) is

applied to the cell. After a 1 min delay the cell is depolarized

about 8 mV. After 5 min the cell is returned to the resting

level and the nerve stimulated. A small depolarization occurs

accompanied by an increased R_{in}. Bottom: After 10 min

continuous perfusion with 5-HT the cell remains depolarized.

Stimulation at the depolarized level results in a very small

depolarization and an increase in the noise level of the

recording.

FIGURE 24

5-HT ⟶

60 sec

10 mV

1 nA

141
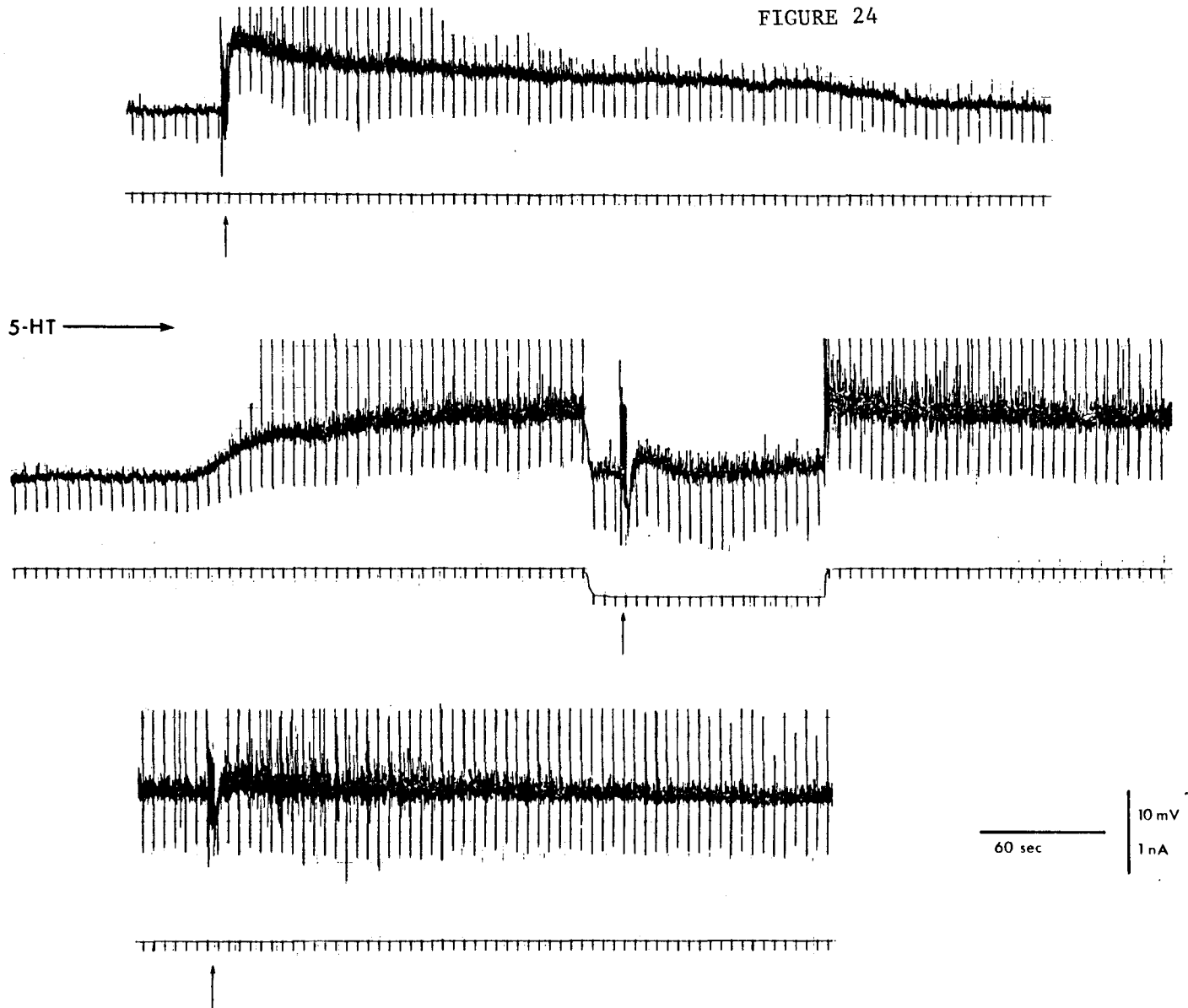
increase in R_{in}. However, repetitive nerve stimulation at the peak of the 5-HT induced depolarization evoked no detectable LS-EPSP (Figure 24, bottom). One interesting property of this cell was its apparent lack of tachyphylaxis to continued application of 5-HT. Rapid desensitization to 5-HT occurs at a variety of other sites, including the guinea pig celiac ganglion (Dun, Kiraly & Ma, 1983). In this cell, however, the depolarization continued, waning by only a few mV, for over one hour of continuous 5-HT application. During this time small depolarizations could be elicited by nerve stimulation. In none of the other cells which were depolarized by 5-HT, nor in the 12 cells not depolarized, was conclusive evidence obtained that prolonged superfusion of 5-HT could desensitize the LS-EPSP.

b. Luteinizing Hormone Releasing Hormone

LHRH was of interest since it has been identified as the mediatior of the LS-EPSP in the bullfrog. LHRH (1-100 μM) had no effect on E_m and R_{in} of the 4 rabbit IMG neurons tested. Similarly, LS-EPSP elicited in these cells was not appreciably altered. Moreover, an LHRH antagonist, $(D-\rho-Glu^1,D-Phe^2,D-Trp^{3,6})$-LHRH (100 μM), which has been shown to block the membrane depolarization induced by LHRH in the bullfrog ganglion cells (Jan & Jan, 1982), was without effect on the LS-EPSP elicited in IMG neurons (n=4).

c. Norepinephrine

NE is the classical postganglionic transmitter in the sympathetic nervous system and is contained in the principal cells of the IMG

(Jacobwitz, 1974). Furthermore, catecholamine fluorescent terminals have been observed abutting on neighboring IMG cells (Elfvin, 1971c) which make contacts with one another. Therefore, the possibility that NE may be released from these terminals and generate the LS-EPSP was examined. At low concentrations (1 µM) NE had no effect on E_m, R_{in} or the LS-EPSP (n=4) With high concentrations (> 100 µM), however, NE did block the LS-EPSP. This effect was not accompanied by any change in E_m nor by a change in R_{in}. The most likely explanation is that NE was acting presynaptically to reduce transmitter output. That NE is not involved in the mediation of the LS-EPSP is further demonstrated by the experiments in which the LS-EPSP was not antagonized by the adrenergic antagonist dihydroergotamine (DHE, 10 µM, n=4).

d. Substance P

SP has been proposed as the mediator of the LS-EPSP in the guinea pig IMG (Dun & Jiang, 1982; Jiang et al., 1982; Tsunoo et al., 1982) and also as the mediator of slow noncholinergic potentials in the guinea pig myenteric plexus (Katayama & North, 1978). In the present study, SP (1-100 µM) caused a slow depolarization in 5 of the 15 cells tested. The R_{in} changes accompanying the depolarization varied from cell to cell; two cells exhibited an increase in R_{in} while in the other three neurons a decrease in R_{in} was observed. However, the LS-EPSP was not affected by prolonged application of SP in any of the cells tested.

Tracings from two of the cells which were depolarized by SP are shown in Figures 25 and 26. In the cell shown in Figure 25, a small LS-EPSP could be elicited prior to SP application (not shown). SP (10

μM) caused a depolarization of about 8 mV in this particular cell. During the SP depolarization repetitive stimulation elicited no detectable LS-EPSP. After a period of wash the LS-EPSP returned as E_m returned to the resting level. Next, the cell was depolarized by current injection to the level of the SP-induced depolarization (Figure 25, bottom). Under these conditions repetitive stimulation again elicited no detectabel LS-EPSP.

The cell in Figure 26 was also depolarized by SP (10 μM). The depolarization was accompanied by a decrease in R_{in}. E_m was then returned to the resting level by hyperpolarizing current during which time nerve stimulation could again elicit a LS-EPSP. Thus, SP had no desensitizing effect on the LS-EPSP evoked in this cell.

Several putative SP antagonists have recently been developed including (D-Pro^2,D-Phe^7,D-Trp^9)-SP and (D-Arg^1,D-Pro^2,D-Trp^{7,9},Leu^{11})-SP (Folkers, Horig, Rosell, & Bjorkroth, 1981; Rosell, Olgart, Gazelius, Panopoulos, Folkers & Horig, 1981; Yanagisawa, Otsuka, Konishi, Akagi, Folkers & Rosell, 1982). Neither of these compounds at concentrations of 10 μM to 100 μM noticeably altered the LS-EPSP, E_r or R_{in} of 5 rabbit IMG neurons tested.

Capsaicin, which causes release and subsequent depletion of SP, (Jessell et al., 1978; Gamse et al., 1981a, 1981b) was also tested to see if it could release SP, thereby causing a LS-EPSP, or deplete SP, thereby blocking the LS-EPSP, in a manner similar to that reported in the guinea pig IMG (Dun & Kiraly, 1983). Capsaicin, at concentrations from 5 μM to 10 μM applied for at least 10 min, did not result in a

FIGURE 25. Effects of substance P on membrane potential, input

resistance and the LS-EPSP in a rabbit IMG neuron.

Substance P (10 µM) application is indicated by the bar. Arrows

indicate stimulation of the ascending mesenteric nerve (30 Hz for

3 sec). Top: SP depolarized this cell by 8 mV and decreased R_{in}

by 20%. Following 3.5 min in SP stimulation of the ascending

mesenteric nerve evoked no detectable LS-EPSP. After washout of

SP the membrane potential returned to the original resting level

at which time repetitive stimulation evoked a small LS-EPSP.

Bottom: After 10 min in normal Krebs solution the cell was

depolarized to the level of the SP depolarization by current

injection. Under these conditions, nerve stimulation did not

result in a LS-EPSP. Atropine (1 µM) was present throughout the

experiment.

FIGURE 25

SP 10 µM

60 sec

10 mV
0.5 nA
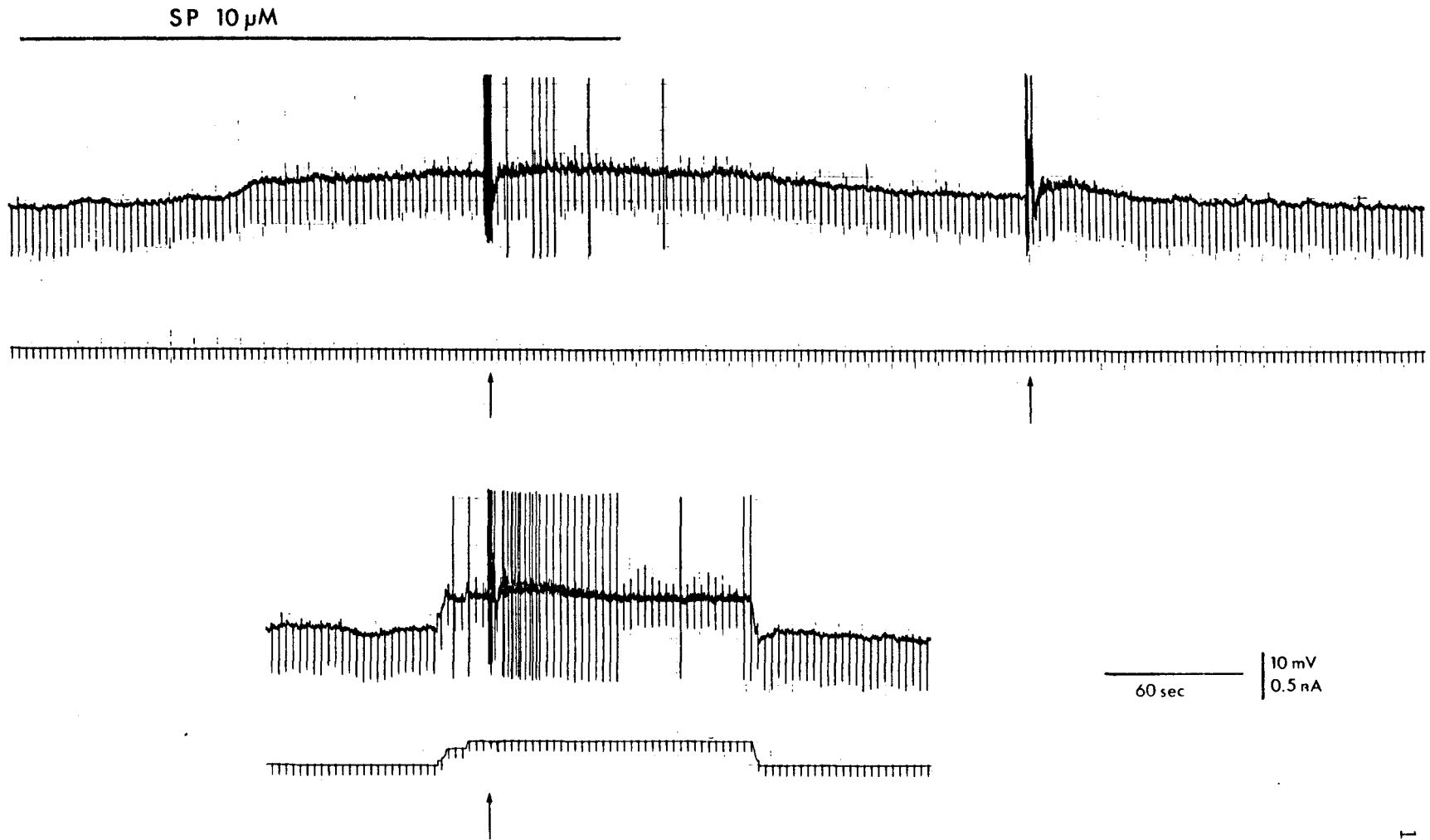
FIGURE 26. Effects of substance P on membrane potential, input

resistance and the LS-EPSP in another rabbit IMG neuron. ·

SP also depolarizes this cell by 8 mV with a decrease in

resistance. During the SP-induced depolarization the cell was

returned to the resting level by current injection. Stimulation

of the ascending mesenteric nerve (16 Hz for 3 sec, arrow)

elicited a LS-EPSP despite the presence of SP. d-TC (50 μM) and

atropine (1 μM) were present throughout the experiment.

FIGURE 26

SP 10 μM

60 sec

10 mV

1 nA
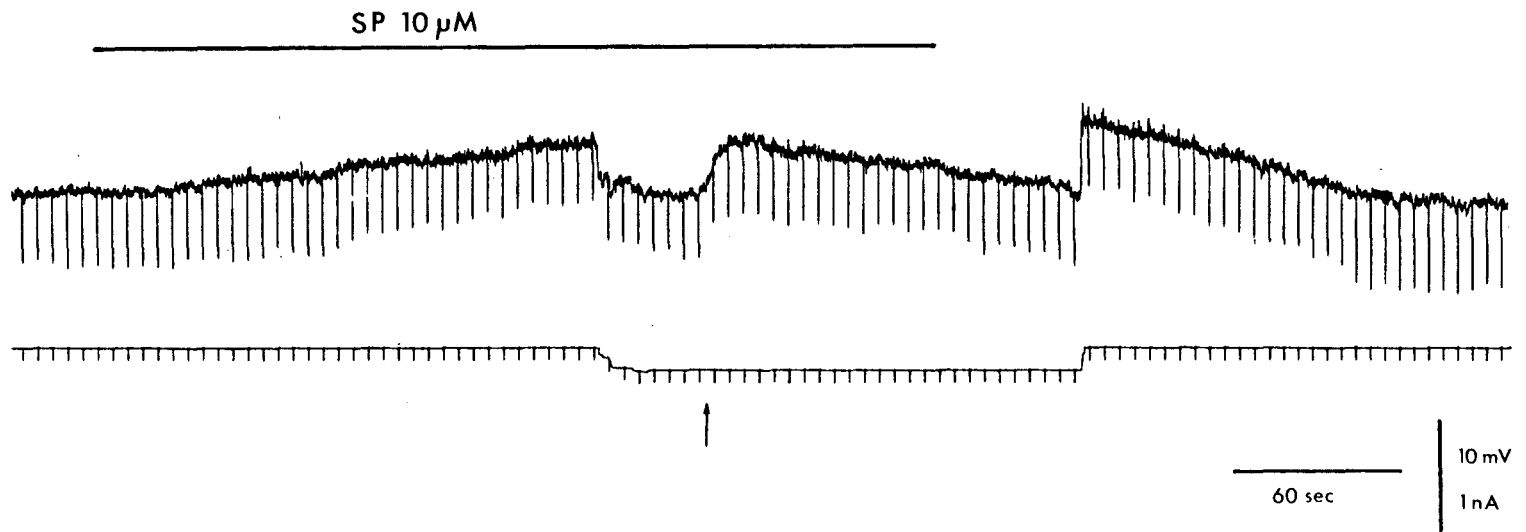
postsynaptic membrane depolarization in any of the cells tested (n=8).

Nor did capsaicin have any affect on the LS-EPSP elicited in these

cells.

e. Vasoactive Intestinal Polypeptide

Very dense networks of VIP-immunoreactivity were observed in the

immunohistochemical studies (see below) and it seemed possible that this

peptide may be involved in non-cholinergic transmission in the rabbit

IMG. VIP (1 nM-10 µM) when applied to the ganglion had no effect on the

E_r or R_{in} of any of the 10 cells tested. In 3 cells, however, a slight

increase in the amplitude of the LS-EPSP was observed in the presence of

VIP.

H. Late Slow Inhibitory Postsynaptic Potential

In addition to the LS-EPSP, a slow hyperpolarizing potential was

observed in a small number of the rabbit IMG neurons. Since this poten-

tial appears with a similar time course to the LS-EPSP but is in oppo-

site direction it was termed the late slow inhibitory postsynatpic

potential (LS-IPSP). A LS-IPSP not preceded by a LS-EPSP was observed

in 3% (6 of 174) of the IMG cells examined. In 10% of the cells both a

LS-IPSP and LS-EPSP were observed. This hyperpolarizing potential was

not affected by nicotinic or muscarinic antagonists, but was blocked in

low Ca^{++}/high Mg^{++} Krebs. Figure 27 shows the response of a cell to

stimulation of the ascending mesenteric nerve and hypogastric nerve

before (top panel) and after (bottom panel) perfusion with atropine (1

µM). Prior to atropine, stimulation of either nerve results in a slow

FIGURE 27. Slow depolarization and slow hyperpolarization in a single

rabbit IMG neuron.

A: Stimulation (30 Hz for 3 sec) of the ascending mesenteric

nerve (AMN) or of the hypogastric nerve (HGN) elicits a slow

depolarization. In the case of hypogastric nerve stimulation the

depolarization is followed by a small hyperpolarization. B:

After perfusion with atropine (1 µM), AMN stimulation elicits a

smaller depolarization. The response to HGN stimulation is now

exclusively in the hyperpolarizing direction.

FIGURE 27
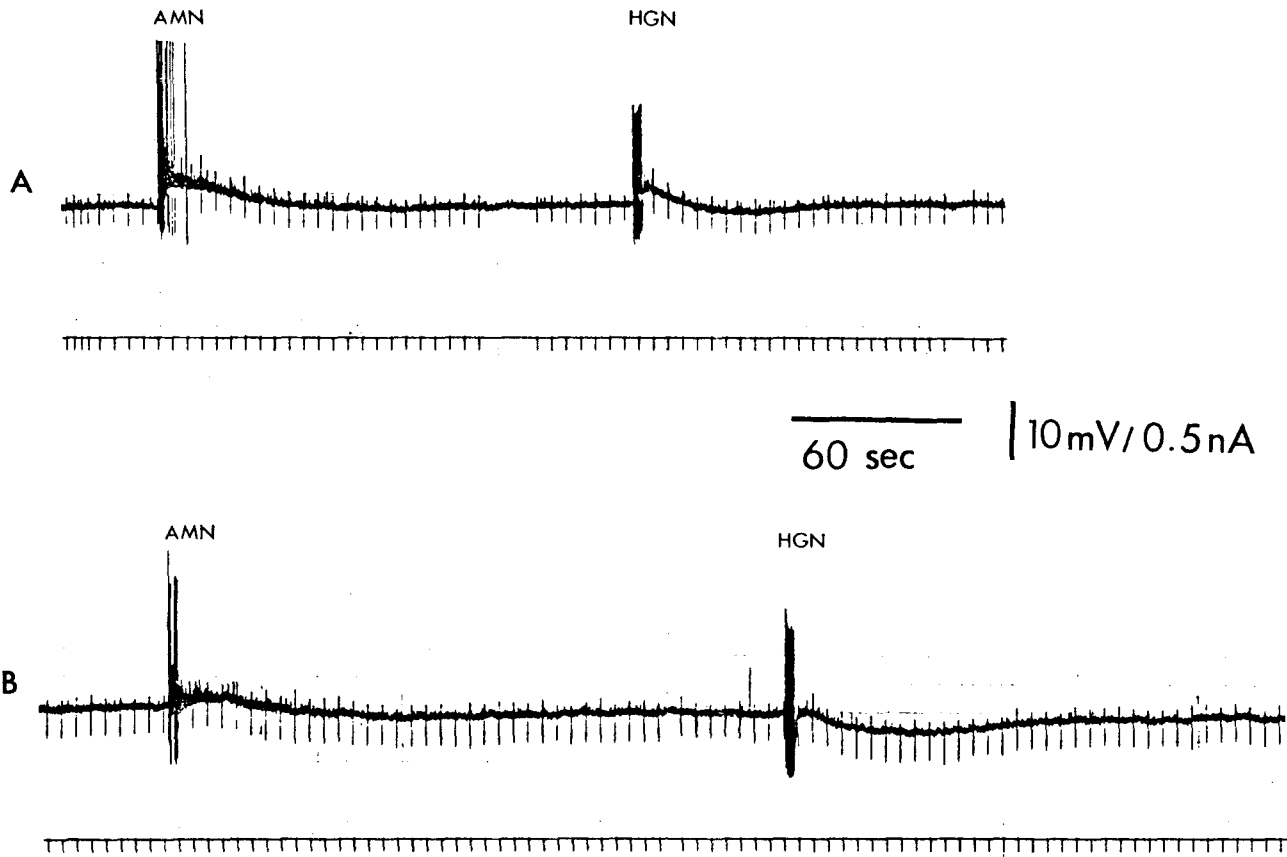
depolarization. A small hyperpolarization following the slow depolarization is apparent after hypogastric nerve stimulation. After atropine perfusion the response to ascending mesenteric nerve stimulation is reduced while the hyperpolarization following hypogastric nerve stimulation is increased.

An interesting, and consistent, property of the LS-IPSP was its voltage sensitivity. The amplitude of the LS-IPSP was always increased in amplitude when the cell was hyperpolarized. Figure 28 illustrates this point. After hyperpolarizing the membrane by only 5 mV the LS-IPSP is greatly increased. The LS-IPSP was always accompanied by an increase in R_{in}.

I. Immunohistochemistry of the Rabbit IMG

The purpose of these studies was to determine whether or not certain peptides were present in the rabbit IMG, which has not been studied previously. Several antigens were chosen for immunohistochemical localization in the rabbit IMG. These include CCK, ENK, LHRH, SOM, SP and VIP. As mentioned in the Methods section, there was some difficulty in examining the rabbit IMG with commercially available antisera, since all of these antisera were raised in rabbits. Consequently, there was a significant amount of nonspecific binding of the secondary antibody, particularly with the FITC technique. These sections were, therefore, pretreated in a solution containing $KMnO_4$ and H_2SO_4 to reduce the unwanted background staining. It is unclear to what extent this treatment might destroy or otherwise alter the antigenic determinants. This may partially explain the relative sparsity of ENK and SP immunoreactiv-

FIGURE 28.   Increase in the amplitude of the LS-IPSP following membrane

hyperpolarization.

Repetitive stimulation (30 Hz for 3 sec) of the aortic branch of

the ascending mesenteric nerve at resting potential elicits a

small depolarization followed by a small hyperpolarization.   When

inward current is passed to hyperpolarize the cell by 5 mV, the

depolarization is nearly abolished while the LS-IPSP is

accentuated.   Note the increased R_{in} accompanying the LS-IPSP.

FIGURE 28

10 mV / 0.5 nA

60 sec

154
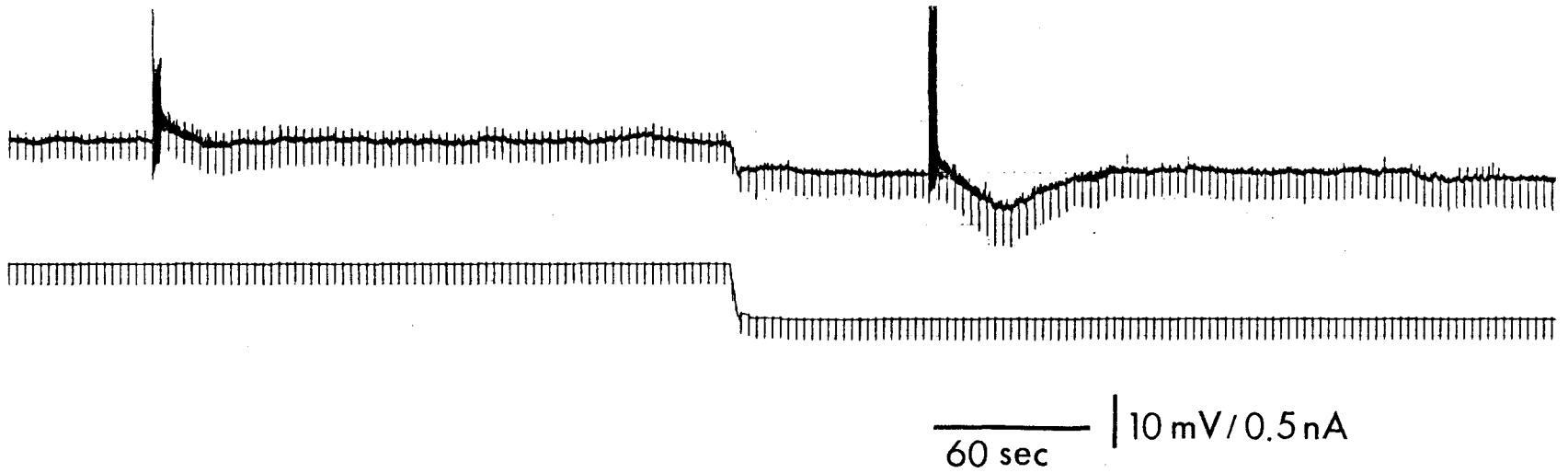
ity we observed in this ganglion. Also, there appeared to be a certain
amount of nonspecific cell body staining with both the FITC and ABC
techniques. Therefore, the presence of substances which have been found
in the cell bodies of other sympathetic ganglia, such as SOM, cannot
definitely determined in the present studies. No significant nonspe-
cific staining of nerve fibers was observed and, therefore, it is con-
cluded that ENK-, SP- and VIP-immunoreactive fibers are present in
fibers in the rabbit IMG. Immunoreactive fibers to CCK, LHRH or SOM
were not observed.

1. Enkephalin Immunoreactivity

The immunoreactivity following incubation with antibody to ENK was
the least intense of the three peptides described here. ENK fibers
appeared throughout the ganglion, usually being more apparent near the
edge of the ganglionic tissue than through the interior of the ganglion.
ENK fibers usually ran seperately to form a weakly immunoreactive net-
work coursing longitudinally through the IMG. Figure 29 illustrates the
ENK fluorescence in the rabbit IMG. The relatively low intensity of ENK
is evident. This was a particular problem in the rabbit IMG due to the
fluorescence of the background, which is evident even with the elution
technique. A section incubated with preabsorbed ENK antibody is shown
in Figure 30. Note the absence of stained fibers and weakly fluorescing
cell bodies. Background was not as much of a problem with the ABC tech-
nique (Figure 31) however, the diffuseness of the ENK immunoreactivity
is still evident here. The lower micrograph in Figure 31 shows the ENK
immunoreactivity around a pair of ganglionic neurons. The ENK fibers

FIGURE 29.   Immunofluorescent micrograph of a rabbit IMG section

incubated with antisera to met-enkephalin.

Faintly ENK-immunoreactive fibers are seen throughout the

ganglionic section.   The fibers generally course longitudinally

through the IMG, rarely encircling the ganglion cells.   (× 350)

FIGURE 29

158
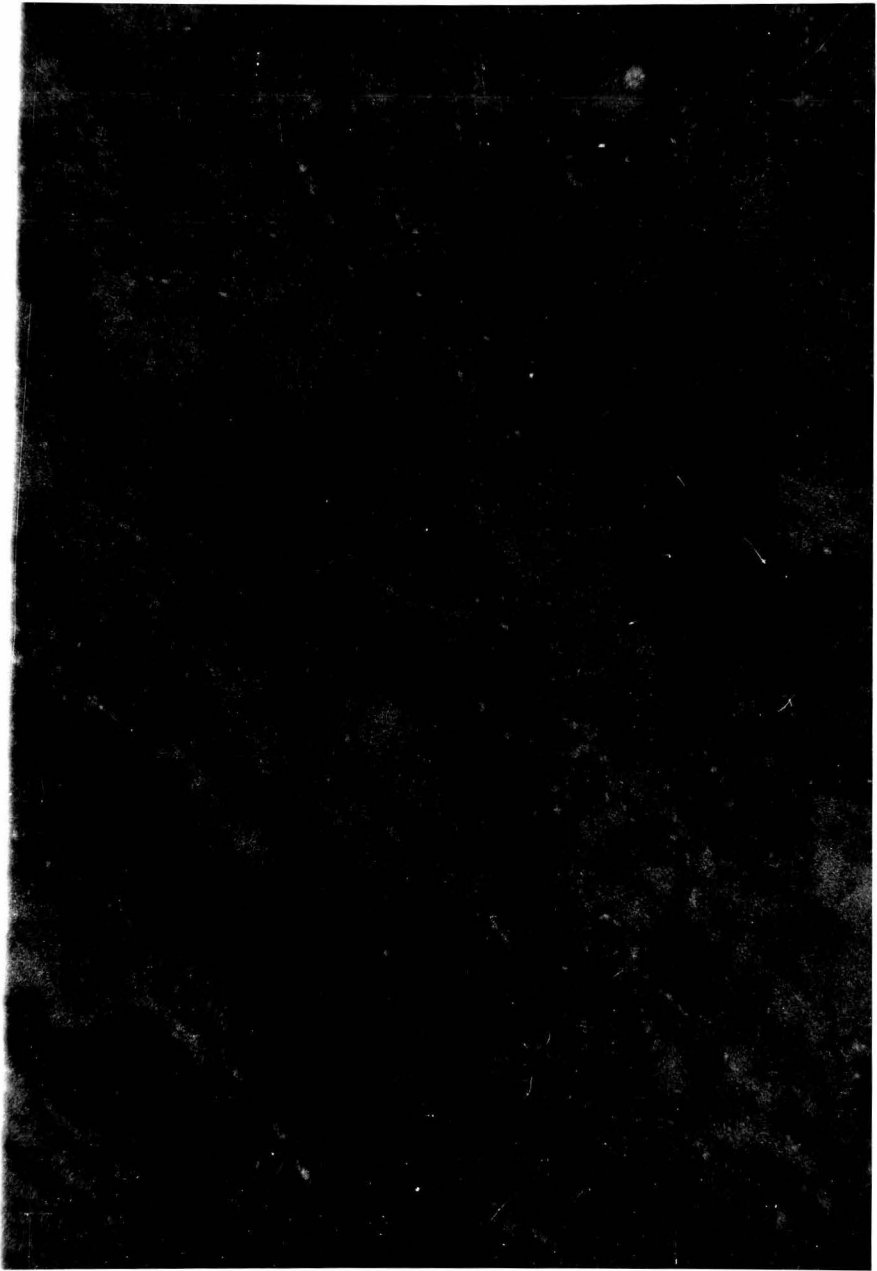
FIGURE 30.   Immunofluorescent micrograph of a rabbit IMG section

incubated with preabsorbed met-enkephalin antisera.

No immunoreactive fibers were seen in sections incubated with

antisera preabsorbed with met-ENK.   Preabsorption was with 100 µg

met-ENK per ml diluted antibody.   (× 350)
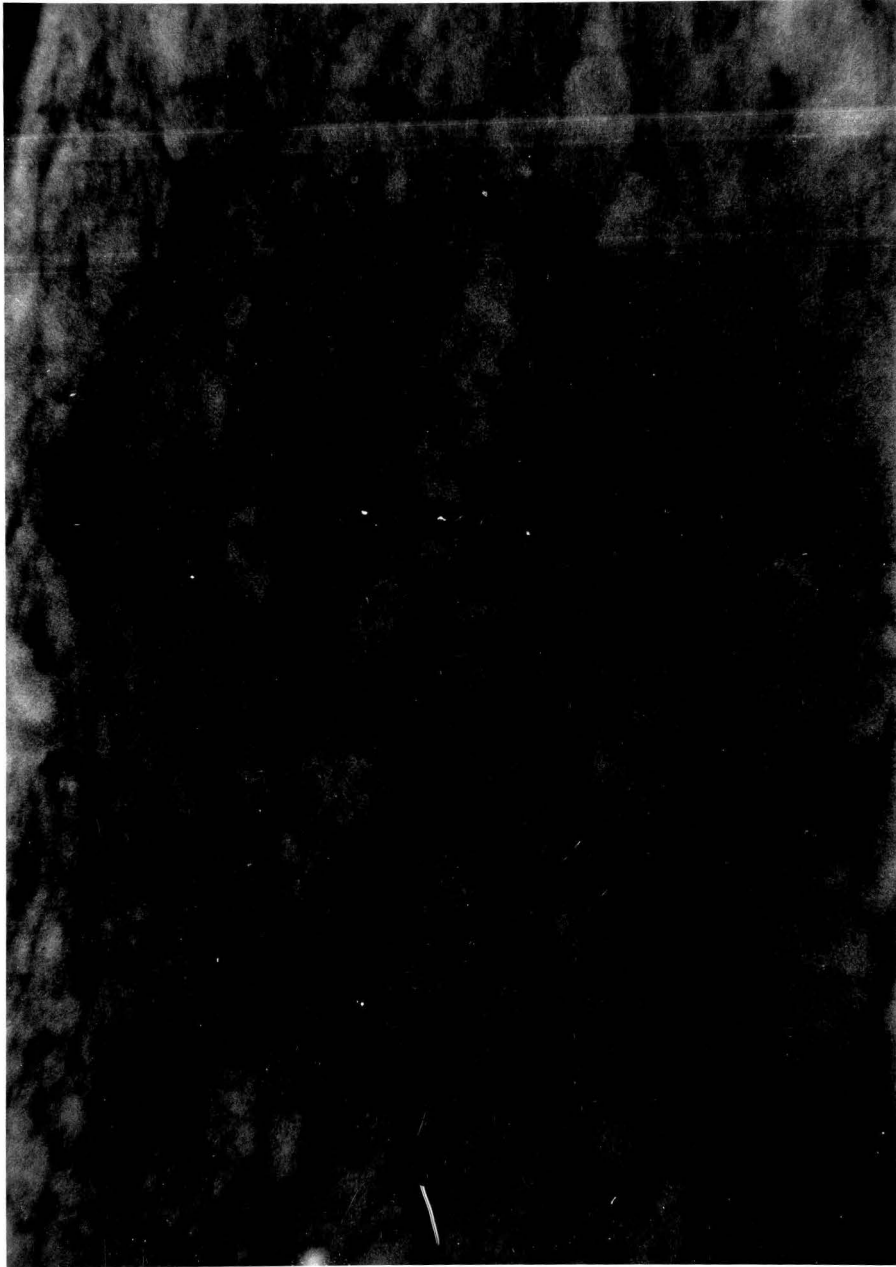
FIGURE 30

FIGURE 31. Micrographs of enkephalin-immunoreactivity in rabbit IMG

sections using the ABC technique.   .

Top: At low power, diffusely distributed ENK-immunoreactive

fibers are seen distributed throughout this ganglion section. (×

525) Bottom: ENK-immunoreactivity distributed around two

ganglionic neurons. Reaction product is seen abutting the cell

bodies at several points, but the fibers do not surround the

cells as do SP or VIP fibers. (× 1050)
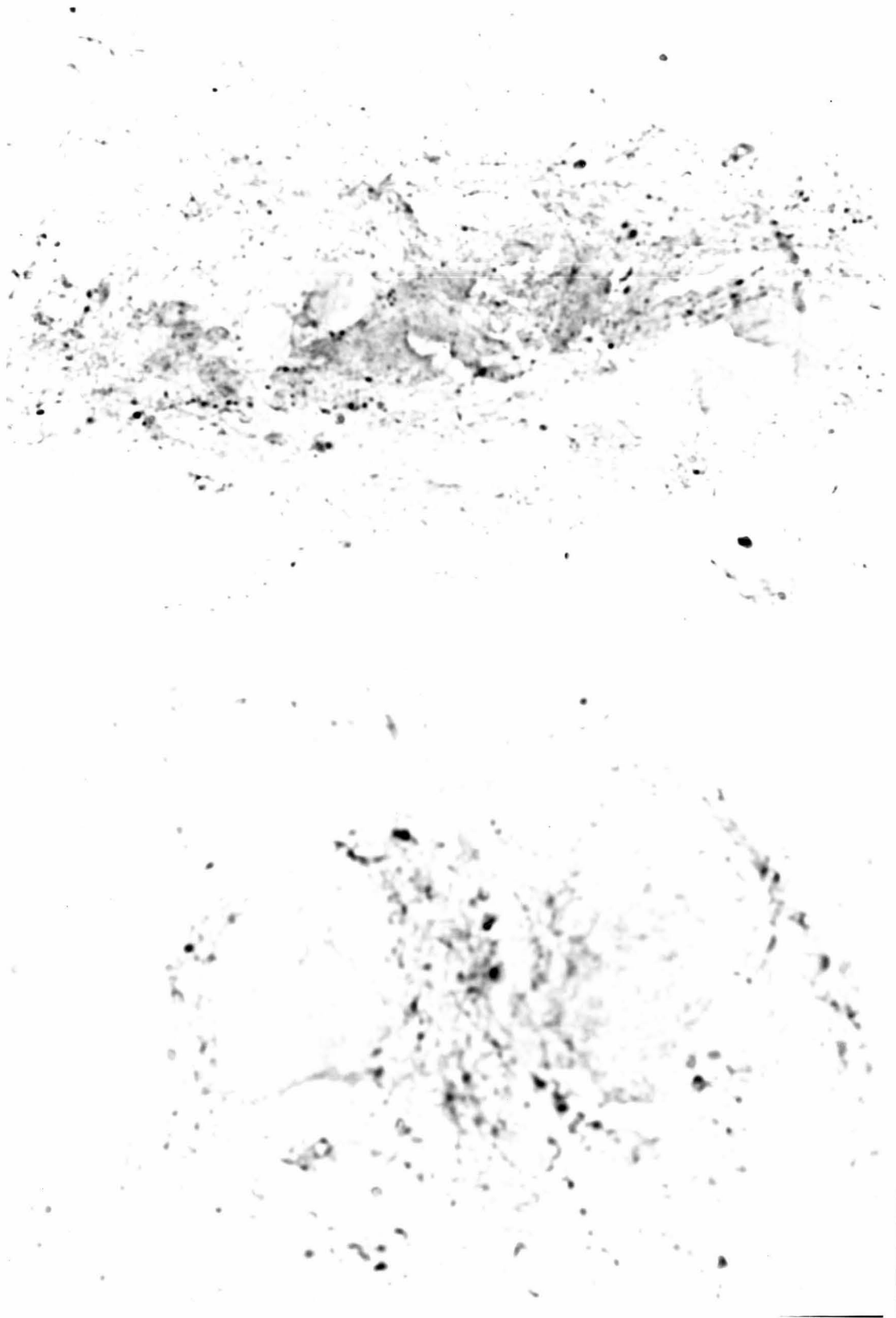
FIGURE 31   161

did not appear to surround the cells as completely as do the SP and VIP fibers. This can be seen in the other micrographs as ENK fibers rarely encircle the ganglionic neurons. ENK fibers reacted by the ABC technique are also shown in Figure 31, top.

2. Substance P Immunoreactivity

The SP immunoreactive fibers were more obvious than the ENK fibers. Figure 32 shows a ganglion section reacted for SP with the FITC technique. The SP fibers course throughout the ganglion, frequently in bundles of fine nerve fibers which branch out to surround the cell bodies. A section incubated with preabsorbed antibody to SP is shown in Figure 33. Note the lack of immunoreactive fibers. A cell surrounded by SP immunoreactive fibers is shown in the bottom panel of Figure 34. The top micrograph, at lower magnification, further illustrates the distribution of SP fibers in the rabbit IMG.

3. Vasoactive Intestinal Peptide Immunoreactivity

The most striking of all the peptide immunoreactivity was that observed following incubation with antibody to VIP (Figure 35). No VIP immunoreactive fibers were observed following preabsorption of the antibodies with VIP (Figure 36). VIP fibers formed a very dense network throughout the IMG, running together in strands and surrounding a majority of the ganglion cells. This network appears as a plexus of fibers in the ganglion. A cell surrounded by VIP immunoreactivity is shown at high magnification in Figure 37.

FIGURE 32.   Fluorescence micrograph of a rabbit IMG section incubated

with antisera to substance P.

Fine, varicose SP-immunoreactive fibers course among the ganglion

cells.   The fibers frequently travel in bundles.   Several fibers

branch to surround the ganglion cell at upper right.   (× 350)

FIGURE 32

FIGURE 33.   Immunofluorescent micrograph of a rabbit IMG section

incubated with preabsorbed substance P antisera.

No immunoreactive fibers were seen in sections incubated with

antisera preabsorbed with SP.   Preabsorption was with 100 μg SP

per ml diluted antibody.   (× 350)
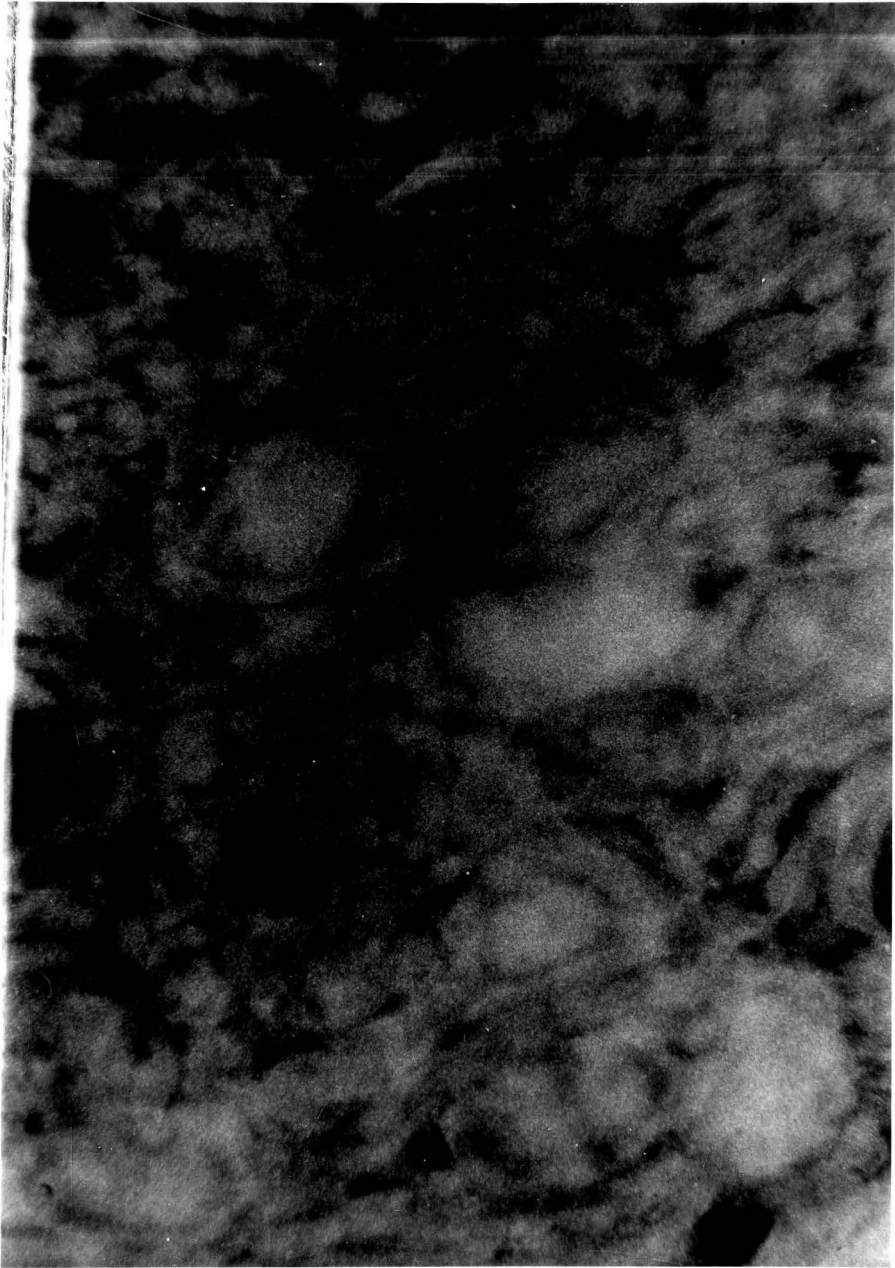
FIGURE 33

FIGURE 34. Micrographs of substance P-immunoreactivity in rabbit IMG

      sections using the ABC technique.

      Top: At low power, bundles of SP-immunoreactive fibers are seen.

      Fibers frequently branch out from these bundles. ($\times$ 525) Bottom:

      SP-immunoreactivity fibers come in close apposition to and

      surround a lightly stained principal ganglionic neuron. ($\times$ 1050)
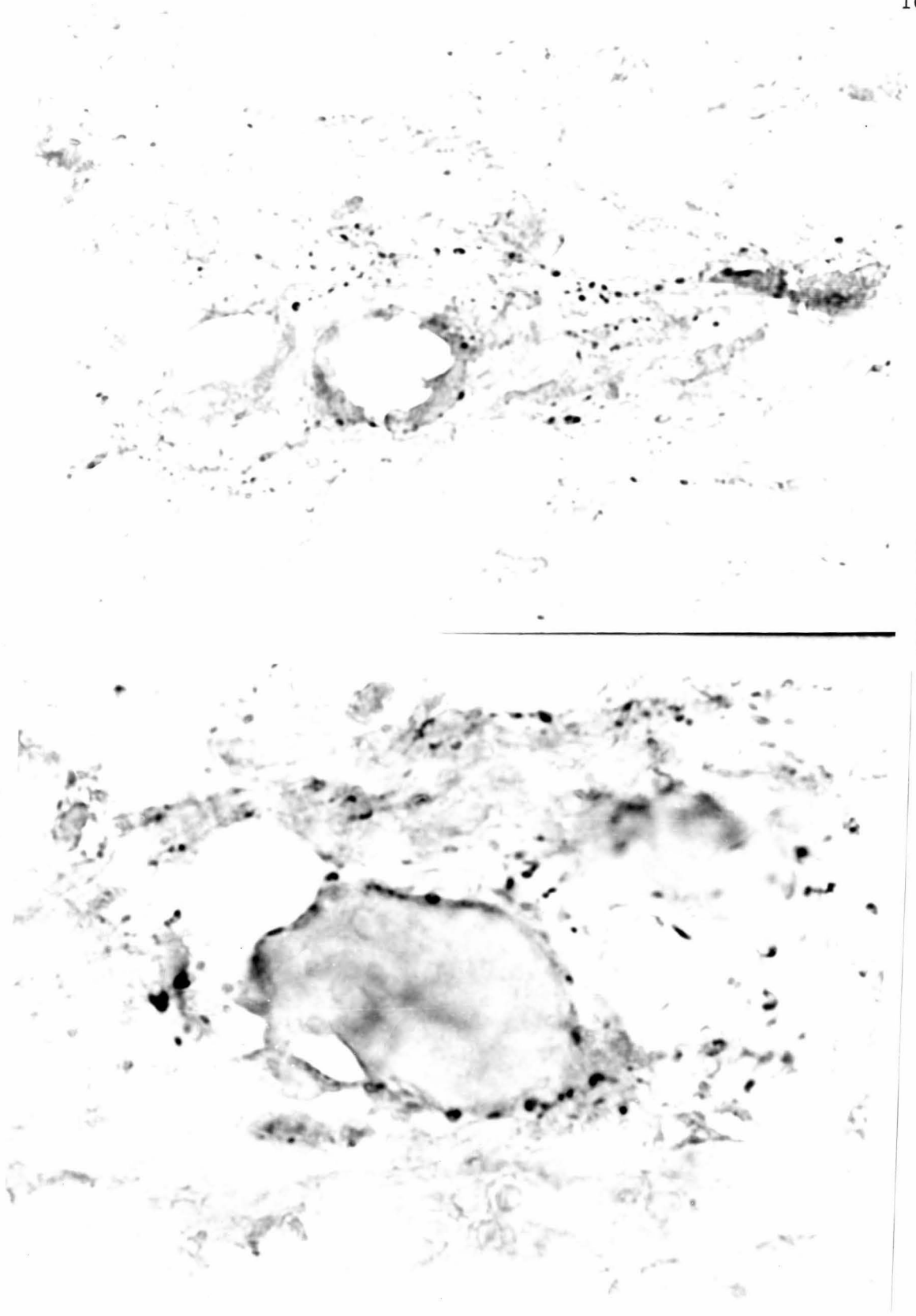
FIGURE 34

FIGURE 35. Fluorescence micrograph of vasoactive intestinal

polypeptideimmunoreactivity in a rabbit IMG section.

A dense network of VIP-immmunoreactivity is seen throughout the

ganglion. Many cells are surrounded by VIP-immunoreactive

fibers. (× 350)

FIGURE 35 170
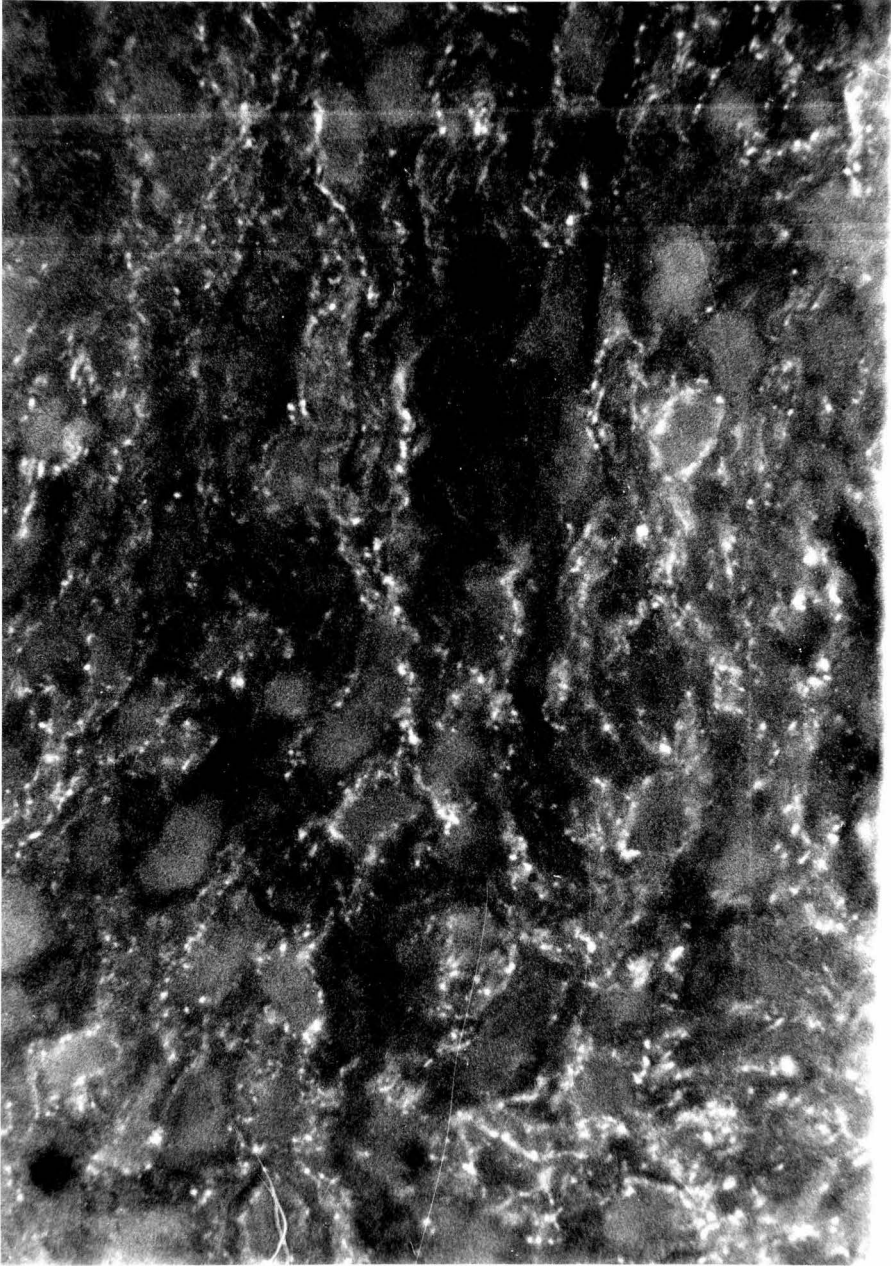
FIGURE 36.   Immunofluorescent micrograph of a rabbit IMG section

incubated with preabsorbed vasoactive intestinal polypeptide

antisera.

No immunoreactive fibers were seen in sections incubated with

antisera preabsorbed with VIP.   Preabsorption was with 100 µg VIP

per ml diluted antibody.   (× 350)

FIGURE 36 172

FIGURE 37. Micrographs of vasoactive intestinal polypeptide-
immunoreactivity in rabbit IMG sections using the ABC technique.
Top: At low power, many VIP-immunoreactive fibers are seen
coursing throughout this ganglion section and surrounding a
ganglion cell in the center. (× 525) Bottom: High power
micrograph of a principal ganglionic neuron encircled by
intensely immunoreactive VIP fibers. (× 1050)
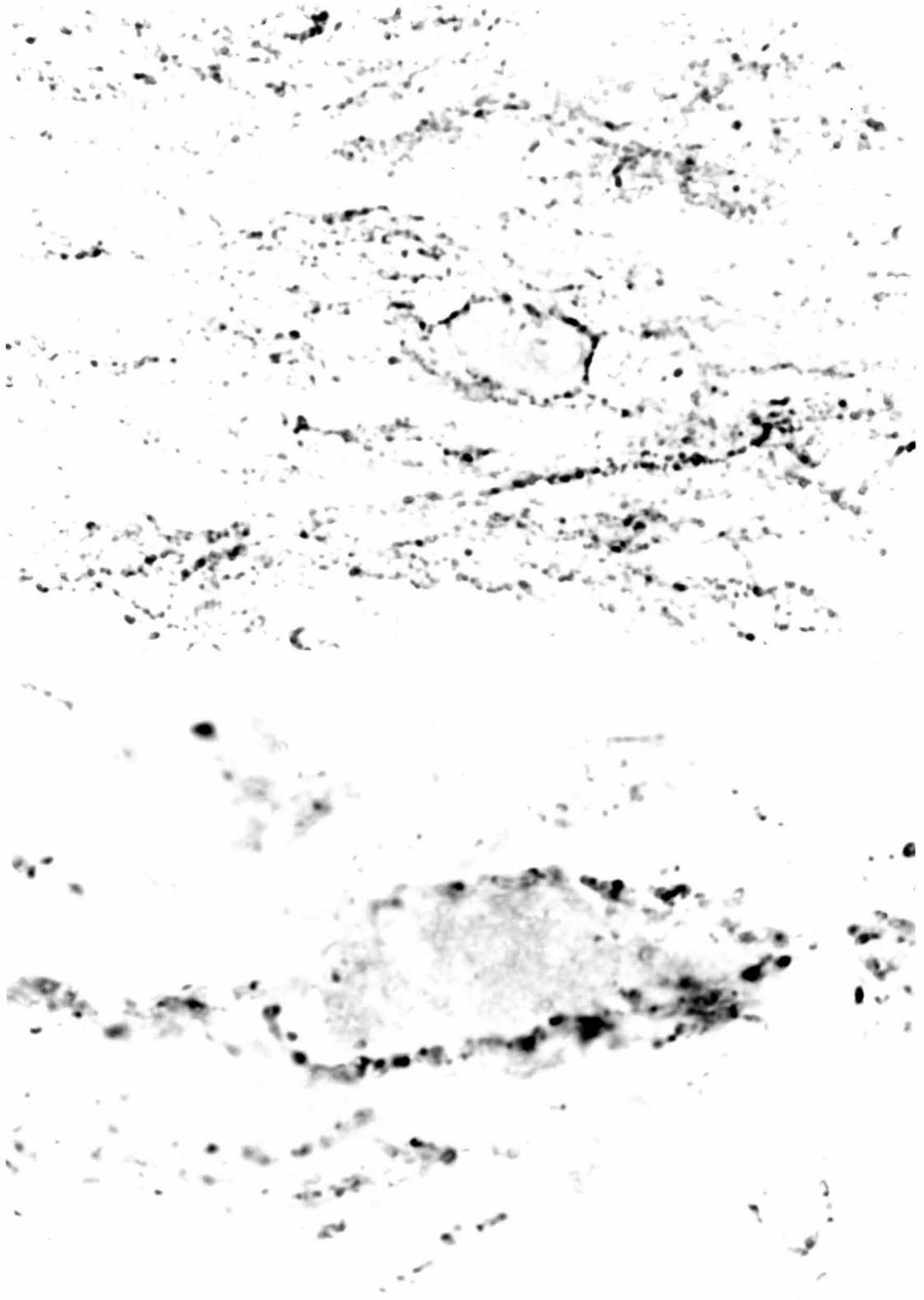
FIGURE 37

All of the above peptides were also observed in the nerve trunks of the IMG. No fibers were observed following omission of the primary antibody (Figure 38) or following preabsorption of the primary antibodies with the antigen of interest (Figures 30, 33 and 36); however, some nonspecific staining of cell bodies was observed with both the FITC and ABC techniques. For example, a cell lightly stained with reaction product is apparent in the right center of Figure 34. This finding made it impossible to determine with certainty whether or not any of these peptides were present in the cell bodies.

176

FIGURE 38. Rabbit IMG section processed with the ABC technique in the

absence of a primary antibody.

This ganglion section was processed identically to the other ABC

sections shown except that a primary antibody was omitted. Note

the lack of immunoreactive fibers in the absence of a primary

antibody. (× 525)

FIGURE 38   177
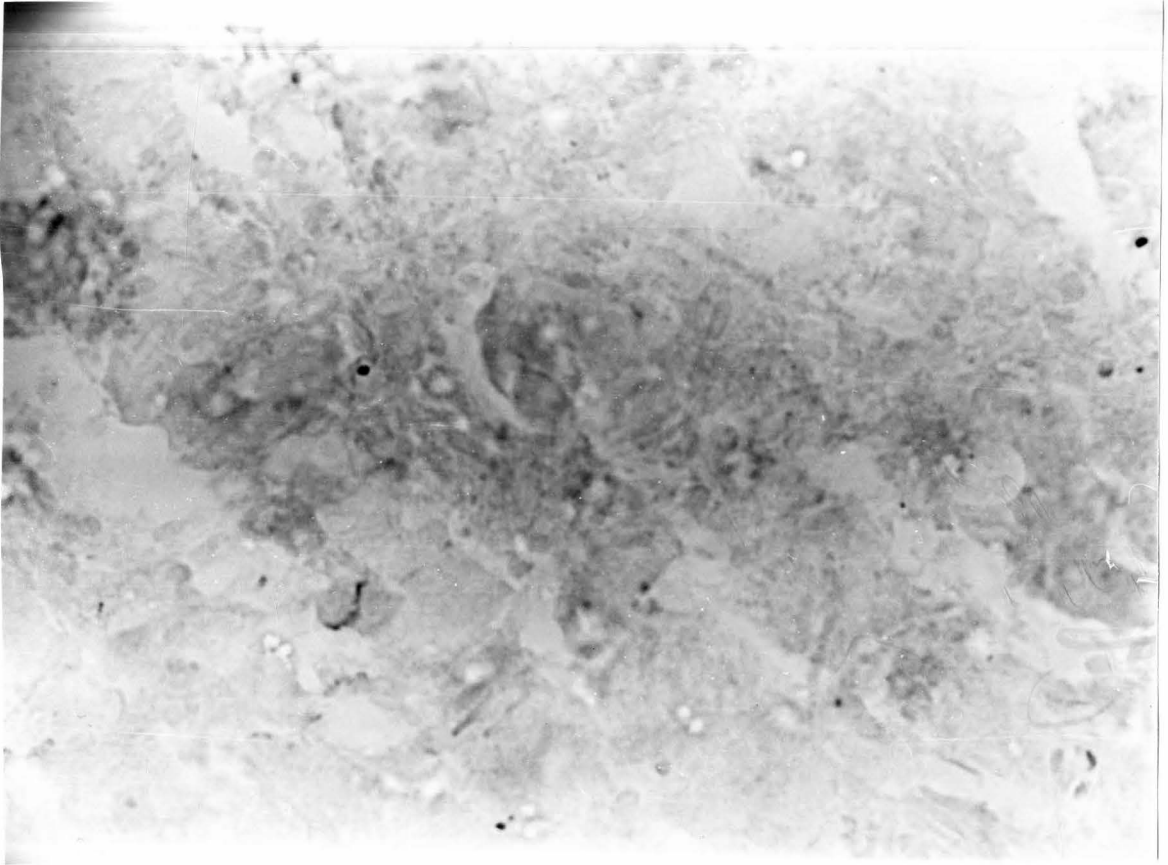
V. DISCUSSION

Previous studies have indicated the complexity of neural transmission in the prevertebral sympathetic ganglia. This complexity is illustrated by the findings that 1) the prevertebral ganglia are innervated not only by preganglionic neurons of central origin but also receive afferent inputs from the effector organs, 2) immunoreactivity to a number of peptides is present in neuronal structures in these ganglia and 3) slow postsynaptic potentials not mediated by ACh can be elicited in the neurons of these ganglia. These results demonstrate that the prevertebral ganglia do not function solely to relay cholinergic preganglionic impulses from the spinal cord to the peripheral visceral organs, but these ganglia are also involved in the integration of both centrally and peripherally originating synaptic impulses involving both ACh and noncholinergic transmitters. These findings have been obtained mainly through investigations on the guinea pig prevertebral ganglia. It was of interest to ascertain whether or not similar phenomena occur in the prevertebral ganglia of other species. Consequently, the present study was undertaken to examine synaptic transmission in the rabbit IMG. Neither the intracellular electrophysiology nor the immunohistochemistry of the rabbit prevertebral ganglia have been previously studied.

A. Anatomy

There are several differences between the anatomy of the rabbit IMG and the IMG of other species, most obviously the size of the ganglion. Apparently, as the size of the animal increases, so does the size of the IMG. For example, in the rat the IMG is a relatively small and difficult to find ganglion, in the guinea pig the ganglion is somewhat larger, in the cat the IMG consists of several large lobes of ganglionic tissue and in the human the IMG appears not as a distinct ganglion but as a plexus. The rabbit IMG is larger than the guinea pig IMG and smaller than the cat IMG. Also, the arrangement of the nerve trunks of the IMG differs from species to species. In the rabbit the ascending mesenteric nerve is the most evident of the nerves associated with the ganglion, while the fibers along the inferior mesenteric artery, the colonic fibers, are fewer and more diffuse than in the guinea pig or cat. This finding led Langley & Anderson (1896b) to suggest that in the rabbit more fibers course to the colon through the ascending mesenteric nerve. The hypogastric nerve in the rabbit most often appears as a single nerve bundle, while in other species two separate nerves are seen.

B. Membrane Properties

While the arrangement of the ganglion shows considerable species variation, the properties of the principal ganglionic neurons are very similar in the different species examined, and are, in fact, also similar to the properties of the cells in other sympathetic ganglia such as the superior cervical ganglion and the paravertebral ganglia (see Table 3). This similarity generally holds for both passive and active mem-

brane properties, although subtle differences do exist. Some of the similarities and differences are discussed below.

1. Current-Voltage Relationship

The current-voltage curves in the rabbit IMG neurons were fairly linear with hyperpolarization to about 40 mV from Er and with very small depolarizing pulses (Figure 3). With larger depolarizations delayed rectification became apparent and with large hyperpolarizations anomalous rectification was seen. Both delayed and anomalous rectification have been reported for a variety of other sympathetic ganglion preparations. Delayed rectification has been reported in the sympathetic neurons of the bullfrog paravertebral ganglia (Nishi & Koketsu, 1960), guinea pig thoracic chain ganglia (Blackman & Purves, 1969), guinea pig pelvic plexus (Blackman, Crowcroft, Devine, Holman & Yonemura, 1969) and in the rabbit SCG (Christ & Nishi, 1973). The delayed rectification involves an increase in membrane conductance as the cell is depolarized. This increase occurs with a delay after the onset of the depolarization and is due to the activation of a voltage dependent K^+ current (Grundfest, 1961). Anomalous rectification has been studied in the rabbit SCG (Christ & Nishi, 1973) and is apparent at approximately 30-40 mV negative to E_r. Anomalous rectification has also been reported for the guinea pig IMG (Crowcroft & Szurszewski, 1971) and pelvic ganglia (Blackman & Purves, 1969; Crowcroft & Szurszewski, 1971). Anomalous rectification also involves an increase in K^+ conductance, but at hyperpolarized levels (Christ & Nishi, 1973). No anomalous rectification was observed in the guinea pig paravertebral ganglia, the guinea pig SCG or

the rat SCG; however, these studies apparently only examined hyperpolar-
izations to levels about 40 mV more negative than the E_r value. It is
possible that with greater hyperpolarizations anomalous rectification
would have been observed. It has been suggested that the conductance
change during anomalous rectification occurs on the dendritic membrane
rather than at the soma membrane (Christ & Nishi, 1973). Thus, there
may be a correlation between the number of dendrites of a cell and the
degree of anomalous rectification. This would be consistent with the
absence of anomalous rectification in bullfrog sympathetic ganglion
cells (Nishi & Koketsu, 1960) and the presence of anomalous rectifica-
tion in the multipolar rabbit IMG neurons. In conclusion, these voltage
dependent properties have been widely observed in sympathetic neurons.

2. Action Potential

In the rabbit IMG, as well as in other sympathetic ganglia
(Haefely, 1972), the depolarization needed to reach threshold for the
action potential is similar following either direct intracellular or
orthodromic stimulation. This threshold is similar for a wide variety
of sympathetic ganglia as shown in Table 3. In general, a depolariza-
tion to between -40 and -35 mV is needed to result in an action poten-
tial.

a. Amplitude

With regard to action potential amplitude, several studies have
noted that the orthodromic spike was slightly smaller than the direct
spike (Nishi & Koketsu, 1960; Blackman et al., 1969; Perri, Sacchi &

Casella,1970). The orthodromic spike in the rabbit IMG averaged 2 mV smaller than the direct spike and 5 mV smaller than the antidromic spike (Table 4); however, statistical tests showed these differences were not significant. Further, a paired t-test for those cells where both direct and orthodromic spikes were measured did not approach significance. A possible explanation for the orthodromic spike being smaller than the direct spike is that during an orthodromic spike the resistance of the membrane at the synapse is decreased by the acting transmitter. This results in a low resistance pathway for the shunting of the current generating the action potential (Fatt & Katz, 1951). In the IMG, however, there are few axosomatic synapses (Elfvin, 1971a) and a decreased resistance of the dendritic membrane would provide little shunting effect on the soma spike. Therefore, it must be concluded that the amplitudes of the direct, antidromic and orthodromic spikes are not different in rabbit IMG cells.

b. Afterhyperpolarization

The action potential in the rabbit IMG was followed by a long afterhyperpolarization, frequently lasting over 250 msec. The afterhyperpolarization is generated by increases in K^+ conductances. Two K^+ conductances have been implicated in the generation of the afterhyperpolarization--a voltage-dependent G_K and a Ca^{++}-dependent G_K. The afterhyperpolarization in sympathetic neurons of the rat SCG were thoroughly investigated by McAfee and Yarowsky (1979). They found both of these G_Ks to be involved in the afterhyperpolarization. The voltage-dependent G_K, also known as the delayed rectifier current, is a short-

latency voltage sensitive conductance while the Ca^{++}-dependent G_K is of
longer latency and largely dependent on Ca^{++}. Considering these find-
ings and the findings of similar Ca^{++}-dependent currents in other neu-
rons, the question arose as to whether a similar Ca^{++}-dependent G_K might
be involved in the long duration of the aftehryperpolarization of the
rabbit IMG cells. The afterhyperpolarization was reduced in amplitude
and duration in low Ca^{++} Krebs (Figure 7B). This indicates that a
Ca^{++}-dependent G_K is present in the rabbit IMG cells. Such a finding
stresses the importance of Ca^{++} in controlling the electrical activity
of the cell. The afterhyperpolarization has been shown to be important
in controlling the rate of firing of guinea pig IMG neurons (Weems &
Szurszewski, 1978). Neuronal excitability is reduced during the afte-
rhyperpolarization as a result of both the hyperpolarization and the
accompanying increased membrane conductance. Thus, the afterhyperpolar-
ization serves to regulate the frequency of firing of the postganglionic
neurons. Another suggested function of Ca^{++}-dependent G_K is to provide
a link between cellular metabolism and membrane conductance (Meech,
1978). Thus, Ca^{++} in the cytoplasm can modify the membrane response to
stimulation and can be modified by the metabolic state of the cell.
This may provide a mechanism whereby the intracellular environment can
influence synaptic transmission.

c. Antidromic Spike

The occurrence of an antidromic spike was rare in the rabbit IMG
cells. Only about 4% of the cells examined in this study exhibited
antidromic spikes. This is similar to what occurs in the guinea pig IMG

(Crowcroft & Szurszewski, 1971; Dun, personal communication) and the cat IMG (Weems, personal communication) where the appearance of an antidromic spike is an infrequent occurrence. The appearance of an antidromic spike does not seem to depend on the nerve being stimulated since three of the antidromic spikes followed hypogastric nerve stimulation, another three followed ascending mesenteric nerve stimulation and the other two following activiation of the aortic branch of the ascending mesenteric nerve. Since stimulation of the nerves almost always resulted in orthodromic action potentials, one possibility would be that the antidromic spike collided with the propagated orthodromic spike along the axon, preventing conduction of the antdromic spike to the soma. This does not seem likely since the conduction velocity of the postganglionic fibers was greater than that of the preganglionic fibers and there is a synaptic delay involved in the orthodromic response; however, such a collision may have been a factor in cells which were innervated by the more rapidly conducting preganglionic fibers or in cells whose axons took a more circuitous route than the preganglionic fibers. Another possibility may be that the axons of these cells have electrical properties which prevent antidromic conduction. There may be points along the axon where antidromic propagation is difficult. Branch points in axons would be one possible point; however, it has not been established whether or not postganglionic axons give off collaterals prior to the terminal arborizations at the effector organ. Another point would be the sudden enlargement at the axon-soma junction.

3. Conduction Velocity

a. Preganglionic Fibers

A wide range of conduction velocities have been reported for sympathetic preganglionic fibers. For the preganglionic fibers in the sympathetic trunk values of conduction velocity range from 0.5-15 m/sec (Erulkar & woodward, 1968; Blackman & Purves, 1969; Blackman et al., 1969; Perri et al., 1970). Also, there is some interspecies variation as in the rat cervical sympathetic trunk two groups of fibers conducting at 0.5-1.0 m/sec and 3-4 m/sec were found while, in the same study, three groups were found in the guinea pig cervical trunk conducting at 1.5, 4.4 and 15.4 m/sec (Perri et al., 1970). The conduction velocity of the slow conducting group of fibers to the rabbit IMG is slower than the above values while the faster group of fibers seen in the present study is in a similar range to those above.

The conduction velocites in the rabbit IMG are more consistent with other studies involving the IMG, particularly those of Brown and Pascoe (1952) and Krier et al. (1982). Both of these studies found two groups of preganglionic fibers with the fastest group conducting at 2-7 m/sec and the slow group at 0.25 m/sec (Brown & Pascoe, 1952) or 0.5-2 m/sec (Krier et al., 1982). In general, the conduction velocity of the preganglionic fibers to the abdominal prevertebral ganglia are slow conducting fibers. These fibers would therefore be classified as C fibers.

b. Postganglionic Fibers

The reported conduction velocities of postganglionic sympathetic fibers are similarly variant, ranging from 0.6-6 m/sec (Eccles, 1935; Bronk, Tower, Solandt & Larrabee, 1938; Douglas & Ritchie, 1956; Kosterlitz, Thompson & Wallis, 1964). The most frequently reported values range from 0.6-3 m/sec. The value obtained in the present work is not far from the value of 0.45 m/sec obtained on the same ganglion with extracellular recordings (Brown & Pascoe, 1952). In the cat hypogastric nerve, composed mainly of postganglionic fibers, the largest group of fibers was found to conduct at 0.9-1.6 m/sec (Lloyd, 1937), which is slightly larger than the value found here.

There are several factors which may contribute to the variability of such estimates. First, in the calculation of both pre- and postganglionic conduction velocities, the distance from the stimulating to recording electrode was estimated as a straight line through the nerve and the ganglion. It is quite possible that the fiber involved does not take such a direct route, but may meander through the ganglion on its way to the cell from which the recording was made. If this is the case, the distance measured would be an underestimate and, resultantly, so would the calculated conduction velocity.

The second factor is synaptic delay and involves only the estimates of preganglionic conduction velocity. One method for the calculation of synaptic delay is to plot latency of the response (y-axis) vs. distance from stimulating to recording electrode (x-axis) while placing the stimulating electrode at various points along the preganglionic

nerve trunk. This gives a line with slope equal to the reciprocal of the conduction velocity and a y-intercept equal to the synaptic delay. This is the method used by Kreulen and Szurszewski (1979b) in the guinea pig celiac plexus. Their value of synaptic delay equal to 9.3 msec was used in the calculation of preganglionic conduction velocity here. Our method of stimulation did not allow for such a calculation. Other estimates of synaptic delay have been somewhat variable. In the cat IMG values of 4.5-6 msec were obtained (Lloyd, 1937; Job & Lundberg, 1952). In the rabbit SCG, the delay from stimulation of the preganglionic nerve terminal to the F-EPSP was only 1.5-2 msec (Christ & Nishi, 1971). If the actual synaptic delay in the rabbit IMG is larger, conduction velocity would be an underestimate, if smaller our conduction velocity is an overestimate.

C. Fast-Excitatory Postsynaptic Potential

The characteristics of the F-EPSP appear very similar for the various sympathetic ganglia studied (Nishi & Koketsu, 1960; Blackman & Purves, 1969; Blackman et al., 1969; Perri et al., 1970). The description of the F-EPSP of rabbit IMG cells presented here is consistent with that presented in these other reports. One invariable finding is that the time constant of decay of the F-EPSP is longer than τ_m. In the rabbit IMG cells the time constant of decay of the F-EPSP was twice as long as τ_m. This has been taken as evidence that the transmitter action outlasts the peak of the F-EPSP (Coombs, Curtis & Eccles, 1956).

The F-EPSP was eliminated in low Ca^{++} solution and, as expected, was antagonized by the nicotinic cholinergic antagonist d-TC. These

results indicate that, as in other sympathetic ganglia, a F-EPSP occurs following the release of ACh from the preganglionic nerve fibers and the interaction of ACh with nicotinic receptors on the postganglionic cell.

D. Number of Cholinergic Inputs

There exist a large number of cholinergic inputs to each rabbit IMG neuron, on average 42. These inputs usually summated to result in the appearance of two, frequently three, action potentials in the post-ganglionic cell. In a study on the inputs to the guinea pig SCG the number of fibers to each cell was estimated at 10 (Nja & Purves, 1977). In the rabbit SCG this number has been estimated at 8 (Wallis & North, 1978). Similar to the rabbit IMG, cells in the guinea pig IMG receive an average of 40 inputs (Crowcroft & Szurszewski, 1971).

The number calculated in the present study may even be an underes-timate. Not all of the fibers which enter the ganglion were examined. Some of the fibers are attached to the ganglion separately from the major nerve trunks examined here. For example, some fibers from the IMG course along the inferior mesenteric artery. These fibers were not stimulated. Also, we cannot be sure that all of the fibers responded to stimulation in a given nerve. Perhaps some fibers were insulated from the stimulus or for some other reason did not respond to the stimulus. Some of the inputs may have been undetected because they occurred at the same threshold and with the same latency as another F-EPSP and, thus, two inputs were counted as one. In any case, the degree of convergence of presynaptic inputs to cells in the rabbit IMG is clearly significant.

On the basis of the results obtained in studies of the SCG, it was calculated that each preganglionic fiber must innervate 50-240 postganglionic cells (Nja & Purves, 1977; Wallis & North, 1978). This has been taken as a further illustration of the diffuse control exerted by the sympathetic nervous system. In order to determine the number of cells innervated by each preganglionic fiber the ratio of preganglionic to postganglionic fibers must be known. This information has not been determined with respect to the rabbit IMG. An estimate has been made in the cat IMG, however. This estimate was 1 preganglionic fiber for every 3 postganglionic neurons (Harris, 1943) assuming that none of the preganglionics passing through the ganglion to the hypogastric nerve synapsed in the ganglion. If these fibers did synapse the ratio would be 1/1.5. Further, this study only counted fibers of lumbar spinal origin. It is now known that the IMG receives cholinergic inputs of peripheral origin (Crowcroft et al., 1971) and preganglionics probably also enter the IMG via the ascending mesenteric nerves. Interspecies differences in the preganglionic/postganglionic ratio have been shown to be related more to differences in the number of postganglionic cells than to differences in the number of preganglionic fibers (Ebbesson, 1963). Since the rabbit IMG is smaller than the cat IMG, and assuming size is related to cell number, one would expect an even higher ratio in the rabbit IMG. Considering these factors a preganglionic/postganglionic ratio near 1/1 does not seem unreasonable in the rabbit IMG. If we accept this ratio then each preganglionic fiber would only innervate approximately 40 postganglionic neurons, a number considerably smaller

than the 200 obtained in the SCG. Since some of these inputs may arise from the gut, the use of the term preganglionic in the present context is not restricted to the classical preganglionic fibers arising in the spinal cord, but may also include cholinergic fibers arising in the gut. Since these fibers of different origin cannot be distinguished, the term preganglionic includes any fiber which causes the appearance of a F-EPSP in a rabbit IMG neuron.

The number of inputs to the rabbit IMG cells may be indicative of the degree of dendritic branching of the cells. In the rabbit ciliary ganglion it has been found that cells which lack dendrites are generally innervated by a single axon, whereas neurons with increasing numbers of dendrites receive innervation from a proportionally greater number of axons (Purves & Hume, 1981). If this organgization extends to the prevertebral ganglia it would be concluded that the rabbit IMG cells have extensive dendrites.

E. Slow Inhibitory Postsynaptic Potential

A slow IPSP was not observed in the rabbit IMG. A hyperpolarization was observed following repetitive neruonal spiking in some cells (see Figure 12); however, this was not a synaptic potential since it was mimicked by direct intracellular stimulation and disappeared when the spiking was blocked by d-TC. Therefore, this potential was the result of summating action potential afterhyperpolarizations. A S-IPSP has been observed in the guinea pig IMG (Ma, Dun & Jiang, 1983). This response differs from the S-IPSP in other sympathetic ganglia in that it is not atropine-sensitive. The response that has been termed the

LS-IPSP in the rabbit IMG does not appear to be equivalent to the S-IPSP because its time course is much longer and the LS-IPSP was accompanied by an increased R_{in} as opposed to the S-IPSP in the guinea pig IMG which was accompanied by a decreased resistance.

F. Slow Excitatory Postsynaptic Potential

Recorded intracellularly as the S-EPSP, this response was first recorded extracellularly from mammalian ganglia as the LN wave (Eccles, 1952). The muscarinic nature of this response was revealed with extracellular recordings (Eccles & Libet, 1961) and subsequently confirmed intracellularly (Libet & Tosaka, 1966). Consistent with other reports (Kobayashi & Libet, 1968; Weight & Votava, 1970) a decrease in membrane conductance was observed during the S-EPSP in the rabbit IMG and the response was blocked by atropine.

Two mechanisms have been proposed as contributing to the S-EPSP in mammalian neurons (Hashiguchi, Kobayashi, Tosaka & Libet, 1982). In the range of E_m from -20 to -60 mV a voltage sensitive outward potassium current, the M current (Brown & Adams, 1980), is active. When E_m is in this range suppression of the M current results in a S-EPSP with an accompanying increase in R_{in}. At E_m more negative than -60 mV the M current is inactivated and unable to contribute to the S-EPSP. At this level an increase in intracellular cylic-GMP has been proposed as responsible for the S-EPSP. No conductance change is involved in this response. An increased R_{in} was observed during the S-EPSP in the rabbit IMG. This may be explained by the fact that the E_r of these cells was above -60 mV, where a suppression of the M current is important.

G. Late Slow Excitatory Postsynaptic Potential

A LS-EPSP was observed in 63% of the cells in the rabbit IMG. This is slightly less than the percentage of cells exhibiting a LS-EPSP in other ganglia. In the guinea pig IMG this figure was 70-80% (Neild, 1978; Tsunoo et al., 1982). In the bullfrog 90% of B cells and 75% of C cells exhibit a LS-EPSP (Jan & Jan, 1982). The amplitude of the LS-EPSP in the rabbit is similar to the response in these other ganglia.

With regard to membrane resistance changes, the LS-EPSP in the rabbit was again similar to the bullfrog and guinea pig. An increase or no change in R_{in} was observed in the rabbit IMG. In the bullfrog the LS-EPSP is accompanied by an incresed R_{in}. In the guinea pig an increase or no change was usually obseved (Dun & Jiang, 1982; Tsunoo et al., 1982), but in some cells a small initial decrease in R_{in} was seen followed by a sustained increase (Dun & Jiang, 1982). Such a decrease in R_{in} was not seen in the rabbit IMG cells.

The synaptic nature of the LS-EPSP is illustrated by the findings that both TTX and low Ca^{++} resulted in a disappearance of the response. That the LS-EPSP is not simply an afterpolarization following repetitive cellular action potentials was shown by the findings that direct intra-cellular stimulation did not elicit a LS-EPSP and application of d-TC, which blocked the repetitive spiking, did not affect the LS-EPSP.

1. Topography

The finding that there is no topographical organization of the cells which show a LS-EPSP in the rabbit IMG is not unusual. F-EPSP inputs to cells in sympathetic ganglia have also been shown not to be

topographically organized (Purves & Wigston, 1983). This does not, how-
ever, mean that the innervation of the cells is unselective or random.
In fact, the pattern of innervation to the guinea pig SCG is somewhat
selective. Neurons which project to particular regions of the periphery
are contacted in an organized manner by preganglionic axons arising from
different levels of the spinal cord. Several findings support the view
that individual postsynaptic cells which are mixed randomly throughout
the ganglion may have identifying characteristics that preganglionic
fibers recognize during synapse formation. In this manner, innervation
is based more on cell recognition than on anatomical considerations. At
certain levels within the autonomic nervous system, however, there are
anatomical organizations. The ganglia of the sympathetic chain are
innervated by preganglionic axons arising at different spinal cord lev-
els (Lichtman, Purves & Yip, 1980). Within the ganglion, however, the
organization is not anatomical. Rather, the preganglionic innervation
received by a cell seems to depend on the end organ which it effects.
For example, the sympathetic fibers to the eye receive a large number of
fibers from T1 while those to the ear are mainly innervated by pregan-
glionics from T4 (Lichtman, Purves & Yip, 1979), although the cells
which project to the eye and ear are scattered throughout the SCG.

Considering these findings, it is not surprising that the LS-EPSP
inputs to the rabbit IMG are not topographically organized. The above
results may suggest a similar selectivity of innervation of the cells in
the IMG. Inputs to the IMG have been found from the spinal cord, the
effector organs and from the solar and pelvic plexuses. A selectivity

of innervation could be important here. Inputs from L1 spinal levels may innervate IMG cells which project to the upper part of the colon while those from L3 may innervate the rectum or genitalia. Also, peripheral inputs from the upper parts of the colon may innervate cells in the IMG which project to the lower portions of the intestine.

The lack of topographical organgization in the IMG is consistent with the HRP tracing studies (Dalsgaard & Elfvin, 1982). When HRP was applied to the hypogastric or colonic nerves of the guinea pig IMG labeled neuronal cell bodies were found to be randomly distributed throughout the ganglion, not regionally localized.

2. Stimulus Frequency

The plot of LS-EPSP amplitude vs. presynaptic stimuli revealed a hyperbolic curve, as described in the Results section. The coefficients calculated for the equations represent the maximum amplitude and the stimulus required to reach a half maximal effect in an average cell. For example, it was calculated from the frequency data that % amplitude = (123 × Hz) / (11 + Hz); thus, the average maximum LS-EPSP amplitude is 123% of the response obtained at 30 Hz for 3 sec. From Table 5, the average amplitude at 30 Hz for 3 sec is 4.3 mV, translating to an average maximum response of 5.3 mV. A half maximal response of 2.6 mV would be obtained with stimulation at 11 Hz for 3 sec. These data may prove useful in the comparison of the LS-EPSP in the rabbit IMG with slow responses observed in other preparations.

3. Pharmacology of the LS-EPSP

In most cells in the rabbit IMG, responses to the perfused drugs were absent. The possibility has been raised that penetration of the compounds when applied by perfusion may present a problem, particularly with the relatively high molecular weight peptides (SP=1350, VIP=3330). In order to avoid these problems several steps were taken. First, a rapid flow rate was used to prevent dilution of the drugs in the bathing solution. Second, connective tissue, which may serve as a diffusion barrier, was removed as thoroughly as possible from the ganglion. Third, an attempt was made to impale cells near the edge of the ganglion. Even with these measures the diffusion problem is difficult to assess. Evidence to suggest that the lack of effects was not due to perfusion barriers includes the finding that when SP did have an effect it did so at low concentrations and also the observation that d-TC was always effective in blocking the F-EPSPs.

a. 5-Hydroxytryptamine

The response of the cells in the rabbit IMG to 5-HT was more similar to the LS-EPSP than the responses to the other substances tested. 5-HT did induce a depolarization and this depolarization was accompanied by an increased R_{in}; however, only 20% of the cells which exhibited a LS-EPSP also responded to 5-HT application. One would not expect diffusion to be a problem with 5-HT which has a molecular weight of 180. In the guinea pig celiac ganglion 60% of the cells which exhibited a LS-EPSP were sensitive to 5-HT. With prolonged application of 5-HT to the celiac ganglion an apparent desensitization was seen. The 5-HT

depolarization returned to resting level with continued application and the LS-EPSP disappeared. In the present study, however, those cells which were depolarized by 5-HT did not return to E_r until 5-HT was washed out. This may indicate that the 5-HT receptors in the guinea pig celiac ganglion and in the rabbit IMG are different. Additionally, conclusive evidence that the LS-EPSP was desensitized by 5-HT was not obtained.

b. Luteinizing Hormone Releasing Hormone

In the bullfrog paravertebral ganglia there is considerable evidence that LHRH mediates the LS-EPSP (see Introduction). LHRH had no effect on the LS-EPSP in the rabbit, nor was the LS-EPSP affected by an LHRH antagonist. Furthermore, no LHRH-like immunoreactivity was observed in the rabbit IMG in the immunohistochemical experiments. In the studies on the LHRH depolarization in bullfrog cells (Jan et al., 1979, 1980; Jan & Jan, 1982) LHRH or the LHRH antagonist was applied by pressure ejection from a pipette; therefore, the exact concentration of LHRH in the bullfrog studies is unknown. The concentration of LHRH or the LHRH analog in the pipette was 100 μM and the volume ejected < 1 μL; thus, the concentration at the cell must be considerably less than 100 μM. Katayama & Nishi (1982) used 5 μM in their voltage clamp investigation of the LS-EPSP in the bullfrog. It would appear then that the concentration used in the present experiments was sufficient. Thus, it must be concluded that LHRH is not involved in the genesis of the LS-EPSP in the rabbit IMG.

c. Substance P

Prior to the pharmacological experiments, the most likely candidate for the mediation of the LS-EPSP in the rabbit IMG was considered to be SP. This is because the response observed in the rabbit IMG was very similar to the response in the guinea pig IMG, SP was found in the fibers in the rabbit IMG and it seemed likely that the transmitter would be the same in mammalian species. Three pharmacological manipulations were performed to investigate the role of SP: application of SP, application of SP antagonists and application of capsaicin.

Substance P. When SP was perfused over the rabbit IMG only 1/3 of the cells were depolarized. In contrast, 90% of the cells were found to be SP-sensitive in the guinea pig IMG (Dun & Minota, 1981). The concentrations used in the present study must be sufficient since Dun & Minota (1981) obtained responses with 0.5 μM SP. Further, 2 of the cells that did respond to SP in the present study were sensitive to 1 μM SP.

In the guinea pig IMG continuous SP perfusion resulted in an apparent desensitization of the LS-EPSP. Desensitization occurred within 4 min of continuous application of 1 μM SP (Dun & Jiang, 1982). Additionally, the LS-EPSP remained depressed for several minutes after SP application (Dun & Jiang, 1982; Tsunoo et al., 1982). In the rabbit IMG the SP concentrations used were usually higher and the peptide was applied for times ranging for 5-15 min; however, no desensitizing effects were observed.

From the SP perfusion experiments, the final line of evidence against SP involvement in the LS-EPSP comes from the different types of

R_{in} changes observed following SP perfusion. The LS-EPSP was never accompanied by a decrease in R_{in}. On the other hand, 60% of the cells depolarized by SP showed a decrease in R_{in} during the depolarization. In this respect the effect of SP resembles SP effects on the guinea pig IMG (Dun & Minota, 1981) and the guinea pig locus coeruleus (Cheeseman, Pinnock & Henderson, 1983) where variable types of R_{in} changes have been observed.

Substance P Antagonists. The SP antagonists used in this thesis have been shown to antagonize the effects of SP at several sites (Folkers et al., 1981; Rosell et al., 1981; Yanagisawa et al., 1982). At 50 μM, (D-Pro[2], D-Phe[7], D-Trp[9])-SP blocked completely the LS-EPSP in the guinea pig within 5 min (Jiang et al., 1982). At lower concentrations the LS-EPSP was partially blocked. This SP analog and another, (D-Arg[1],D-Pro[2],D-Trp[7,9],Leu[11])-SP, which is supposedly more potent and specific (Yanigisawa, Otsuka, Konishi, Akagi, Folkers & Rosell, 1982) did not block the LS-EPSP in the rabbit IMG.

Capsaicin. Capsaicin has been shown to cause the release and subsequent depletion of SP from sensory neurons (Jessell et al., 1978; Gamse et al., 1981a, 1981b). Likewise, capsaicin (0.9-1.5 μM) caused release of SP from the guinea pig IMG (Tsunoo et al., 1982). In the guinea pig IMG, capsaicin (0.5-100 μM) perfusion resulted in a depolarization of the postganglionic cells (Dun & Kiraly, 1983). This depolarization appeared within seconds of the capsaicin application. Also, capsaicin was effective only on those cells which exhibited a LS-EPSP. In the rabbit IMG capsaicin was tested at concentrations of 5-100 μM and

was completely ineffective with perfusions for up to 15 min. Also in the guinea pig IMG, capsaicin perfusion apparently resulted in a deple- tion of SP since following capsaicin application a LS-EPSP could not be elicited. Even with 15 min perfusion of 100 µM capsaicin the LS-EPSP in the rabbit IMG persisted.

That capsaicin did not result in a depolarization of the rabbit IMG cells nor in a disappearance of the LS-EPSP was surprising. Capsai- cin clearly results in a depletion of SP in sympathetic ganglia (Gamse et al., 1981b) and a release of SP (Tsunoo et al., 1982). If this is the case in the rabbit IMG, capsaicin's ineffectiveness would indicate that SP is not involved in the LS-EPSP. In primary sensory neurons in the spinal cord capsaicin was shown not only to result in a decrease in SP-immunoreactivity, but also in CCK-, SOM- and VIP-immunoreactivity (Jansco, Hokfelt, Lundberg, Kiraly, Halasz, Nilsson, Terenius, Rehfeld, Steinbusch, Verhofstad, Elde, Said & Brown, 1981). These findings may also suggest that CCK, SOM and VIP are not involved in the LS-EPSP. These authors suggest that capsaicin not only affects SP fibers but is specific for sensory neurons, since immunoreactivity to 5-HT, ENK and neurotensin, found in fibers which do not subserve a sensory role, were not affected. These results and the present findings are not easily reconciled. If capsaicin affects only sensory fibers then it would be assumed that the SP fibers seen in the immunohistochemical studies are not of a sensory nature as they are in the guinea pig IMG. Alterna- tively, if capsaicin causes the release of transmitter from sensory fibers then the LS-EPSP in the rabbit IMG is not the result of a trans-

mitter released from sensory fibers as is the LS-EPSP in the guinea pig IMG. All of the above studies on the actions of capsaicin have used the rat or guinea pig. It may be possible that the nervous system of the rabbit is for some reason unresponsive to capsaicin.

These three pharmacological manipulations provide very good evidence that SP is not involved in the LS-EPSP in the rabbit IMG. The finding that the LS-EPSP in the rabbit IMG is not mediated by SP while the LS-EPSP in the guinea pig is mediated by SP correlates with studies which have examined the SP content in the gut. The SP fibers in the guinea pig IMG are thought to be sensory fibers from the colon which traverse the ganglion. In the transverse colon of the guinea pig the concentration of SP-immunoreactivity was found to be over 100 pmol/g wet tissue. In the rabbit transverse colon there was only 1/10 this amount (Holzer, Bucsics, Saria & Lembeck, 1982). Since there are SP-containing cell bodies in the guinea pig intestine (Schultzberg et al., 1980), these differences may reflect differences in the population of these cells in the guinea pig and rabbit. However, these differences may partly reflect a large and small number of SP sensory fibers in the guinea pig and rabbit colon, respectively. This study also serves to illustrate the differences in neuropeptides among various species.

d. Vasoactive Intestinal Polypeptide

VIP-immunoreactivity was particularly striking in the rabbit IMG. VIP is released in a Ca^{++}-dependent manner from in vitro brain preparations indicating it may subserve a transmitter role in the central nervous system (Giachetti, Said, Reynolds and Koniges, 1977; Emson, Fahren-

krug, Schaffalitzky de Muckadell, Jessell & Iversen, 1978).
Electrophysiologically, VIP has been shown to exert a depolarizing
effect on rat cerebral cortical neurons and toad motoneurons (Phillis,
Kirkpatrick & Said, 1978), rat dorsal horn neurons (Jeftinija, Murase,
Nedeljkov & Randic, 1982) and rat hippocampal pyramidal neurons (Dodd,
Kelly & Said, 1979). Where resistance changes have been examined, VIP
depolarization is accompanied by an increased membrane conductance.
This is in contrast to the LS-EPSP which involves an increased R_{in}. VIP
did not depolarize the rabbit IMG neurons. In a few cells, however, a
slight increase in the amplitude of the LS-EPSP was noticed. This sug-
gests that VIP may play a role in the modulation of the LS-EPSP, but
further studies must be done to obtain conclusive evidence.

The results of the pharmacological experiments emphasize the div-
ersity of synaptic transmission in various sympathetic ganglia. In the
bullfrog paravertebral ganglia the LS-EPSP is mediated by LHRH, in the
guinea pig IMG by SP and in some cells of the guinea pig celiac ganglia
by 5-HT. The present studies indicate that neither of these substances
is involved in the LS-EPSP in the majority of rabbit IMG neurons. A
possible explanation is that the LS-EPSP is mediated by more than one
substance with some cells responding to one substance and the remainder
responding to a different transmitter. Alternatively, two substances
may be acting simultaneously to produce a LS-EPSP.

4. Functional Significance of the LS-EPSP

One of the most obvious implications of the LS-EPSP would be to increase the probability of an action potential being generated following impingement of a F-EPSP onto a postganglionic cell. The depolarization during the LS-EPSP would bring the cell closer to the threshold and the increased R_{in} would make the current flow generated during the F-EPSP result in a greater voltage change. Take as an example a cell with E_r=-50 mV, R_{in}=40 MΩ and threshold=-38 mV. In the absence of a LS-EPSP, a F-EPSP of 10 mV in this cell does not result in a spike. During a LS-EPSP, however, an R_{in} increase of 20% would allow a F-EPSP generated by a similar current to depolarize the cell by 12 mV and, with an accompanying depolarization of only a few mV would allow this F-EPSP to easily reach threshold and generate an action potential. That such a phenomenon does occur during slow postsynaptic potentials has been demonstrated. In the bullfrog paravertebral ganglia, injection of current pulses which did not initiate action potentials in the resting state frequently produced impulses during the LS-EPSP (Jan et al., 1979). Further analysis showed that three factors contributed to this increased excitability--the membrane depolarization and increased R_{in} as described above and a third factor, a lowering of the threshold for action potential initiation by 1-3 mV. An increased excitability also occurs during the muscarinic S-EPSP in the bullfrog ganglia (Schulman & Weight, 1976). A slight increase in the excitability of the postganglionic neurons could be important in the IMG since most of the cholinergic inputs to this ganglion are subthreshold and a summation of inputs is required to elicit an action potential.

Another implication of this increased excitiability would be to expand the time during which temporal summation would be effective (Hartzell, 1981). The summation of subthreshold F-EPSPs would have to involve a synchronism with a few milliseconds of converging inputs. During a LS-EPSP the time span of the activity of the synapse would be increased, thereby maximizing the likelihood of temporal summation of responses. Additionally, a decrease in membrane conductance would increase the space constant of the dendrite. In this situation a given F-EPSP would be conducted along the cell processes with less of a decrement per unit length, consequently increasing the likelihood of spatial summation of F-EPSPs.

H. Concluding Comments

The present studies have demonstrated both the diversity and the complexity of synaptic transmission in the abdominal prevertebral sympathetic ganglia. In terms of basic cellular properties these cells are similar to the sympathetic neurons found in the paravertebral ganglia. This similarity extends to the mediation of the F- and S-EPSPs by nicotinic and muscarinic actions of ACh, respectively. In contrast to the paravertebral ganglia, the prevertebral ganglia receive a large number of subthreshold cholinergic inputs which converge onto the ganglionic neurons. These converging fibers enter the ganglion from all directions--rostral, caudal, medial and lateral--and most likely oringinate in peripheral sites as well as in the preganglionic nuclei in the spinal cord.

The paravertebral ganglia are also distinguished by the occurrence of noncholinergic slow postsynaptic potentials. These slow postsynaptic potentials play an important role in the input-output relationships of these ganglia. A unique property of the slow postsynaptic potentials is the variability which exists in the pharmacology of the slow responses in the different ganglia examined. A LS-EPSP has been found to occur in the bullfrog paravertebral ganglia, in the guinea pig IMG and celiac ganglion, and in the rabbit IMG. In each of these ganglia the noncholinergic response to nerve sitmulation is similar; however; the pharmacology of the response is diverse, with the slow response in each ganglion exhibiting unique pharmacological properties. This may be indicative of a specialization of function with regard to noncholinergic transmission in the different ganglia. This specialization may be related to species-specific differences in the functional role played by the slow postsynaptic potentials in the interaction of the prevertebral ganglia with the effector organs.

REFERENCES

Adrian, E. D. (1931). Potential changes in the isolated nervous system of Dytiscus marginalis. J. Physiol. (Lond.) 72, 132-151.

Adrian, E. D, Bronk, D. W. and Phillips, G. (1932). Discharges in mammalian sympathetic nerves. J. Physiol. (Lond.) 74, 115-133.

Aidley, D. J. (1978). The Physiology of Excitable Cells. Cambridge University Press, Cambridge.

Ashe, J. H. and Libet, B. (1981). Orthodromic production of non-cholinergic slow depolarizing response in the superior cervical ganglion of the rabbit. J. Physiol. (Lond.) 320, 333-346.

Bayliss, W. M. and Starling, E. A. (1900). The movements and the innervation of the large intestine. J. Physiol. (Lond.) 26, 107-118.

Baylor, D. A., Fuortes, M. G. F. and O'Bryan, P. M. (1971). Receptive fields of cones in the retina of the turtle. J. Physiol. (Lond.) 214, 265-294.

Billingsley, P. R. and Ranson, S. W. (1918). On the number of nerve cells in the ganglion cervicale superius and of nerve fibers in the cephalic end of the truncus sympatheticus in the cat and on the numerical relations of preganglionic and postganglionic neurons. J. Comp. Neurol. 29, 359-366.

Blackman, J. G., Crowcroft, P. J., Devine, C. E., Holman, M. E. and Yonemura, K. (1969). Transmission from preganglionic fibres in the hypogastric nerve to peripheral ganglia in male guinea-pigs. J. Physiol. (Lond.) 201, 723-743.

Blackman, J. G., Ginsborg, B. L. and Ray, C. (1963). Synaptic transmission in the sympathetic ganglion of the frog. J. Physiol. (Lond.) 167, 355-373.

Blackman, J. G. and Purves, R. D. (1969). Intracellular recordings from ganglia of the thoracic sympathetic chain of the guinea-pig. J. Physiol. (Lond.) 203, 173-198.

Bronk, D. W., Tower, S. S., Solandt, D. Y. and Larrabee, M. G. (1938). The transmission of trains of impulses through a sympathetic ganglion and in its postganglionic nerves. Amer. J. Physiol. 122, 1-15.

Brooks-Fournier, R. and Coggeshall, R. E. (1981). The ratio of preganglionic axons to postganglionic cells in the sympathetic nervous system of the rat. J. Comp. Neurol. 197, 217-236.

Brown, D. A. and Adams, P. R. (1980). Muscarinic suppression of a novel voltage-sensitive K^+ current in a vertebrate neurone. Nature 283, 673-676.

Brown, G. L. and Pascoe, J. E. (1952). Conduction through the inferior mesenteric ganglion of the rabbit. J. Physiol. (Lond.) 118, 113-123.

Cheeseman, H. J., Pinnock, R. O. and Henderson, G. (1983). Excitatory action of substance P in the locus coeruleus. Irish J. Med. Sci. 152, Suppl. 1, 18.

Christ, D. D. and Nishi, S. (1971). Effects of adrenaline on nerve terminals in the superior cervical ganglion of the rabbit. Br. J Pharmacol. 41, 331-338.

Christ, D. D. and Nishi, S. (1973). Anomalous rectification of mammalian sympathetic ganglion cells. Exp. Neurol. 40, 806-815.

Coombs, J. S., Curtis, D. R. and Eccles, J. C. (1956). Time course of motoneuronal responses. Nature 178, 1049-1050.

Crowcroft, P. J. and Szurszewski, J. H. (1971). A study of the inferior mesenteric and pelvic ganglia of guinea-pigs with intracellular electrodes. J. Physiol. (Lond.) 219, 421-441.

Crowcroft, P. J., Holman, M. E. and Szurszewski, J. H. (1971). Excitatory input from the distal colon to the inferior mesenteric ganglion in the guinea-pig. J. Physiol. (Lond.) 219, 443-461.

Dalsgaard, C.-J. and Elfvin, L.-G. (1979). Spinal origin of preganglionic fibers projecting onto the superior cervical ganglion and inferior mesenteric ganglion of the guinea pig, as demonstrated by the horseradish peroxidase technique. Brain Res. 172, 139-143.

Dalsgaard, C.-J. and Elfvin, L.-G. (1982). Structural studies on the connectivity of the inferior mesenteric ganglion of the guinea pig. J. Autonom. Nerv. Sys. 5, 265-278.

Dalsgaard, C.-J., Hokfelt, T., Elfvin, L.-G., Skirboll, L. and Emson, P. (1982a). Substance P-containing primary sensory neurons projecting to the inferior mesenteric ganglion: evidence from combined retrograde tracing and immunohistochemistry. Neurosci. 7, 647-654.

Dalsgaard, C.-J., Hokfelt, T., Elfvin, L.-G. and Terenius, L. (1982b). Enkephalin-containing sympathetic preganglionic neurons projecting to the inferior mesenteric ganglion: evidence from combined retrograde tracing and immunohistochemistry. Neurosci. 7, 2039-2050.

Dalsgaard, C.-J., Hokfelt, T., Schultzberg, M., Lundberg, J. M., Terenius, L., Dockray, G. J. and Goldstein, M. (1983). Origin of peptide-containing fibers in the inferior mesenteric ganglion of the guinea pig: immunohistochemical studies with antisera to substance P, enkephalin, vasoactive intestinal polypeptide, cholecystokinin and bombesin. Neurosci. 9, 191-211.

Davison, J. S. and Hersteinsson, P. (1975). Functional organization of the guinea-pig inferior mesenteric ganglion. J. Physiol. (Lond.) 250, 27P-28P.

De Groat, W. C. and Krier, J. (1979). The central control of the lumbar sympathetic pathway to the large intestine of the cat. J. Physiol. (Lond.) 289, 449-468

Dockray, G. J., Vaillant, C. and Walsh, I. H. (1979). Bombesin-like immunoreactivity in the rat gastrointestinal tract. Neurosci. 4, 1561-1568.

Dodd, J., Kelly, J. S. and Said, S. I. (1979). Excitation of the rat hippocampus by the octacosapeptide, vasoactive intestinal polypeptides (VIP). Br. J. Pharmacol. 66, 125P.

Douglas, W. W. and Ritchie, J. M. (1956). The conduction of impulses through the superior cervical and accessory cervical ganglia of the rabbit. J. Physiol. (Lond.) 133, 220-231.

Dun, N. J. and Jiang, Z. G. (1982). Non-cholinergic excitatory transmission in inferior mesenteric ganglia of the guinea pig: possible mediation by substance P. J. Physiol. (Lond.) 325, 145-159.

Dun, N. J. and Karczmar, A. G. (1979). Actions of substance P on sympathetic neurons. Neuropharmacol. 13, 219-223.

Dun, N. J. and Kiraly, M. (1983). Capsaicin causes release of a substance P-like peptide in guinea-pig inferior mesenteric ganglia. J. Physiol. (Lond.) 340, 107-120.

Dun, N. J., Kiraly, M. and Ma, R. C. (1983). Evidence for a serotonin mediated slow excitatory potential in the guinea-pig celiac ganglia. Submitted for publication.

Dun, N. J. and Ma, R. C. (1983). Slow non-cholinergic excitatory potentials in neurones of the guinea-pig celiac ganglia. Submitted for publication.

Dun, N. J. and Minota, S. (1981). Effects of substnace P on neurones of the inferior mesenteric ganglia of the guinea pig. J. Physiol. (Lond.) 321, 259-271.

Ebbesson, S. O. E. (1963). A quantitative study of human superior cervical sympathetic ganglia. Anat. Rec. 146, 353-356.

Ebbesson, S. O. E. (1968). Quantitative studies of superior cervical sympathetic ganglia in a variety of primates including man. I. The ratio of preganglionic fibers to ganglionic neurons. J. Morphol. 124, 117-132.

Eccles, J. C. (1935). The action potential of the superior cervical ganglion. J. Physiol. (Lond.) 85, 179-206.

Eccles, R. M. (1952). Action potentials of isolated mammalian sympathetic ganglia. J. Physiol. (Lond.) 117, 181-195.

Eccles, R. M. (1963). Orthodromic activation of single ganglion cells. J. Physiol. (Lond.) 165, 387-391.

Eccles, R. M. and Libet, B. (1961). Origin and blockade of the sympathetic responses of curarized sympathetic ganglia. J. Physiol. (Lond.) 157, 484-503.

Elfvin, L.-G. (1968). A new granule-containing nerve cell in the inferior mesenteric ganglion of the rabbit. J. Ultrastruct. Res. 22, 37-44.

Elfvin, L.-G. (1971a). Ultrastructural studies on the synaptology of the inferior mesenteric ganglion of the cat. I. Observations on the cell surface of the postganglionic perikarya. J. Ultrastruct. Res. 37, 411-425.

Elfvin, L.-G. (1971b). Ultrastructural studies on the synaptology of the inferior mesenteric ganglion of the cat. II. Specialized serial neuronal contacts between preganglionic end fibers. J. Ultrastruct. Res. 37, 426-431.

Elfvin, L.-G. (1971c). Ultrastructural studies on the synaptology of the inferior mesenteric ganglion of the cat. III. The structure and distribution of the axodendritic and dendrodendritic contacts. J. Ultrastruct. Res. 37, 432-448

Elfvin, L.-G. and Dalsgaard, C.-J. (1977). Retrograde axonal transport of horseradish peroxidase in afferent fibers of the inferior mesenteric ganglion of the guinea pig. Identification of the cells of origin in dorsal root ganglia. Brain Res. 126, 149-153.

Emson, P. C., Fahrenkrug, J., Schaffalitzky de Muckadell, O. B., Jessell, T. M. and Iversen, L. L. (1978). Vasoactive intestinal polypeptide (VIP): vesicular localization and potassium evoked release from rat hypothalamus. Brain Res. 143, 174-178.

Erulkar, S. D. and Woodward, J. K. (1968). Intracellular recording from mammalian superior cervical ganglion in situ. J. Physiol. (Lond.) 199, 189-203.

Falck, B. (1962). Observations on the possibilities of the cellular localization of monoamines by a fluorescence method. Acta Physiol. Scand. 56, Suppl. 197.

Fatt, P. and Katz, B. (1951). An analysis of the end-plate potential recorded with an intracellular electrode. J. Physiol. (Lond.) 115, 320-370.

Folkers, K., Horig, J., Rosell, S. and Bjorkroth, U. (1981). Chemical design of antagonists of substance P. Acta Physiol. Scand. 111, 505-506.

Gabella, G. (1976). Structure of the Autonomic Nervous System. Wiley, New York.

Gamse, R., Leeman, S. E., Holzer, P. and Lembeck, F. (1981a). Differential effects of capsaicin on the content of somatostatin, substance P, and neurotensin in the nervous system of the rat. Naunyn-Schmiedeberg's Arch. Pharmacol. 317, 140-148.

Gamse, R., Wax, A., Zigmond, R. E. and Leeman, S. E. (1981b). Immunoreactive substance P in sympathetic ganglia: distribution and sensitivity towards capsaicin. Neurosci. 6, 437-441.

Garry, R. C. (1933a). The nervous control of the caudal region of the large bowel in the cat. J. Physiol. (Lond.) 77, 422-431.

Garry, R. C. (1933b). The response to stimulation of the caudal end of the large bowel in the cat. J. Physiol. (Lond.) 78, 208-224.

Garry, R. C. and Gillespie, J. S. (1955). The responses of the musculature of the colon of the rabbit to stimulation, in vitro, of the parasympathetic and of the sympathetic outflows. J. Physiol. (Lond.) 128, 557-576.

Gaskell, W. H. (1916). The Involuntary Nervous System. Longmans Green, London.

Giachetti, A., Said, S. I., Reynolds, R. C. and Koniges, F. C. (1977). Vasoactive intestinal polypeptide in brain: localization in and release from isolated nerve terminals. Proc. Nat. Acad. Sci., U.S.A. 74, 3424-3428.

Gillespie, J. S. and Mackenna, B. R. (1961). The inhibitory action of the sympathetic nerves on the smooth muscle of the rabbit gut, its reversal by reserpine and restoration by catechol amines and by dopa. J. Physiol. (Lond.) 156, 17-34.

Grundfest, H. (1961). Ionic mechanisms in electrogenesis. Ann. N. Y. Acad. Sci. 94, 405-457.

Haefely, W (1972). Electrophysiology of the adrenergic neuron. Hand. Exp. Pharmacol., 33, 660-725.

Hamberger, B. and Norberg, K.-A. (1965). Studies on some systems of adrenergic synaptic terminals in the abdominal ganglia of the cat. Acta Physiol. Scand. 65, 235-242

Hamberger, B., Norberg, K.-A. and Sjoqvist, F. (1964). Evidence for adrenergic nerve terminals and synapses in sympathetic ganglia. Int. J. Neuropharmacol. 2, 279-282.

Hamberger, B., Norberg, K.-A. and Ungerstedt, U. (1965). Adrenergic synaptic terminals in autonomic ganglia. Acta Physiol. Scand. 64, 285-286

Harris, A. J. (1943). An experimental anlysis of the inferior mesenteric plexus. J. Comp. Neurol. 79, 1-17.

Hartzell, H. C. (1981). Mechanisms of slow postsynaptic potentials. Nature 291, 539-544.

Hashiguchi, T., Kobayashi, H., Tosaka, T. and Libet, B. (1982). Two muscarinic depolarizaing mechanisms in mammalian sympathetic neurons. Brain Res. 242, 378-382.

Hokfelt, T., Elfvin, L.-G., Elde, R., Schultzberg, M., Goldstein, M. and Luft, R. (1977a). Occurrence of somatostatin-like immunoreactivity in some peripheral sympathetic noradrenergic neurons. Proc. Natl. Acad. Sci., U.S.A. 74, 3587-3591.

Hokfelt, T., Elfvin, L.-G., Schultzberg, M., Fuxe, K., Said, S. I., Mutt, V. and Goldstein, M. (1977b). Immunohistochemical evidence of vasoactive intestinal polypeptide-containing neurons and nerve fibers in sympathetic ganglia. Neurosci. 2, 885-896.

Hokfelt, T., Elfvin, L.-G., Schultzberg, M., Goldstein, M. and Nilsson, G. (1977c). On the occurrence of substance P-containing fibers in sympathetic ganglia: immunohistochemical evidence. Brain Res. 132, 29-41.

Hokfelt, T., Lundberg, J. M., Schultzberg, M., Johansson, O., Skirboll, L., Anggard, A., Fredholm, B., Hamberger, B., Pernow, B., Rehfeld, J. and Goldstein, M. (1980). Cellular localization of peptides in neural structures. Proc. Roy. Soc. Lond. B 210, 63-77.

Holzer, P., Bucsics, A., Saria, A. and Lembeck, F. (1982). A study of the concentrations of substance P and neurotensin in the gastrointestinal tract of various mammals. Neurosci. 7, 2919-2924.

Horn, J. P. and Dodd, J. (1983). Inhibitory cholinergic synapses in autonomic ganglia. Trends Neurosci. 6, 180-184.

Hunt, C. C. and Riker, W. K. (1966). Properties of frog sympathetic neurons in normal ganglia and after axon section. J. Neurophysiol. 29, 1096-1114.

Jacobwitz, D. M. (1974). The peripheral autonomic system. In: The Peripheral Nervous System, Hubbard, J. I. (Ed.), pp. 87-110, Plenum Press, New York.

Jan, Y. N., Jan, L. Y. and Kuffler (1979). A peptide as a possible transmitter in sympathetic ganglia of the frog. Proc. Natl. Acad. Sci., U.S.A. 76, 1501-1505.

Jan, Y. N., Jan, L. Y. and Kuffler (1980). Further evidence for peptidergic transmission in sympathetic ganglia. Proc. Natl. Acad. Sci., U.S.A. 77, 5008-5012.

Jan, L. Y. and Jan, Y. N. (1982). Peptidergic transmission in sympathetic ganglia of the frog. J. Physiol. (Lond.) 327, 219-246.

Jansco, G., Hokfelt, T., Lundberg, J. M., Kiraly, E., Halasz, N., Nilsson, G., Terenius, L., Rehfeld, J., Steinbusch, H., Verhofstad, A., Elde, R., Said, S. and Brown, M. (1981). Immunohistochemical studies on the effect of capsaicin on spinal and medullary peptide and monoamine neurons using antisera to substance P, gastrin/CCK, somatostatin, VIP, enkephalin, neurotensin and 5-hydroxytryptamine. J. Neurocytol. 10, 963-980.

Jeftinija, S., Murase, K., Nedeljkov, V. and Randic, M. (1982). Vasoactive intestinal polypeptide excites mammalian dorsal horn neurons both in vivo and in vitro. Brain Res., 243, 158-164.

Jessell, T. M., Iversen, L. L. and Cuello, A. C. (1978). Capsaicin-induced depletion of substance P from primary sensory neurones. Brain Res. 152, 183-188.

Jiang, Z. G., Dun, N. J. and Karczmar, A. G. (1982a). Substance P: a putative sensory transmitter in mammalian autonomic ganglia. Science 217, 739-741.

Jiang, Z. G., Simmons, M. A. and Dun, N. J. (1982b). Enkephalinergic modulation of non-cholinergic transmission in mammalian prevertebral ganglia. Brain Res. 235, 185-191.

Job, C. and Lundberg, A. (1952). Reflex excitation of cells in the inferior mesenteric ganglion on stimulation of the hypogastric nerve. Acta Physiol. Scand. 26, 366-382.

Katayama, Y. and Nishi, S. (1982). Voltage-clamp analysis of peptidergic slow depolarizations in bullfrog sympathetic ganglion cells. J. Physiol. (Lond.) 333, 305-313.

Katayama, Y. and North, R. A. (1978). Does substance P mediate slow synaptic excitation within the myenteric plexus? Nature 274, 387-388.

Kessler, J. A., Adler, J. E., Bohn, M. C. and Black, I. B. (1981). Substance P in principal sympathetic neurons: regulation by impulse activity. Science 214, 335-336.

Kleinhaus, S., Boley, S. J., Sheran, M. and Sieber, W. K. (1979). Hirschprung's disease: a survey of the members of the surgical section of the American Academy of Pediatrics. J. Ped. Surg. 14, 588-597.

Kobayashi, H. and Libet, B (1968). Generation of slow postsynaptic potential without increases in ionic conductance. Proc. Nat. Acad. Sci., U.S.A. 69, 1304-1311.

Konishi, S., Tsunoo, A. and Otsuka, M. (1979a). Enkephalins presynaptically inhibit cholinergic transmission in sympathetic ganglia. Nature 282, 515-516.

Konishi, S., Tsunoo, A. and Otsuka, M. (1979b). Substance P and noncholinergic excitatory synaptic transmission in guinea pig sympathetic ganglia. Proc. Jap. Acad. 55, 525-530.

Kosterlitz, H. W., Thompson, J. W. and Wallis, D. I. (1964). The compound action potential in the nerve supplying the medial smooth muscle of the nictitating membrane of the cat. J. Physiol. (Lond.) 171, 426-433.

Kreulen, D. L. and Szurszewski, J. H. (1979a). Reflex pathways in the abdominal prevertebral ganglia: evidence for a colo-colonic inhibitory reflex. J. Physiol. (Lond.) 295, 21-32.

Kreulen, D. L. and Szurszewski, J. H. (1979b). Electrophysiologic and morphologic basis for organization of neurons in prevertebral ganglia. In: Frontiers of Knowledge in the Diarrheal Diseases, Janowitz, H. D. and Sachar, D. B. (Eds), pp. 211-226, Projects in Health, Upper Montclair, New York.

Krier, J., Schmalz, P. F. and Szurszewski, J. H. (1982). Central innervation of neurones in the inferior mesenteric ganglion and of the large intestine of the cat. J. Physiol. (Lond.) 332, 125-138.

Krnjevic, K. (1977). Effects of substance P on central neurons in cats. In: Substance P, von Euler, U. S. and Pernow, B. (Eds.), pp. 217-230, Raven Press, New York.

Kuba, K. and Koketsu, K. (1978). Synaptic events in sympathetic ganglia. Prog. Neurobiol. 11, 77-169.

Kuntz, A. J. (1940). The structural organization of the inferior mesenteric ganglia. J. Comp. Neurol. 72, 371-382.

Kuntz, A. J. and Saccomanno, G. (1944). Reflex inhibition of intestinal motility mediated through decentralized prevertebral ganglia. J. Neurophysiol. 7, 163-170.

Langley, J. N. (1891). The innervation of the pelvic viscera. J. Physiol. (Lond.) 12, xxiii-xxvi.

Langley, J. N. (1921). The Autonomic Nervous System. Heffer, Cambridge, Mass.

Langley, J. N. and Anderson, H. K. (1895a). On the innervation of the pelvic and adjoining viscera. Part I. The lower portion of the intestine. J. Physiol. (Lond.) 18, 67-105.

Langley, J. N. and Anderson, H. K. (1895b). On the innervation of the pelvic and adjoining viscera. Part II. The bladder. J. Physiol. (Lond.) 19, 71-84.

Langley, J. N. and Anderson, H. K. (1895c). On the innervation of the pelvic and adjoining viscera. Part IV. The internal generative organs. J. Physiol. (Lond.) 19, 122-130.

Langley, J. N. and Anderson, H. K. (1895d). On the innervation of the pelvic and adjoining viscera. Part V. Position of the nerve cells on the course of the efferent nerve fibers. J. Physiol. (Lond.) 19, 131-139.

Langley, J. N. and Anderson, H. K. (1896a). On the innervation of the pelvic and adjoining viscera. Part VI. Histological and physiological observations upon the effects of section of the sacral nerves. J. Physiol. (Lond.) 19, 372-384.

Langley, J. N. and Anderson, H. K. (1896b). On the innervation of the pelvic and adjoining viscera. Part VII. Anatomical observations. J. Physiol. (Lond.) 20, 372-406.

Larsson, L.-I. (1981). Peptide immunocytochemistry. Prog. Histochem. Cytochem. 13, 1-85

Lawson, H. (1934). The role of the inferior mesenteric ganglia in the diphasic response of the colon to sympathetic stimuli. Am. J. Physiol. 109, 257-273.

Lawson, H. and Holt, J. P. (1937). The control of the large intestine by the decentralized inferior mesenteric ganglion. Am. J. Physiol. 118, 780-785.

Learmonth, J. R. and Markowitz, J. (1929). Studies on the function of the lumbar sympathetic outflow. I. The relation of the lumbar sympathetic outflow to the sphincter ani internus. Am. J. Physiol. 89, 686-691.

Learmonth, J. R. and Markowitz, J. (1930). Studies on the innervation of the large bowel. II. The influence of the lumbar colonic nerves on the distal portion of the colon. Am. J. Physiol. 94, 501-504.

Libet, B. (1970). Generation of slow inhibitory and excitatory postsynaptic potentials. Fed. Proc. 29, 1945-1956.

Libet, B. and Tosaka, T. (1966). Slow postsynaptic potentials recorded intracellularly in sympathetic ganglia. Fed. Proc. 25, 270.

Lichtman, J. W., Purves, D. and Yip, J. W. (1979). On the purpose of selective innervation of guinea-pig superior cervical ganglion. J. Physiol. (Lond.) 292, 69-84.

Lichtman, J. W., Purves, D. and Yip, J. W. (1980). Innervation of sympathetic neurones in the guinea-pig thoracic chain. J. Physiol. (Lond.) 298, 285-299.

Lloyd, D. P. C. (1937). The transmission of impulses through the inferior mesenteric ganglia. J. Physiol. (Lond.) 91, 296-313.

Lundberg, J. M., Hokfelt, T., Anggard, A., Kimmel, J., Goldstein, M. and Markey, K. (1980). Coexistence of an avian pancreatic polypeptide (APP) immunoreactive substance and catecholamines in some peripheral and central neurons. Acta Physiol. Scand. 110, 107-109.

Lundberg, J. M., Hokfelt, T., Anggard, A., Terenius, L., Elde, R., Markey, K., Goldstein, M. and Kimmel, J. (1982). Organizational principles in the peripheral sympathetic nervous system: subdivision by coexisting peptides (somatostatin-, avian pancreatic polypeptide-, and vasoactive intestinal polypeptide-like immunoreactive materials). Proc. Natl. Acad. Sci., U.S.A. 79, 1303-1307.

Ma, R. C., Dun, N. J. and Jiang, Z. G. (1983). Evidence of slow IPSP in mammalian prevertebral ganglia. Brain Res. 270, 350-354.

Matthews, M. R. and Cuello, A. C. (1982). Substance P-immunoreactive peripheral branches of sensory neurons innervate guinea pig sympathetic neurons. Proc. Natl. Acad. Sci., U.S.A. 79, 1668-1672.

McAfee, D. A. and Yarowsky, P. J. (1979). Calcium-dependent potentials in the mammalian sympathetic neurone. J. Physiol. (Lond.) 290, 507-523.

McLennan, H. and Pascoe, J. E. (1954). The origin of certain non-medullated nerve fibers which form synapses in the inferior mesenteric ganglion of the rabbit. J. Physiol. (Lond.) 124, 145-156.

Meech, R. W. (1978). Calcium-dependent potassium activation in nervous tissues. Ann. Rev. Biophys. Bioeng. 7, 1-18.

M'Fadden, G. D. F., Loughridge, J. S. and Milroy, T. H. (1935). The nerve control of the distal colon. Q. J. Exp. Physiol. 25, 315-327.

Narahasi, T. (1974). Chemicals as tools in the study of excitable membranes. Physiol. Rev. 54, 812-889.

Neild, T. O. (1978). Slowly-developing depolarization of neurons in the guinea-pig inferior mesenteric ganglion following repetitive stimulation of the preganglionic nerves. Brain Res. 140, 231-239.

Nicoll, R. A. (1978). The action of thyrotropin-releasing hormone, substance P and related peptides on frog spinal motoneurons. J. Pharmacol. Exp. Ther. 207, 817-824.

Nishi, S. (1974). Ganglionic transmission. In: The Peripheral Nervous System, Hubbard, J. I. (Ed.), pp. 225-255, Plenum Press, New York.

Nishi, S. and Koketsu, K. (1960). Electrical properties and activities of single sympathetic neurons in frogs. J. Cell. Comp. Physiol. 55, 15-30.

Nishi, S. and Koketsu, K. (1968). Early and late afterdischarges of amphibian sympathetic ganglion cells. J. Neurophysiol. 31, 109-121.

Nja, A. and Purves, D. (1977). Specific innervation of guinea-pig superior cervical ganglion cells by preganglionic fibres arising from different levels of the spinal cord. J. Physiol. (Lond.) 264, 565-583.

Otsuka, M. and Konishi, K. (1977). Electrophysiological and neurochemical evidence for substance P as a transmitter of primary sensory neurons. In: Substance P, von Euler, U. S. and Pernow, B., (Eds.), pp. 207-214, Raven Press, New York.

Perri, V., Sacchi, O. and Casella, C. (1970). Electrical properties and synaptic connections of the sympathetic neurons in the rat and guinea-pig superior cervical ganglion. Pflugers Arch. 314, 40-54.

Phillis, J. W., Kirkpatrick, J. R. and Said, S. F. (1978). Vasoactive intestinal polypeptide excitation of central neurons. Can. J. Physiol. Pharmacol. 56, 337-340.

Purves, D. and Hume, R. I. (1981). The relation of postsynaptic geometry to the number of presynaptic axons that innervate autonomic ganglion cells. J. Neurosci. 1, 441-452.

Purves, D. and Wigston, D. J. (1983). Neural units in the superior cervical ganglion of the guinea-pig. J. Physiol. (Lond.) 334, 169-178.

Purves, R. D. (1981). Microelectrode Methods for Intracellular Recording and Ionophoresis. Academic Press, New York.

Rankin, F. W. and Learmonth, J. R. (1930). Section of the sympathetic nerves of the distal part of the colon and the rectum in the treatment of Hirschprung's disease and certain types of constipation. Ann. Surg. 92, 710-720.

Rankin, F. W. and Learmonth, J. R. (1932). The present status of the treatment of Hirschprung's disease. Am. J. Surg. 15, 219-227.

Rosell, S., Olgart, L., Gazelius, B., Panopoulos, P., Folkers, K. and Horig, J. (1981). Inhibition of antidromic and substance P-induced vasodilatation by a substance P antagonist. Acta Physiol. Scand. 111, 381-382.

Ross, J. P. (1935). The results of sympathectomy: an analysis of the cases reported by fellows of the association of surgeons. Br. J. Surg. 23, 433-443.

Sanbe, S. (1961). Studies on the incoming and outgoing myelinated fibers of the sympathetic superior cervical ganglion. Fukushima J. Med. Sci. 8, 109-129.

Schulman, J. A. and Weight, F. F. (1976). Synaptic transmission: long-lasting potentiation by a postsynaptic mechanism. Science 194, 1437-1439.

Schultzberg, M. (1983). Bombesin-like immunoreactivity in sympathetic ganglia. Neurosci. 8, 363-374.

Schultzberg, M., Hokfelt, T., Lundberg, J. M., Terenius, L., Elfvin, L.-G. and Elde, R. (1978). Enkephalin-like immunoreactivity in nerve terminals in sympathetic ganglia and adrenal medulla and in adrenal medullary gland cells. Acta Physiol. Scand. 103, 475-477.

Schultzberg, M., Hokfelt, T., Nilsson, G., Terenius, L., Rehfeld, J. F., Brown, M., Elde, R. P., Goldstein, M. and Said, S. (1980). Distribution of peptide- and catecholamine-containing neurons in the gastrointestinal tract of rat and guinea-pig: immunohistochemical studies with antisera to substance P, vasoactive intestinal polypeptide, enkephalin, somatostatin, gastrin/cholecystokinin, neurotensin and dopamine-β-hydroxylase. Neurosci. 5, 689-744.

Schultzberg, M., Hokfelt, T., Terenius, L., Elfvin, L.-G., Lundberg, J. M., Brandt, J., Elde, R. P. and Goldstein, M. (1979). Enkephalin immunoreactive nerve fibres and cell bodies in sympathetic ganglia of the guinea pig and rat. Neurosci. 4, 249-270.

Skok, V. I. (1973). Physiology of Autonomic Ganglia. Igaku Shoin, Tokyo.

Sternberger, L. A. (1979). Immunocytochemistry. Wiley, New York.

Szurszewski, J. H. and Weems, W. A. (1976). A study of peripheral input to and its control by post-ganglionic neurones of the inferior mesenteric ganglion. J. Physiol. (Lond.) 256, 541-556.

Tallarida, R. J. and Jacob, L. S. (1979). The Dose-Response Relation in Pharmacology. Springer-Verlag, New York.

Tramu, G., Pillez, A. and Leonardelli, J. (1978). An efficient method of antibody elution for the successive or simultaneous localization of two antigens by immunocytochemistry. J. Histochem. Cytochem. 26, 322-324.

Trumble, H. C. (1933). The plan of the visceral nerves in the lumbar and sacral outflows of the autonomic nervous system. Br. J. Surg. 21, 664-676.

Tsunoo, A., Konishi, S. and Otsuka, M. (1982). Substance P as an excitatory transmitter of primary afferent neurons in guinea-pig sympathetic ganglia. Neurosci. 7, 2025-2037.

Wallis, D. I. and North, R. A. (1978). Synaptic input to cells of the rabbit superior cervical ganglion. Pflugers Arch. 374, 145-152.

Webber, R. H. (1955). Analysis of the sympathetic trunks, communicating rami, sympathetic roots and visceral rami in the lumbar region in man. Ann. Surg. 141, 398-413.

Weems, W. A. and Szurszewski, J. H. (1977). Modulation of colonic motility by peripheral neural inputs to neurons of the inferior mesenteric ganglion. Gastroenterol. 73, 273-278.

Weems, W. A. and Szurszewski, J. H. (1978). An intracellular analysis of some intrinsic factors controlling neural output from inferior mesentric ganglion of guinea pigs. J. Neurophysiol. 41, 305-321.

Weight, F. F. and Votava, J. (1970). Slow synaptic excitation in sympathetic ganglion cells: evidence for synaptic inactivation of potassium conductance. Science, 170, 755-758.

Wolf, G. A., Jr. (1941). The ratio of preganglionic neurons to postganglionic neurons in the visceral nervous system. J. Comp. Neurol. 75, 235-243.

Wood, J. D. and Mayer, C. J. (1978). Slow synaptic excitation mediated by serotonin in Auerbach's plexus. Nature 276, 836-837.

Yanagisawa, M., Otsuka, M., Konishi, S., Akagi, H., Folkers, K. and Rosell, S. (1982). A substance P antagonist inhibits a slow reflex response in the spinal cord of the newborn rat. Acta Physiol. Scand. 116, 109-112.

Youmans, W. B., Karstens, A. I. and Aumann, K. W. (1942). Nervous pathways for the reflex regulation of intestinal pressure. Am. J. Physiol. 135, 619-627.

The dissertation submitted by Mark Alan Simmons has been read and approved by the following committee:

>   Dr. Nae J. Dun, Director
>   Associate Professor, Pharmacology, Loyola
>
>   Dr. William C. de Groat, Professor, Pharmacology
>   University of Pittsburgh
>
>   Dr. Alexander G. Karczmar, Professor and Chairman,
>   Pharmacology, Loyola
>
>   Dr. Sarah A. Shefner, Research Assistant Professor,
>   Physiology and Biophysics, University of Illinois
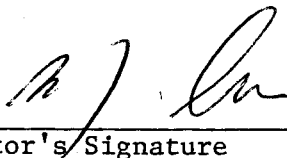>
>   Dr. Jay Z. Yeh, Associate Professor, Pharmacology,
>   Northwestern University

The final copies have been examined by the director of the dissertation and the signature which appears below verifies the fact that any necessary changes have been incorporated and that the dissertation is now given final approval by the Committee with reference to content and form.

The dissertation is therefore accepted in partial fulfillment of the requirements for the degree of Doctor of Philosophy.

11/22/83
_____
Date

_____
Director's Signature